



UNIVERSIDADE FEDERAL DE SANTA CATARINA
CENTRO TECNOLÓGICO
PROGRAMA DE PÓS-GRADUAÇÃO EM ENGENHARIA QUÍMICA

Viviane Chiaradia

**UNSATURATED MACROLACTONE POLYMERIZATION FOLLOWED BY ITS
MODIFICATION AND CROSSLINKING VIA CLICK CHEMISTRY-BASED
REACTIONS**

Florianópolis

2019

Viviane Chiaradia

**UNSATURATED MACROLACTONE POLYMERIZATION FOLLOWED BY ITS
MODIFICATION AND CROSSLINKING VIA CLICK CHEMISTRY-BASED
REACTIONS**

Tese submetida ao Programa de Pós-Graduação da
Universidade Federal de Santa Catarina para a obtenção
do título de Doutor em Engenharia Química.

Orientador: Prof^ª. Dr^ª. Claudia Sayer

Coorientador: Prof. Dr. Pedro Henrique Hermes de
Araújo

Coorientadora: Prof^ª. Dr^ª. Débora de Oliveira

Florianópolis

2019

Ficha de identificação da obra elaborada pelo autor,
através do Programa de Geração Automática da Biblioteca Universitária da UFSC.

Chiaradia, Viviane

Unsaturated macrolactone polymerization followed by its modification and crosslinking via click chemistry-based reactions. / Viviane Chiaradia; orientadora, Claudia Sayer, coorientador, Pedro Henrique Hermes de Araújo, coorientadora, Débora de Oliveira, 2019. 168 p.

Tese (doutorado) - Universidade Federal de Santa Catarina, Centro Tecnológico, Programa de Pós-Graduação em Engenharia Química, Florianópolis, 2019.

Inclui referências

1. Engenharia Química. 2. Globalide. 3. Polimerização enzimática por abertura de anel. 4. Reações tiol-eno. 5. Reações Alder-eno. I. Sayer, Claudia. II. Hermes de Araújo, Pedro Henrique. III. De Oliveira, Débora. IV. Universidade Federal de Santa Catarina. Programa de Pós-Graduação em Engenharia Química. V. Título.

Viviane Chiaradia

**UNSATURATED MACROLACTONE POLYMERIZATION FOLLOWED BY ITS
MODIFICATION AND CROSSLINKING VIA CLICK CHEMISTRY-BASED
REACTIONS**

O presente trabalho em nível de doutorado foi avaliado e aprovado por banca examinadora composta pelos seguintes membros:

Prof.^a Claudia Sayer, Dr.^a

Universidade Federal de Santa Catarina

Prof. Cristiano José de Andrade, Dr.

Universidade Federal de Santa Catarina

Prof.^a Ana Paula Serafini Immich Bueno, Dr.^a

Universidade Federal de Santa Catarina

Prof. Luiz Henrique Catalani, Dr.

Universidade de São Paulo

Certificamos que esta é a **versão original e final** do trabalho de conclusão que foi julgado adequado para obtenção do título de doutor em Engenharia Química.

Prof.^a Dr.^a Cíntia Soares

Coordenadora do Programa

Prof.^a Dr.^a Claudia Sayer

Orientadora

Florianópolis, 02 de julho de 2019.

ACKNOWLEDGMENTS

Primeiramente, agradeço aos meus pais Zenaide e José pelo incentivo e pelo esforço que sempre fizeram para investir na minha educação. Eles foram meus primeiros professores e sem sombra de dúvidas a base que me conduziu até aqui. Aos meus irmãos Rogério e Gustavo, por acreditarem em mim e apoiarem todas minhas decisões mesmo que elas me fizessem ficar longe deles. Amo vocês!

Aos meus orientadores Dr.^a Claudia Sayer e Dr. Pedro Araújo pela oportunidade de trabalhar ao lado deles desde meu mestrado. À minha coorientadora Dr.^a Débora de Oliveira pelos 11 anos de parceria, desde o início da minha graduação. Ao professor Dr. Andreas Heise por ter aberto as portas do seu laboratório na Irlanda e ter me dado a oportunidade de conhecer um novo mundo na pesquisa.

Ao André, por ter sido meu parceirinho e ter me incentivado a continuar lutando mesmo quando tudo parecia dar errado. Sou eternamente grata ao teu amor, paciência (foram muitas lamentações e choradeiras) e palhaçadas durante esta etapa. Tenho certeza que este trabalho é motivo de orgulho para ti também. Obrigada!

Aos meus amigos do Laboratório de Controle e Processos de Polimerização (LCP), vou levar vocês no meu coração. Aos meus amigos do *Royal College of Surgeons in Ireland*, minha estadia na Irlanda não seria tão maravilhosa sem o acolhimento e parceria de vocês. *Go raibh maith agat.*

À Universidade Federal de Santa Catarina e ao Programa de Pós-Graduação em Engenharia Química por todos os recursos disponibilizados. Ao Laboratório Central de Microscopia Eletrônica da Universidade Federal de Santa Catarina (LCME/UFSC) pelas análises de microscopia eletrônica de transmissão. À Coordenação de Aperfeiçoamento de Pessoal de Nível Superior (CAPES) e ao Conselho Nacional de Desenvolvimento Científico e Tecnológico (CNPq) pelo apoio financeiro no Brasil e no exterior.

A todos que passaram pela minha vida nessa jornada e torceram pelo meu sucesso.

Obrigada!

RESUMO

Poliésteres alifáticos estão entre os polímeros biodegradáveis mais utilizados em aplicações biomédicas. A síntese de poliésteres pode ser conduzida por duas rotas principais: polimerização por abertura de anel e policondensação. Neste trabalho, o poliéster poli(globalide) foi sintetizado via polimerização enzimática por abertura de anel em solução e em miniemulsão a partir da macrolactona insaturada globalide. O efeito da concentração de enzima na e-ROP em solução utilizando Novozym 435 (NVZ 435, lipase B de *Candida antarctica* imobilizada em suporte poroso) mostrou que as massas molares não foram alteradas (de forma acentuada) quando utilizadas diferentes concentrações de enzima, permanecendo em torno de 30.000 g mol⁻¹ (M_w). As reações conduzidas em solução com a lipase NS88011 (lipase B de *Candida antarctica* imobilizada em suporte mais barato quando comparado com a lipase NVZ435) mostraram que maiores massas molares (M_w 60.500 g mol⁻¹) podem ser obtidas quando esta enzima é utilizada na e-ROP, em comparação aos poliésteres obtidos com a Novozym 435, e períodos de reação mais longos são necessários para a obtenção de rendimentos na faixa de 80-90%. Lipases livres (CALB e NS40116) foram utilizadas para a obtenção de nanopartículas de PGI via polimerização enzimática por abertura de anel (e-ROP) em miniemulsão. Diâmetros na faixa de 70 a 280 nm foram obtidos quando CALB foi utilizada como biocatalisador e massas molares na faixa entre 6.800 a 23.200 g mol⁻¹ foram atingidas. Entretanto, nanopartículas sintetizadas com NS40116 mostraram-se instáveis e apenas diâmetros acima do limite de detecção do equipamento foram encontrados (6 µm). Após a síntese e caracterização de PGI via e-ROP em solução e miniemulsão, duas estratégias diferentes de *click-chemistry* foram utilizadas para a modificação da cadeia polimérica. A primeira estratégia utilizada foi a modificação pós-polimerização de PGI via reações tiol-eno. Três tióis contendo grupamentos fosfoéster foram sintetizados em tolueno para obter compostos puros com rendimentos acima de 60% após purificação em coluna de sílica. Assim, os tióis sintetizados foram adicionados na cadeia de PGI e parâmetros como razão molar tiol:eno e concentração de iniciador foram avaliados. Resultados de conversão em dupla ligação e propriedades térmicas dos polímeros foram afetados pelo tamanho da cadeia do tiol utilizado. Quando TF2 foi adicionado na cadeia de PGI, conversões em dupla ligação de 14 a 84% foram obtidas e o polímero com 14% de modificação foi escolhido para produzir fibras via eletrofiação. Fibras homogêneas e sem a presença de grânulos na faixa de 11 µm foram obtidas e este material mostrou-se não tóxico em células de fibroblastos. Em uma segunda metodologia, a cadeia polimérica de PGI foi modificada ou reticulada via reações com triazolinedionas (TADs). PGI foi modificado com TAD monofuncional (*4-phenyl-1,2,4-triazoline-3,5-dione*) para obter polímeros com elevado grau de modificação (97%) em reação conduzida em THF em um sistema livre de catalisador e iniciadores. Com o intuito de obter *scaffolds* porosos, fibras de PGI foram obtidas por eletrofiação e reticuladas com TADs bifuncionais para uma melhoria nas propriedades mecânicas do material. De uma forma geral, a química de triazolinedionas mostrou-se eficiente para introduzir funcionalidades e reticulações na cadeia de PGI e modificar as propriedades térmicas e mecânicas do polímero.

Palavras-chave: Polimerização enzimática por abertura de anel, macrolactona, globalide, tiol-eno, triazolinedionas, modificação, reticulação.

RESUMO EXPANDIDO

Introdução

Polímeros biodegradáveis, biocompatíveis e não-tóxicos vêm sendo utilizados como biomateriais para aplicações na área biomédica, incluindo fios de sutura, parafusos, *scaffolds* para regeneração de tecidos e nanopartículas para liberação prolongada de fármacos (SEYEDNEJAD et al., 2011). Neste sentido, poliésteres alifáticos são uma excelente alternativa e podem ser sintetizados por policondensação e polimerização por abertura de anel (ROP) de ésteres cíclicos (lactonas e macrolactonas). A síntese de poliésteres via ROP enzimática (e-ROP) possui algumas vantagens quando comparada com a ROP mediada por catalisadores químicos, uma vez que enzimas são altamente seletivas e derivadas de fontes naturais. Além disso, a polimerização pode ocorrer em condições reacionais brandas e o polímero final não apresenta traços tóxicos de catalisador residual (SEYEDNEJAD et al., 2011; YANG et al., 2014). Macrolactonas insaturadas, como o globalide (GI), são interessantes no desenvolvimento de biomateriais, uma vez que a presença de insaturação na cadeia polimérica final (após a polimerização de GI) permite a adição de grupos funcionais de interesse com o intuito de melhorar o desempenho do material para aplicações específicas. Devido ao seu elevado caráter hidrofóbico, polímeros derivados de macrolactonas possuem lenta degradação no organismo e para permitir seu uso como biomateriais biodegradáveis, geralmente são funcionalizados para redução de sua cristalinidade. Neste trabalho, a polimerização enzimática por abertura de anel da macrolactona insaturada globalide foi estudada via ROP em solução e em miniemulsão. Ainda, foi realizada a modificação pós-polimerização do polímero insaturado poli(globalide) (PGI) via reações *click* tiol-eno e alder-eno.

Objetivo

Este trabalho propõe a síntese de poliéster insaturado PGI via e-ROP em solução ou em miniemulsão e sua modificação via reações *click*. Para a modificação pós-polimerização, duas rotas químicas distintas foram utilizadas: tiol-eno e alder-eno. Na modificação via tiol-eno, o trabalho teve como objetivo a conjugação de grupamento fosfoésteres nas insaturações de PGI disponíveis e posterior caracterização dos materiais obtidos via conversão de dupla ligação e propriedades térmicas. Ainda, teve como objetivo a produção de fibras por *electrospinning* e análise da biocompatibilidade dos *scaffolds* obtidos. Para a metodologia alder-eno, o objetivo principal do trabalho consistiu na modificação e reticulação de PGI utilizando triazolidonas (TADs) monofuncionais e bifuncionais e a caracterização dos materiais obtidos. Em adição, a reticulação de fibras de PGI foi estudada *in-situ* (durante o *electrospinning*) e após o processo de *electrospinning*.

Metodologia

A polimerização enzimática por abertura de anel foi conduzida em solução e em miniemulsão. Para a primeira metodologia, foi estudado o efeito da concentração de enzima (2, 6 e 10 m/m% em relação ao monômero) na polimerização de globalide na presença das lipases imobilizadas Novozym 435 (NVZ 435) ou NS88011 utilizando tolueno como solvente. Após a polimerização, o polímero foi precipitado em metanol e caracterizado quanto suas propriedades térmicas, cristalinas e de massa molar.

Para o preparo de nanopartículas de poli(globalide), as reações foram conduzidas em miniemulsão e catalisadas pelas lipases livres de *Candida antarctica* B ou *Thermomyces*

lanuginosus. Para o preparo da fase aquosa foram utilizados água, lipase livre e Lutensol AT50 (surfactante) e para a fase orgânica foram utilizados monômero G1 e hexadecano ou crodamol (co-estabilizadores). As polimerizações foram conduzidas avaliando o efeito da concentração de surfactante (1; 2,5 e 5 m/m% em relação a água) e da temperatura reacional (45 ou 60 °C) no diâmetro final das nanopartículas e suas respectivas massas molares.

Duas rotas químicas diferentes foram utilizadas para a modificação pós-polimerização do homopolímero poli(globalide), ambas fazendo uso da insaturação na cadeia polimérica para adição de grupamentos via *click-chemistry*. Quando a modificação foi conduzida via reações de adição tiol-eno, tióis contendo grupamento fosfoéster foram sintetizados para posterior adição na cadeia polimérica com a finalidade de reduzir a hidrofobicidade do material - pela adição de um composto mais hidrofílico. Após a síntese, os tióis-fosfoésteres foram adicionados na cadeia de PGI via reações tiol-eno na presença de iniciador térmico (AIBN) a 80 °C em um período de 8 horas. Parâmetros como concentração de iniciador (1 e 5 mol% em relação ao tiol) e razão molar tiol:eno (0,5:1; 1:1 e 2:1) foram avaliados. A adição dos tióis à cadeia de PGI foi confirmada por ¹H-RMN e a redução da cristalinidade foi associada ao comportamento térmico dos materiais funcionalizados. Ainda, polímeros puro e modificado foram utilizados para o preparo de fibras via *electrospinning*.

Por fim, a cadeia do homopolímero PGI foi modificada via reações alder-eno utilizando triazolinedionas (TADs). Primeiramente, triazolinedionas bifuncionais foram sintetizadas a partir de diisocianatos de acordo com protocolo descrito na literatura. A reação entre PGI e TAD monofuncional comercial (PTAD) foi realizada em temperatura ambiente, na ausência de catalisadores/iniciadores utilizando diferentes solventes orgânicos. Fibras de PGI foram obtidas via *electrospinning* e reticuladas com TADs bifuncionais (HM bis-TAD e MDP bis-TAD) durante ou após o processo de *electrospinning*. Propriedades térmicas e mecânicas foram avaliadas para verificar o impacto da reticulação nas propriedades finais das fibras.

Resultados e Discussão

Na ROP enzimática em solução (Capítulo 3), altos rendimentos (entre 85 a 93%) e massas molares na faixa de 30.000 g mol⁻¹ foram observados nos minutos iniciais da reação (10 min) catalisada por lipase NVZ 435. Quando NS88011 foi utilizada, o rendimento aumentou gradativamente com o tempo reacional (de 10, 23 e 50% em 10 minutos de reação para 72, 90 e 88% em 360 minutos quando concentrações de enzima de 2, 6 e 10 m/m% foram utilizadas, respectivamente). Massas molares mais elevadas, na faixa de 60.000 g mol⁻¹ foram obtidas com o uso de NS88011, porém, dispersidades mais elevadas foram atingidas.

Na ROP enzimática via miniemulsão (Capítulo 4), parâmetros como concentração de surfactante e temperatura reacional foram avaliados. Nanopartículas com diâmetros de 70 a 280 nm foram obtidas e o aumento na concentração de surfactante acarretou a redução dos diâmetros. Massas molares foram medidas por GPC na faixa de 6.800 a 23.200 g mol⁻¹.

No capítulo 5, tióis contendo grupamento fosfoéster foram sintetizados para resultar em compostos altamente puros e com elevados rendimentos após coluna cromatográfica de sílica (acima de 60%). Após, os tióis sintetizados foram adicionados nas insaturações de PGI e a eficiência de conjugação foi relacionada com o tipo e tamanho da cadeia do respectivo tiol-fosfoéster. Quando TF1 foi utilizado, apenas baixas conversões foram obtidas (de até 15%). No entanto, polímeros funcionalizados com TF2 e TF3 apresentaram conversões de dupla ligação de 84 e 30%, respectivamente, quando uma proporção de tiol-eno 2:1 foi utilizada. Após a funcionalização, foi observada a mudança nas propriedades térmicas dos polímeros formados pela redução da temperatura de fusão e obtenção de polímeros completamente amorfos. Polímero modificado com TF2 (14% de dupla conversão) foi selecionado para a produção de fibras por *electrospinning* e fibras homogêneas com diâmetros na faixa de 11 µm foram obtidas.

A biocompatibilidade de fibras de polímero puro e funcionalizado foi avaliada em células de fibroblastos e os polímeros demonstraram-se não tóxicos.

No capítulo 6, a pós-polimerização de PGI foi estudada pela reação com TADs. Altas conversões (de 64 a 97%) foram obtidas na reação de PGI com TAD monofuncional (PTAD) e as propriedades térmicas do polímero final foram modificadas pela inserção de grupamentos *urazole* (derivadas do PTAD). Após teste preliminar confirmando a possibilidade da reticulação de PGI com TADs bifuncionais, *scaffolds* foram obtidos por *electrospinning* e coletados em uma solução contendo TAD bifuncional para obtenção de fibras com 9,8 μm de diâmetro. Devido a obtenção de fibras com defeitos, uma nova metodologia foi testada, onde após a obtenção das fibras por *electrospinning*, estas foram incubadas em soluções contendo HM ou MDP bis-TAD. Após 24 h de incubação, fibras com a superfície reticulada e núcleo não reticulado foram obtidas, preservando as propriedades térmicas de PGI, com temperatura de fusão na faixa de 40 °C. Com o intuito de obter fibras completamente reticuladas, as fibras parcialmente reticuladas foram inchadas e incubadas pela segunda vez em solução contendo os reticulantes e desta vez, materiais totalmente reticulados e amorfos foram obtidos. Após a reticulação, houve um aumento considerável nas propriedades mecânicas das fibras e a resistência a tensão aumentou 1000%. Ademais, a deformação aumentou de 24,5% (PGI puro) para 45% (após reticulação com HM bis-TAD) e 32% (após reticulação com MDP bis-TAD).

Considerações finais

Poliésteres obtidos a partir de macrolactonas são atrativos na área biomédica devido sua biocompatibilidade e biodegradabilidade. Este trabalho é dividido em dois tópicos principais. Os dois primeiros capítulos correspondem a avaliação da polimerização da macrolactona insaturada globalmente via polimerização enzimática por abertura de anel via solução ou miniemulsão. Polimerizações conduzidas em solução utilizando tolueno como solvente e diferentes enzimas como biocatalisadores levaram a formação de polímeros de alta massa molar com boas dispersidades para este tipo de polimerização. Diferentes cinéticas reacionais foram observadas quando NVZ435 e NS88011 foram utilizadas. Para NVZ435, altos rendimentos foram obtidos nos instantes iniciais de reação e estes mantiveram-se estáveis no decorrer da polimerização, na faixa de 88 a 91% e o mesmo comportamento foi observado quando a massa molar foi medida (na faixa de 30.000 g mol^{-1} durante todo o curso reacional). Por outro lado, quando NS88011 foi utilizada, os rendimentos e massas molares aumentaram gradativamente com o tempo reacional até atingir um *plateau* e estas diferenças na cinética são atribuídas a características do suporte de cada enzima, como porosidade por exemplo.

Na e-ROP via miniemulsão, é mais difícil ter um controle no teor de água do sistema, que é o iniciador da polimerização. Assim, massas molares mais baixas (entre 6.760 e 23.200 g mol^{-1}) do que aquelas obtidas via e-ROP em solução foram atingidas, como esperado. Nanopartículas em diâmetros entre 80 a 280 nm foram obtidas e a polimerização confirmada por ^1H RMN.

O segundo tópico da tese foi a modificação pós-polimerização de PGI com o intuito de alterar as propriedades do polímero, altamente hidrofóbico. No capítulo 5 foi demonstrada a possibilidade de adição de grupamentos fosfoéster na cadeia de PGI via reações de adição tioleno. A adição de grupamentos fosfoésteres pendentos na cadeia de PGI alteraram as propriedades térmicas do polímero, reduzindo os domínios cristalinos do polímero de origem. Com o intuito de mostrar a versatilidade do polímero, no capítulo 6, a cadeia polimérica foi modificada fazendo uso da química de triazolinedionas (TADs). TADs mostraram ser eficientes na rápida funcionalização ou reticulação do polímero na ausência de iniciadores, catalisadores e temperatura, na fração de segundos. Propriedades mecânicas de fibras de PGI foram potencializadas após a reticulação, assim como a modificação do seu domínio cristalino, possibilitando o futuro uso destes materiais como polímeros biodegradáveis.

ABSTRACT

Aliphatic polyesters are among the most used biodegradable polymers in biomedical applications. Polyesters synthesis can be conducted by two main routes: polycondensation and ring-opening polymerization. In this work, poly(globalide) (PGI) polyester was synthesized by enzymatic ring-opening polymerization in solution and miniemulsion from the unsaturated macrolactone globalide (GI). Polymerization kinetics of GI e-ROP in solution showed that different enzyme concentrations did not affect polymer molecular weight when Novozym 435 (NVZ 435, *Candida antarctica* B lipase immobilized on a porous support) was used as biocatalyst and, molecular weights in a range of 30,000 g mol⁻¹ (M_w) were obtained. On the contrary, when NS88011 (*Candida antarctica* B lipase immobilized on a cheaper support than NVZ 435) was used as biocatalyst, the molecular weights and yields were highly affected by the enzyme concentration and the kinetics were slower than in the NVZ435 case. However, higher molecular weights were reached when NS88011 was used. Free lipases (CALB and NS40116) were used to conduct miniemulsion e-ROP of GI. PGI nanoparticles diameters from 70 to 280 nm and molecular weights ranging from 6,800 to 23,200 g mol⁻¹ were obtained with CALB. Nanoparticles formed by the NS40116 catalyzed system were non-stable under the tested conditions and diameters were always above the measurement limit of the dynamic light scattering equipment (6 μm). After PGI synthesis and characterization via e-ROP in solution and miniemulsion, two different strategies were used to modify their structure via click chemistry. In the first approach, post-polymerization modification of PGI was conducted via thiol-ene reactions. Three different thiols containing phosphoester groups were synthesized in toluene resulting in yields greater than 60% after silica column purification. After that, these compounds were attached to the poly(globalide) backbone and the effects of thiol:ene ratio and initiator concentration were evaluated. Double bond conversions and polymer thermal properties were related to the thiol chain length. When diethyl 6-mercapto-1-hexyl phosphate was added to PGI chain, double bond conversions from 14 to 84% were reached. Modified polymer with 14% of double bond conversion was processed to obtain fibers with diameters around 11 μm via electrospinning, which were non-toxic to fibroblast cells. In the second approach, PGI chain was either modified or crosslinked via triazolinedione (TAD) reactions. PGI was modified with 4-phenyl-1,2,4-triazoline-3,5-dione (PTAD) to obtain high degree of modification (97%) in a reaction conducted with THF as solvent and without catalyst or initiator. In order to obtain porous scaffolds, plain PGI fibers were obtained by electrospinning and crosslinked with two different bifunctional TAD molecules (hexamethylene bis-TAD or MDP bis-TAD) to tune the mechanical properties of the fibers. In summary, TAD chemistry proved to be efficient in introducing functionalities and chemical crosslinks in the PGI chain and changing its thermal and mechanical properties.

Keywords: enzymatic ring-opening polymerization, macrolactone, globalide, thiol-ene, modification, crosslinking.

LIST OF FIGURES

Figure 1 - Different carriers for tissue engineering applications.....	39
Figure 2 - Electrospinning apparatus in vertical (a) and horizontal (b) positions.	40
Figure 3 - Different methods to obtain drug-loaded fibers.....	41
Figure 4 - Nanocapsules and nanospheres morphologies.....	42
Figure 5 - Schematic representation of the action of conventional drugs and drugs encapsulated in polymer nanoparticles.	43
Figure 6 - Schematic representation of miniemulsion technique.	44
Figure 7 - Polyesters application in biomedicine.	45
Figure 8 - Structure of lactones and macrolactones with different ring size.....	48
Figure 9 - Reaction mechanism in e-ROP of ϵ -caprolactone in the model proposed by Johnson.	52
Figure 10 - Schematic representation of the mechanism involved between the lipase active site and ϵ -CL during e-ROP.	54
Figure 11 - Mechanism of thiol-ene addition via free radicals.....	59
Figure 12 - Urazole synthesis from isocyanates.....	61
Figure 13 - TAD synthesis via urazole oxidation.....	61
Figure 14 - Alder-ene reaction between TAD and a substituted alkene.....	62
Figure 15 - PGI-PEG materials (a) before and (b) after thiol-ene photopolymerization and after purification in (c) THF and (d) water.	65
Figure 16 - Post-polymerization modification of unsaturated polymers with distinct functional groups.	66
Figure 17 - Schematic representation of PGI synthesis via e-ROP.	72
Figure 18 - Yield of poly(globalide) after different reaction times at 60 °C using different Novozym 435 lipase concentrations (2, 6 and 10 wt.%) and toluene as solvent (solvent to monomer mass ratio 2:1).	74
Figure 19 - Yield of poly(globalide) after different reaction times at 60 °C using different NS88011 lipase concentrations (2, 6 and 10 wt.%) and toluene as solvent (solvent to monomer mass ratio 2:1).	76
Figure 20 - Weight average molecular weights of poly(globalide) produced at 60 °C with different Novozym 435 concentrations (2, 6, and 10 wt.%) and toluene as solvent (solvent to monomer mass ratio 2:1) in function of reaction time.	77

Figure 21 - Weight average molecular weights of poly(globalide) produced at 60 °C with different NS88011 concentrations (2, 6, and 10 wt.%) and toluene as solvent (solvent to monomer mass ratio 2:1) in function of reaction time.	78
Figure 22 - Molecular weight distribution of poly(globalide) produced using toluene as solvent (solvent to monomer mass ratio 2:1) at 60 °C, in 30 min of reaction and using 10 wt.% of lipase.	79
Figure 23 - DSC curve of PGI obtained from e-ROP using 10 wt.% of Novozym 435.....	80
Figure 24 - X-ray diffraction spectra of PGI obtained from e-ROP using 10 wt.% of Novozym 435.	81
Figure 25 - e-ROP in aqueous miniemulsion - nanodroplets before polymerization.....	85
Figure 26 - Procedure for macrolactone e-ROP in aqueous miniemulsion.	88
Figure 27 - Particle size distribution of P(GI) NPs obtained by miniemulsion e-ROP using free CALB and hexadecane as co-stabilizer at different surfactant concentrations (1, 2.5 and 5 wt.%) at 45 °C (Table 1, entries GC1 to GC3).	91
Figure 28 - Particle size distribution of P(GI) NPs obtained by miniemulsion e-ROP using free CALB and hexadecane as co-stabilizer at different surfactant concentrations (1, 2.5 and 5 wt.%) at 60 °C (Table 1, entries GC4 to GC6).	92
Figure 29 - Molecular weight distribution of P(GI) NPs produced using free CALB and hexadecane as co-stabilizer at different surfactant concentrations (1, 2.5 and 5 wt.%) at 45 °C (Table 2, entries GC1 to GC3).....	93
Figure 30 - ¹ H-NMR spectrum of PGI nanoparticles obtained via miniemulsion e-ROP (400 MHz in CDCl ₃).....	94
Figure 31 - DSC traces of NPs obtained via miniemulsion e-ROP (Table 3, entry GC3 and Table 4, entry GC7).	96
Figure 32 - TEM images of PGI NPs obtained via miniemulsion e-ROP. (a) P(GI) with hexadecane (entry GC6 in Table 3) and (b) P(GI) with crodamol (entry GC8 in Table 4).....	97
Figure 33 - Synthesis of diethyl 2-mercaptoethyl phosphate (TF1).....	102
Figure 34 - Synthesis of diethyl 6-mercapto-1-hexyl phosphate (TF2).	103
Figure 35 - Synthesis of diphenyl 6-mercapto-hexyl phosphate (TF3).....	103
Figure 36 - Modification of PGI with thiol-phosphoesters.	104
Figure 37 - ¹ H-NMR spectrum of diethyl 2-mercaptoethyl phosphate - TF1 (400 MHz in CDCl ₃).....	108

Figure 38 - ¹ H-NMR spectrum of diethyl 6-mercapto-1-hexyl phosphate - TF2 (400 MHz in CDCl ₃).	108
Figure 39 - ¹ H-NMR spectrum of diphenyl 6-mercapto-1-hexyl phosphate - TF3 (400 MHz in CDCl ₃).	109
Figure 40 - GPC trace of PGI homopolymer.	110
Figure 41 - ¹ H-NMR spectrum of PGI homopolymer (400 MHz) in CDCl ₃ .	110
Figure 42 - ¹ H-NMR spectrum of PGI modified with TF1 (400 MHz) in CDCl ₃ .	111
Figure 43 - Differential scanning calorimetry thermograms (second heating curve) before and after post-polymerization modification of PGI with diethyl 2-mercaptoethyl phosphate (TF1).	112
Figure 44 - ¹ H-NMR spectrum of PGI modified with TF2 (400 MHz) in CDCl ₃ (Entry 6M6 in Table 6).	113
Figure 45 - PGI double bond consumption after TF2 addition in PGI backbone.	113
Figure 46 - Differential scanning calorimetry thermograms (second heating curve) before and after post-polymerization modification of PGI with diethyl 6-mercapto-1-hexyl phosphate (TF2).	114
Figure 47 - PGI after modification with TF2 using different ratios of thiol:ene.	114
Figure 48 - ¹ H-NMR spectrum of PGI modified with TF3 (400 MHz) in CDCl ₃ (Entry Ph6).	116
Figure 49 - Differential scanning calorimetry thermograms (second heating curve) before and after post-polymerization modification of PGI with diphenyl 6-mercapto-hexyl phosphate (TF3).	117
Figure 50 - SEM images of (a) PGI - 500 μm, (b) 6M1 - 500 μm, (c) PGI - 20 μm and (d) 6M1 - 20 μm.	119
Figure 51 - Fiber size distribution of (a) PGI and (b) 6M1 fibers.	119
Figure 52 - Proliferation of cells seeded on PGI and 6M1 fibers at day 1, 4 and 7. Data is reported as mean ± standard deviation, *** p < 0.001 (n=3).	120
Figure 53 - Live/dead images of cells at day 7 in PGI (a,b) and 6M1 (c,d).	121
Figure 54 - Hexamethylene bishydrazine carboxylate.	126
Figure 55 - Hexamethylene bisurazole synthesis.	126
Figure 56 - Hexamethylene bis-TAD synthesis.	127
Figure 57 - Methylene diphenyl bishydrazine carboxylate.	127
Figure 58 - Methylene diphenyl bisurazole synthesis.	127

Figure 59 - Methylene diphenyl bis-TAD synthesis.	128
Figure 60 - Modification of PGI with monofunctional PTAD.	129
Figure 61 - Crosslinking of PGI with bifunctional HM bis-TAD.	130
Figure 62 - Schematic illustration of PGI electrospinning followed by fiber deposition in TAD solution.	131
Figure 63 - Schematic illustration of post-crosslinking PGI fibers with HM bis-TAD/MDP bis-TAD.	132
Figure 64 - ¹ H-NMR of hexamethylene bishydrazine carboxylate in DMSO-d ₆	133
Figure 65 - ¹ H-NMR of hexamethylene bisurazole in DMSO-d ₆	134
Figure 66 - ¹ H-NMR of hexamethylene bisTAD in DMSO-d ₆	135
Figure 67 - ¹ H-NMR of methylene diphenyl bishydrazine carboxylate in DMSO-d ₆	136
Figure 68 - ¹ H-NMR of methylene diphenyl bishydrazine carboxilate in DMSO-d ₆	136
Figure 69 - ¹ H-NMR of methylene diphenyl bisTAD in DMSO-d ₆	137
Figure 70 - PTAD reaction (a) after 3 hours in different solvents and (b) in THF.	138
Figure 71 - ¹ H-NMR spectra of (a) PGI before and (b) after PTAD conjugation (entry PP5 in table 6) in CDCl ₃ (400 MHz).	139
Figure 72 - Differential scanning calorimetry thermograms (second heating curve) before and after modification of PGI with PTAD.	140
Figure 73 - Crosslinking reaction between PGI and HM bis-TAD.	141
Figure 74 - SEM images of PGI (a, b and c) and PGI modified with MDP bis-TAD during the electrospinning process (d, e and f).	142
Figure 75 - Fiber size distribution of (a) PGI fibers and (b) crosslinked fibers with MDP bis-TAD after electrospinning of PGI and fiber collection in TAD solution.	142
Figure 76 - Fig. 8 SEM images of plain PGI (a,d); crosslinked PGI/HM bis-TAD (b, e) and crosslinked PGI MDP bis-TAD (c,f).	144
Figure 77 - SEM images of crosslinked (a,c) PGI/HM bis-TAD and (b,d) PGI/MDP bis-TAD after swelling in chloroform.	144
Figure 78 - Fiber size distribution of crosslinked PGI/HM bis-TAD fibers (a) and crosslinked PGI/MDP bis-TAD (b) after second incubation in TAD solutions.	145
Figure 79 - Differential scanning calorimetry thermograms (second heating curve) of first incubation of PGI fibers in HM bis-TAD (a) and second incubation of partial crosslinked PGI fibers in HM bis-TAD and MDP bis-TAD (b).	146

Figure 80 - Stress strain curves of PGI, PGI HM bis-TAD* (first incubation), PGI HM bis-TAD** (second incubation), PGI MDP bis-TAD* (first incubation) and PGI MDP bis-TAD (second incubation) fibers. 147

Figure 81 - Tensile strength of PGI, PGI HM bis-TAD* (first incubation), PGI HM bis-TAD** (second incubation), PGI MDP bis-TAD* (first incubation) and PGI MDP bis-TAD (second incubation) fibers. 147

LIST OF TABLES

Table 1 - Formulations of miniemulsion e-ROP using CALB as biocatalyst.	88
Table 2 - e-ROP in miniemulsion of GI using free CALB as lipase and hexadecane as co-stabilizer.	91
Table 3 - e-ROP in miniemulsion of macrolactones GI using free CALB as lipase and crodamol as co-stabilizer.	95
Table 4 - Thermal properties of NPs obtained by miniemulsion e-ROP using different co-stabilizers.	95
Table 5 - Poly(globalide) functionalization via thiol-ene reactions using TF2.	112
Table 6 - Poly(globalide) functionalization via thiol-ene reactions using TF3.	115
Table 7 - Experimental conditions selected for the preparation of PGI and PGI-PEs fibers using a flow rate of 100 μ L/min and a distance from tip to collector of 15 cm.	118
Table 8 - Modification of PGI with PTAD in different solvents using an equivalent molar ratio of the reactants at room temperature.	138

LIST OF ABBREVIATIONS AND SYMBOLS

- $^1\text{H-NMR}$ - Proton Nuclear Magnetic Resonance
- ϵ -CL - ϵ -Caprolactone
- ϵ -PCL - Poly(ϵ -Caprolactone)
- δ -VL - δ -valerolactone
- ω -PDL - Omega-pentadecalactone
- ω -PPDL - Omega poly(pentadecalactone)
- $^{\circ}\text{C}$ - Degree Celsius
- D - Dispersity
- % - Percentage
- ΔH_m - Melting enthalpy
- A (U/g)- Unit of enzymatic activity
- AIBN - Azobisisobutyronitrile
- CALB - Lipase B of *Candida antarctica*
- CDCl_3 - Deuterated Chloroform
- CH_3CN - Acetonitrile
- DCM - Dichloromethane
- DLS - Dynamic Light Scattering
- DMSO - Dimethyl sulfoxide
- D_p - Particle diameter (nm)
- DSC - Differential Scanning Calorimetry
- EAM - Enzyme activated monomer
- e-ROP - Enzymatic ring-opening polymerization
- FDA - Food and Drug Administration
- Gl - Globalide
- GPC - Gel Permeation Chromatography
- HD - Hexadecanolide
- HFIP - Hexafluoro-2-propanol
- HM bis-TAD - Hexamethylene bis-TAD
- MDP bis-TAD - Methylene bis-TAD
- M_n - Number Average Molecular Weight (g mol^{-1})
- Mol% - Mol percentage

M_w - Weight Average Molecular Weight (g mol⁻¹)

MWCO - Molecular Weight Cut off

nm - Nanometers

NPs - Nanoparticles

NS40116 - Lipase of *Thermomyces lanuginosus*

NVZ 435 - Novozym 435

OH - Hydroxyl

PBS - Phosphate buffered saline

PDI - Polydispersion index

PEG - Poly(ethylene glycol)

PEs - Phosphoesters

PGI - Poly(globalide)

PLA - Polylactic acid

PPEs - Poly(phosphoesters)

PTAD - 4-phenyl-1,2,4-triazole-3,5-dione

ROP - Ring-opening polymerization

SEM - Scanning Electron Microscopy

T - Temperature (°C)

T_m - Melting temperature (°C)

TEM - Transmission Electron Microscopy

TF1 - Diethyl 2-mercaptoethyl phosphate

TF2 - Diethyl 6-mercapto-1-hexyl phosphate

TF3 - Diphenyl 6-mercapto-1-hexyl phosphate

THF - Tetrahydrofuran

TMS - Tetramethylsilane

wt.% - Weight-weight percentage

XRD - X-ray diffraction

TABLE OF CONTENTS

CHAPTER 1	33
1 INTRODUCTION	33
1.1 OBJECTIVES	34
1.1.1 General objective	34
1.1.2 Specific objectives	35
CHAPTER II	37
2 LITERATURE REVIEW	37
2.1 BIOCOMPATIBLE POLYMERS IN BIOMEDICAL FIELD.....	37
2.1.1 Polymers in tissue engineering	37
2.1.1.1 Use of electrospinning technique to obtain polymeric scaffolds.....	39
2.1.1.2 Fiber modification and crosslinking.....	40
2.1.2 Polymers in drug delivery systems	42
2.1.2.1 Use of miniemulsion polymerization technique to obtain polymer nanoparticles	43
2.2 POLYESTERS	45
2.3 POLYESTER SYNTHESIS	46
2.3.1 Polyester synthesis via ROP of lactones	46
2.3.2 Macrolactones in ROP	47
2.3.3 Polyester synthesis via enzymatic ROP of lactones and macrolactones	49
2.4 ENZYMES IN POLYESTER SYNTHESIS	51
2.4.1 Enzymatic ring-opening mechanism	51
2.5 POLYESTER DEGRADATION	54
2.6 POST-POLYMERIZATION FUNCTIONALIZATION OF POLYESTERS	55
2.6.1 Click reactions	56
2.6.2 Thiol-ene click reactions	57
2.6.2.1 Thiol-ene polymerization mechanism	58
2.6.3 Triazolinedione (TAD) in click reactions	59

2.6.3.1 TAD synthesis	60
2.6.3.2 Reactions involving TAD.....	62
2.6.4 Poly(globalide) post-polymerization modification.....	64
2.6.5 Phosphoesters use in polymer modification	66
2.7 FINAL CONSIDERATIONS.....	67
CHAPTER III.....	69
3. POLYESTERS FROM UNSATURATED MACROLACTONE GLOBALIDE USING COMMERCIAL LIPASE NS 88011 AND NOVOZYM 435 AS BIOCATALYSTS	69
3.1 INTRODUCTION.....	69
3.2 MATERIALS AND METHODS	71
3.2.1 Materials.....	71
3.2.2 Methods	71
3.2.2.1 Enzymatic ring-opening polymerization of globalide.....	71
3.2.3 Characterization	72
3.2.3.1 Molecular Weight Distribution.....	72
3.2.3.2 Thermal Properties	72
3.2.3.3 Crystallinity properties	73
3.2.3.4 Enzyme activity	73
3.3 RESULTS AND DISCUSSION.....	73
3.3.1 e-ROP of globalide using different lipases	74
3.3.1.1 Yield of PGI as a function of reaction time.....	74
3.3.1.2 PGI molecular weight as a function of reaction time	76
3.3.1.3 Thermal and crystalline properties	79
3.4 CONCLUSIONS	81
CHAPTER IV	83
4. POLYESTER NANOPARTICLES FROM UNSATURATED MACROLACTONE GLOBALIDE VIA MINIEMULSION ENZYMATIC RING-OPENING POLYMERIZATION	83

4.1 INTRODUCTION	83
4.2 MATERIALS AND METHODS	86
4.2.1 Materials.....	86
4.2.2 Methods	87
4.2.2.1 Enzyme concentration	87
4.2.2.2 Enzyme catalyzed miniemulsion polymerization of unsaturated macrolactone	87
4.2.3 Characterization	88
4.2.3.1 Chemical characterization	88
4.2.3.2 Morphology and particle size	89
4.2.3.3 Molecular Weight Distribution.....	89
4.2.3.4 Thermal analysis.....	90
4.3 RESULTS AND DISCUSSION.....	90
4.3.1 Poly(globalide) nanoparticles obtained via miniemulsion e-ROP.....	90
4.3.1.1 Nanoparticles synthesis using hexadecane as co-stabilizer.....	90
4.3.1.2 Nanoparticles synthesis using crodamol as co-stabilizer	94
4.3.2 Thermal analysis of PGI NPs obtained by miniemulsion e-ROP	95
4.3.3 Morphology of PGI NPs	96
4.4 CONCLUSIONS	97
CHAPTER V.....	99
5. POST-POLYMERIZATION MODIFICATION OF POLY(GLOBALIDE) WITH PHOSPHOESTER GROUPS VIA THIOL-ENE CHEMISTRY	99
5.1 INTRODUCTION	99
5.2 MATERIALS AND METHODS	101
5.2.1 Materials.....	101
5.2.2 Methods	102
5.2.2.1 Synthesis of thiols containing phosphoester groups (PEs-SH)	102
5.2.2.2 Synthesis of PGI homopolymer.....	103
5.2.2.3 Post-polymerization modification of PGI.....	104

5.2.2.4 Electrospinning of PGI and PGI-phosphoester (PGI-PEs)	105
5.2.2.5 Biocompatibility assays.....	105
5.2.3 Characterization	106
5.2.3.1 Chemical Characterization	106
5.2.3.2 Thermal Properties	106
5.2.3.3 Molecular Weight Distribution.....	106
5.2.3.4 Fibers morphology.....	106
5.3 RESULTS AND DISCUSSION.....	107
5.3.1 Synthesis of phosphoester containing thiol group (PEs-SH)	107
5.3.2 Post-polymerization modification of PGI	109
5.3.3 Electrospun PGI and PGI-PEs.....	118
5.3.4 Biocompatibility of PGI and PGI-PEs fibers.....	120
5.4 CONCLUSIONS	121
CHAPTER VI	123
6. CLICK MODIFICATION AND CROSSLINKING OF POLY(GLOBALIDE) VIA ALDER-ENE REACTIONS.....	123
6.1 INTRODUCTION	123
6.2 MATERIALS AND METHODS	125
6.2.1 Materials.....	125
6.2.2 Methods	125
6.2.2.1 Synthesis of PGI	125
6.2.2.2 Synthesis of triazolinediones	125
6.2.2.3 Modification of PGI with PTAD	128
6.2.2.4 Crosslinking of PGI with HM-bisTAD	129
6.2.2.5 <i>In-situ</i> crosslinking of PGI fibers	130
6.2.2.6 Post-crosslinking of PGI fibers.....	131
6.2.3 Polymer characterization.....	132
6.2.3.1 Chemical Characterization	132

6.2.3.2 Thermal Properties	132
6.2.3.3 Morphology	132
6.2.3.4 Mechanical properties.....	133
6.3 RESULTS AND DISCUSSION.....	133
6.3.1 Bifunctional TADs synthesis.....	133
6.3.2 PGI modification with PTAD	137
6.3.3 Crosslinking of PGI with HM-bisTAD	140
6.3.4 <i>In-situ</i> crosslinking of PGI fibers.....	141
6.3.5 Post-crosslinking of PGI fibers	142
6.4 CONCLUSIONS	148
CHAPTER VII.....	149
7. FINAL CONSIDERATIONS	149
7.1 CONCLUSION	149
7.2 FURTHER WORK.....	150
REFERENCES	153

CHAPTER 1

1 INTRODUCTION

Innumerous methodologies of polymer synthesis have been described in literature in the last decades in order to supply the growing demand for polymeric materials. Among the available ones, enzymatic polymerization is an interesting route once it makes use of enzymes from different sources (plants, animals or microorganisms) and the final materials usually present purity and high molecular weights (KOBAYASHI, 2015).

Biodegradable, biocompatible and non-toxic polymers have been utilized in biomedical applications including sutures, screws, scaffolds for tissue engineering and nanoparticles for drug delivery (SEYEDNEJAD et al., 2011). Aliphatic polyesters attend this desired characteristics and they can be synthesized by two main methods: polycondensation and ring-opening polymerization (ROP) of cyclic esters (lactones and macrolactones) (KOBAYASHI, 1999, 2010, 2015; KOBAYASHI; UYAMA; TAKAMOTO, 2000; MILETIĆ; LOOS; GROSS, 2010; SEYEDNEJAD et al., 2011).

Polyester synthesis via enzymatic ring-opening polymerization (e-ROP) has some advantages over ROP using chemical catalysts once enzymes are very selective and derived from natural sources. Besides, the polymerization occurs under mild reaction conditions (SEYEDNEJAD et al., 2011; YANG et al., 2014). Lactones as ϵ -caprolactone (ϵ -CL) and δ -valerolactone (δ -VL) are well known in polymer chemistry and recent studies have been conducted making use of cyclic esters with more carbons in the structure (macrolactones) (DE OLIVEIRA et al., 2017a; POLLONI et al., 2017; SAVIN et al., 2018). Considering the available macrolactones, unsaturated globalide (Gl) has interesting properties and one of the main advantages of its use is related to the unsaturation in the polymer backbone. Thus, different functional groups can be added in its chain to modify polymer properties.

Over the past years, studies showed Gl e-ROP followed by post-polymerization modification of the respective homopolymer, poly(globalide) (PGl). Functional groups such as hydroxy, amines, amides, and poly(ethylene glycol) (PEG) were previously reported to modify PGI chain via thiol-ene reactions (ATES; THORNTON; HEISE, 2011; ATES; HEISE, 2014a; SAVIN et al., 2018; GUINDANI et al., 2019). The functionalization or crosslinking of the PGI usually caused a transition from semicrystalline to an amorphous state and, in combination with

an increased hydrophilicity, an accelerated degradation (MEULEN et al., 2011; ATES; HEISE, 2014a).

Among the available groups to modify PGI chain, phosphoester have interesting properties as high hydrophilicity, biodegradability and biocompatibility. The combination of phosphoesters with aliphatic polyesters is an attractive target structure due to the biocompatibility and degradability of both segments. To date, two different polymer structures have been developed in literature making use of phosphoesters and poly(phosphoesters), such as block copolymers containing a poly(phosphoester) block and polymers with side chain phosphoesters. The latter were mostly obtained by the (controlled) radical polymerization of phosphoester functional acrylates or methacrylates (MONGE et al., 2011a).

In this work, unsaturated macrolactone polymerization was investigated by enzymatic ring-opening polymerization in solution and miniemulsion. Besides, we propose the introduction of phosphoester side groups to the unsaturated aliphatic polyester as this would hinder chain crystallization as well as facilitate cell adhesion. Synthetically, this is challenging because common aliphatic polyester such as poly(ϵ -caprolactone) (ϵ -PCL) and polylactic acid (PLA) do not offer functional anchor points for the attachment of phosphoesters. We therefore propose utilizing PGI, which can readily be prepared by ring-opening polymerization. In addition, highly efficient functionalization and crosslinking of PGI was performed via triazolinedione (TAD) conjugation chemistry and PGI fibers obtained via electrospinning were modified via alder-ene reactions. In general, biomaterials with modulated properties were obtained and they showed to have potential to be applied in biomedical areas.

1.1 OBJECTIVES

1.1.1 General objective

This work proposes the synthesis of the aliphatic unsaturated polyester poly(globalide) by e-ROP in solution or in miniemulsion and its modification via click-like reactions and more specifically thiol-ene and alder-ene systems. The introduction of side-groups in the polymer chain can hinder chain crystallization as well as facilitate cell adhesion.

1.1.2 Specific objectives

1 - Polyester synthesis via solution enzymatic ring-opening polymerization from unsaturated macrolactone globalide using immobilized lipase preparations (Novozym 435 and NS88011).

2 - Polyester nanoparticles preparation via miniemulsion enzymatic ring-opening polymerization from unsaturated macrolactone globalide using free lipase of *Candida antarctica* B (free CALB) and free lipase of *Thermomyces lanuginosus* (free NS40116).

3 - Conjugation of phosphoesters groups in poly(globalide) backbone via thiol-ene click-like reactions and characterization of the final materials regarding double bond conversion and thermal properties.

4 - Fiber production via electrospinning using PGI modified with phosphoester group and evaluation of biocompatibility.

5 - Modification and crosslinking of PGI chain via triazolinedione (TAD) click reactions using monofunctional and bifunctional TADs and characterization of the final polymers regarding conversion and thermal properties.

6 - Crosslinking of electrospun PGI fibers via *in-situ* crosslinking (during electrospinning) and post-electrospinning and characterization of the final fibers regarding mechanical and thermal properties.

In order to facilitate the reader's comprehension, this work was divided in seven chapters, including a brief introduction and the thesis main objectives in Chapter 1. Chapter 2 presents a literature review on the main topics of the thesis, such as biodegradable polymers, polyesters, enzymatic ring-opening polymerization and post-polymerization modification and crosslinking strategies. Chapters 3 and 4 describe the enzymatic ring-opening polymerization of globalide either in solution using toluene as solvent (Chapter 3) and in miniemulsion to obtain polyester nanoparticles (Chapter 4). Chapters 5 and 6 correspond to the post-polymerization modification of poly(globalide) via thiol-ene reactions adding phosphoester groups in the polymer chain (Chapter 5) and post-polymerization modification or crosslinking of PGI making use of triazolinediones via alder-ene reactions (Chapter 6). The main conclusions and suggestions for future works are shown in Chapter 7.

CHAPTER II

2 LITERATURE REVIEW

2.1 BIOCOMPATIBLE POLYMERS IN BIOMEDICAL FIELD

Natural and synthetic polymers with unique properties have been explored along the years as materials for several applications. Among them, biomedical and pharmaceutical fields have gained attention due to the great demand in the market. Thus, biodegradable, biocompatible, renewable and inexpensive polymers are of great interest for applications such as tissue engineering (LEE et al., 2009; ZHAO et al., 2016), controlled/sustained drug release (ALMOUAZEN et al., 2012; SAMPATH; LAKRA; KORRAPATI, 2014), therapeutics, diagnostics and beyond.

Different characteristics could affect polymer biocompatibility. In implants, for example, the biocompatibility is strongly related to polymer molecular weight, solubility, hydrophilicity/hydrophobicity, mechanism of degradation and/or erosion, morphology and shape of the implant. Aside of having good properties, the degradation products of the material should not be toxic, and they need to be easily metabolized from the organism (KOHANE; LANGER, 2008). The degradation products of biodegradable materials after hydrolysis comprehend different substances that are soluble in water. Thus, the length and the nature of the polymeric material will determine how it will be excreted from the body via renal clearance (MELCHELS et al., 2010).

A wide range of requirements must be considered while developing a biocompatible material for biomedical applications. Polymer mechanical properties, degradation time and permeability can be tailored in order to attend the desired application. The facilities available nowadays enable the use of these materials as large (bone screws) and small implants (sutures), membranes, porous structures and nanoscale materials for drug delivery (SONG et al., 2018).

2.1.1 Polymers in tissue engineering

Highly porous tridimensional scaffolds have been designed recently as potential alternatives in tissue engineering platforms. The combination of these porous materials and

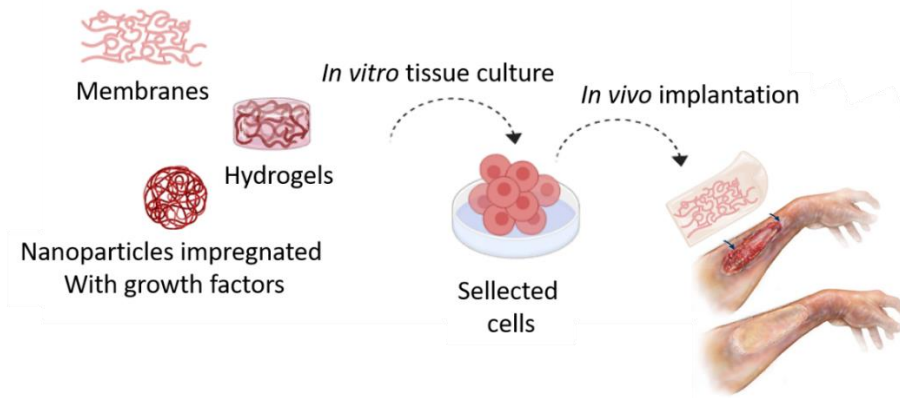
cells from the body is one of the cornerstones of tissue engineering. Biodegradable scaffolds act as a short-term strategy to help damaged systems to regenerate and after total site recovery, the material is degraded leaving behind a viable biologic system (KOHANE; LANGER, 2008). Thus, aspects as scaffold topography (shape, rugosity and pores connectivity) and surface chemistry (wettability, functional groups, surface charge and density) must be evaluated in order to create a good environment for cell proliferation, differentiation and excretion (ITO, 1999; O'BRIEN, 2011; IDASZEK et al., 2016).

Scaffolds properties can be tuned according to the desired site of implantation. Tough materials are required in bone applications while soft ones are more convenient in skin regeneration. To attend these requirements, mechanical properties can be tuned by crosslinking, for example, to form more dense networks to obtain rigid scaffolds. Cell attachment also plays an important role in tissue regeneration (KOHANE; LANGER, 2008). Hydrophobic materials reduce cell adhesion and usually surface modifications are employed to reduce material crystallinity. Furthermore, functional groups can be added in its structure to increase cell interaction.

Both natural and synthetic polymers are usually utilized as supports in tissue engineering. Marine-derived polysaccharides such as chitosan, alginate, fucoidan and carrageenan are the most popular amongst the natural ones (SEZER et al., 2007; MURAKAMI et al., 2010; VAKILI et al., 2017; HU et al., 2019). Alongside, many studies can be found making use of synthetic materials as polyesters, specially ϵ -PCL, polyethylene glycol (PEG), poly(lactic-co-glycolic acid) (PLGA) and many others (ABDAL-HAY et al., 2018; MADER et al., 2018).

These materials can be developed to be used as either hydrogels, nanoparticles, porous membranes and others. Basically, they act as a template to regenerate damaged tissues and are usually seeded with cells before implantation in the injured site (Figure 1).

Figure 1 - Different carriers for tissue engineering applications.



2.1.1.1 Use of electrospinning technique to obtain polymeric scaffolds

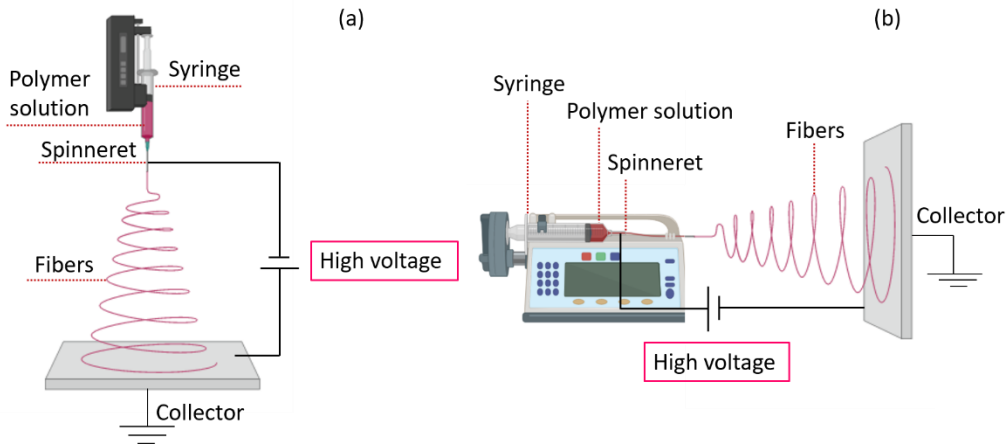
Numerous methodologies can be used to prepare porous tridimensional scaffolds such as 3D printing (SEITZ et al., 2005; BERGEMANN et al., 2016), solvent casting (TORABINEJAD et al., 2014), solvent casting/particulate leaching (LARRAÑAGA et al., 2014) and many others (PUPPI et al., 2010; RAVICHANDRAN et al., 2012; JANIK; MARZEC, 2015). Electrospinning technique stands out from the others due to its simplicity and the possibility of scaling up the process. In tandem, fibers from nanometers to micrometers with high surface area and tunable porosity are obtained and they are similar to the extracellular matrix components.

Electrospinning has drawn attention for the development of biomedical materials. The combination of fibers and drugs is an excellent alternative for applications like tissue engineering, drug release, wound dressing, protein immobilization and others (AGARWAL; WENDORFF; GREINER, 2008).

The basic concept of the technique consists in fiber production by the application of a strong electric field in a polymer solution. Thus, the strong mutual repulsive forces overcome weaker forces of surface tension in the charged polymer solution. Usually, electrospinning is conducted at room temperature in atmosphere conditions and the structure is basically composed of a syringe pump, a high voltage power supply, a spinneret (needle tip) and a metal collector (Figure 2). The polymer solution is injected into the tubing by the pump and the electrical voltage generated from the source causes a cone-shaped deformation of the drop of

polymer solution. Then, the solution is accelerated through the collector of opposite polarity while the solvent evaporates to form solid fibers (BHARDWAJ; KUNDU, 2010).

Figure 2 - Electrospinning apparatus in vertical (a) and horizontal (b) positions.

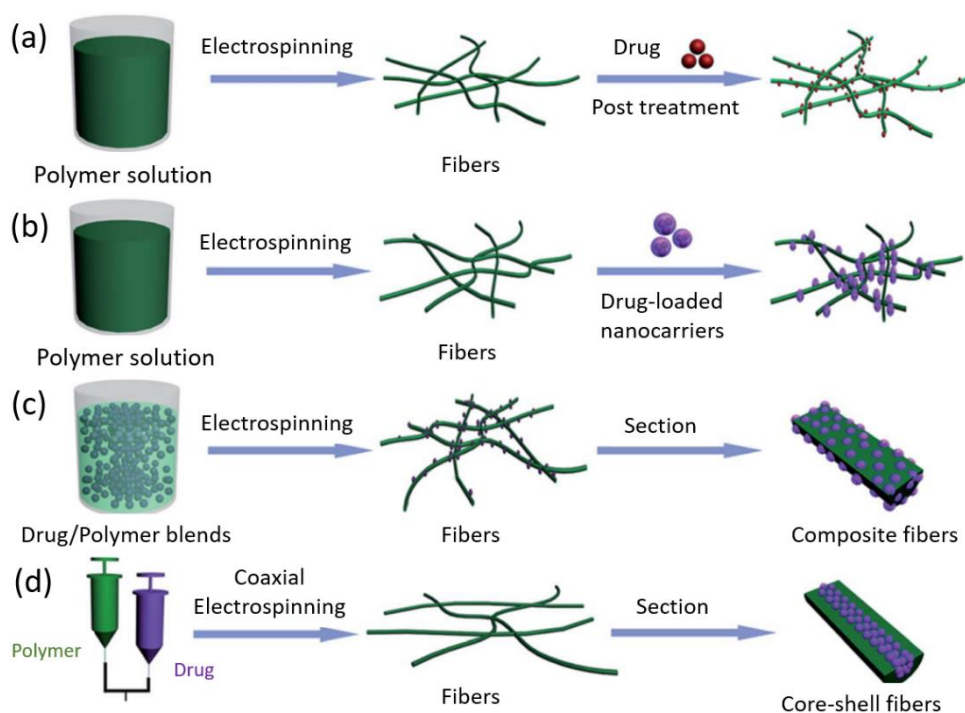


Certain parameters can highly affect the electrospinning process including polymer type and molecular weight, environmental (solution temperature, humidity and air velocity inside of the electrospinning chamber), solution (elasticity, viscosity, conductivity and surface tension) and governing (distance from tip to collector, electrical potential, flow rate, , type of collector and many others) variables (BRAGHIROLI; STEFFENS; PRANKE, 2014). A balance between these parameters can be a solution to obtain homogeneous and well-defined fibers. Although, sometimes electrospun membranes are composed of a mixture of fibers and beads. The occurrence of beads is usually related to the surface tension, electrostatic repulsion and viscoelastic force and can be avoided by the balance between these three parameters - that are affected mostly by polymer and solution properties (LI et al., 2014).

2.1.1.2 Fiber modification and crosslinking

Nanometric and micrometric fibers obtained via electrospinning are of great importance in tissue engineering materials. Apart of mimicking natural structures, fibers can be impregnated with distinct drugs to facilitate the regeneration of damaged tissues and many approaches can be developed to obtain these materials (Figure 3).

Figure 3 - Different methods to obtain drug-loaded fibers.



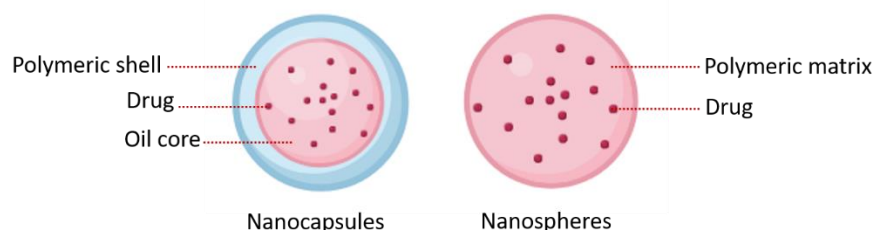
Source: Adapted from He et al. (2014).

Fibers surface modification allows the improvement in mechanical and degradation properties and a number of different methodologies have been used, such as plasma modification, wet chemical methods and surface graft polymerization. Crosslinking of electrospun fibers is an interesting approach to improve typically poor mechanical properties of these materials. In addition to improving fiber properties, crosslinked can result in sustained drug delivery from the matrix and different release profiles can be designed by varying the crosslinking degree. Usually, crosslinkers as glutaraldehyde and *N*-(3-dimethylaminopropyl)-*N*'-ethylcarbodiimide hydrochloride/*N*-hydroxysuccinimide (EDC/NHS) are used to crosslink natural fibers (collagen, elastin, gelatin, fibrinogen, silk fibroin, chitosan and cellulose). Meanwhile, fibers crosslinked with glutaraldehyde can be toxic and induce side effects, such as infection and, fibers treated with EDC/NHS are not stable in aqueous solution (HE; NIE; FENG, 2014). In section 2.6.3 a fast and versatile chemistry is described to crosslink fibers from unsaturated materials.

2.1.2 Polymers in drug delivery systems

Biodegradable polymeric nanoparticles (NPs) have been studied in the last few years as platforms in drug delivery systems (MURA et al., 2011; THAUVIN et al., 2018). In particular, the polymeric materials should be biocompatible and easily excreted from the body by biodegradation or bioerosion. Nanosystems are very interesting in sustained drug release once they increase the drug bioavailability in the organism and they can be shaped in different morphologies (Figure 4).

Figure 4 - Nanocapsules and nanospheres morphologies.

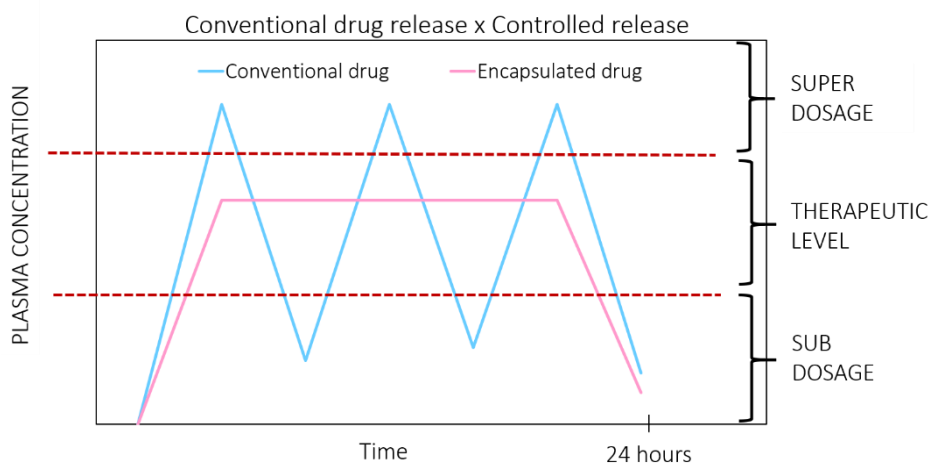


In nanospheres, the drug is adsorbed on the surface and/or incorporated within the polymeric matrix. Alternatively, nanocapsules can be produced and in this case the drug stays encapsulated in the core surrounded by a polymeric shell (core-shell structure) (ROMIO et al., 2009; TEBALDI; BELARDI; MONTORO, 2015; STEINMACHER et al., 2017; RONCO et al., 2018). Particles size and dispersity are very important once they are related to drug kinetics stability, cellular absorption, bioavailability and release. The use of these systems in sustained release has several advantages. One of the main ones includes the reduction of side effects, once the drug is maintained in a therapeutic level in the blood - without reaching toxic levels (super dosage in Figure 5). Besides, the number of doses is reduced once the release is modulated according to the characteristics of the system as polymer biodegradability and/or drug diffusion from the particle (DAS; DAS, 2003).

Aside of modulating drug release, nanoparticles surface can be modified to add functional molecules and/or markers. This way, drugs can be delivered to a specific target such as cancer cells or tissues. Once in contact with the organism, NPs are covered by plasma proteins composing what we know as “protein corona”. In the past few years, poly(ethylene glycol) PEG has been utilized to modify nanoparticles surface (PELAZ et al., 2015; VALÉRIO

et al., 2015; SCHÖTTLER et al., 2016). Studies showed that functionalized PEG nanoparticles have a longer retention time in blood circulation. Also, the PEG repulsion on NPs surface promotes a good colloidal stability and limits protein adsorption (SETTANNI et al., 2017a).

Figure 5 - Schematic representation of the action of conventional drugs and drugs encapsulated in polymer nanoparticles.



Source: Adapted from Das and Das (2003).

2.1.2.1 Use of miniemulsion polymerization technique to obtain polymer nanoparticles

Polymerization reactions conducted in miniemulsion are widely utilized to synthesize polymer nanoparticles from 50 to 500 nm using different mechanisms such as free-radical, ring-opening, step-growth and so on. Miniemulsion polymerization reactions have several advantages over other polymerization techniques once they are versatile and present droplet nucleation - where the droplets are the polymerization *locus* and consequently every droplet formed after sonication may become a particle after polymerization (LANDFESTER; RAMIREZ, 2003).

The miniemulsion preparation consist in a mixture of two immiscible liquids by the homogenization in equipment with high shear rate, such as sonifiers in laboratory scale and high-pressure homogenizers in large industrial scale. The sonifiers produce ultrasound waves and this movement causes the oscillation of the molecules from their initial position. Thus, the droplets size decreases with the sonication time until a certain point where they are maintained

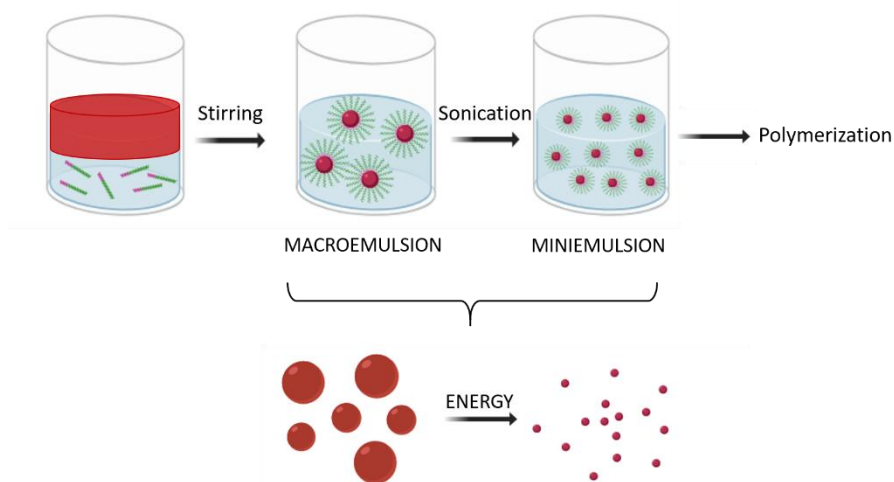
constant and, this behavior is dependent of the formulation, applied energy and the volume of the reactional medium (ASUA, 2002).

Direct miniemulsions (oil-in-water) are formed by the dispersion of an organic phase (containing hydrophobic monomer and co-stabilizer) in an aqueous phase (containing water, surfactant and initiator - this last one in case of radical polymerization) (ASUA, 2002).

First, both phases are mixed vigorously to form micrometric droplets. Then, the previous emulsion is miniemulsified in an equipment with high shear rate to form droplets with reduced diameters - in a nanometric range (Figure 6). Overall, in miniemulsion systems the droplets are the polymerization *locus* and for this, the system requires droplets with high surface area to allow the polymerization to occur inside of the surfactant-stabilized nanodroplets.

Unlike microemulsion systems, miniemulsions are not stable thermodynamically and usually they are stabilized against coalescence and diffusional degradation with surfactants and co-stabilizers (usually water-insoluble compounds of low molecular weight), respectively (ASUA, 2002; LANDFESTER; RAMÍREZ, 2003).

Figure 6 - Schematic representation of miniemulsion technique.



Polyester nanoparticles are of great interest in drug delivery systems in which some authors described the use of large cyclic esters (macrolactones) to obtain biodegradable nanocarriers by miniemulsion polymerization. Macrolactones such as ω -pentadecalactone (ω -PDL) and hexadecanolide (HDL) were used before to obtain particles with approximately 534 nm via enzymatic ring-opening polymerization (MÅLBERG; FINNE-WISTRAND; ALBERTSSON, 2010). Later, Pascual and co-workers reported the organic acid catalyzed

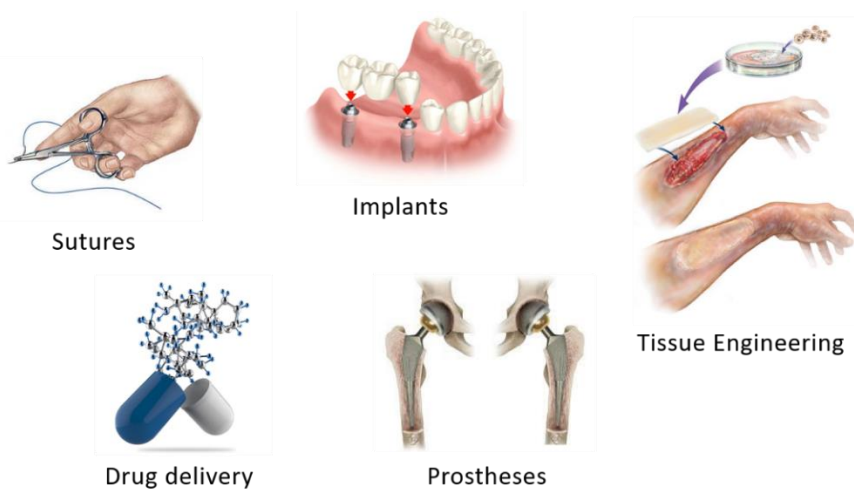
polymerization of ω -PDL and globalide in miniemulsion and only oligoesters with molecular weight of $2,000 \text{ g mol}^{-1}$ were obtained (PASCUAL; LEIZA; MECERREYES, 2013a).

2.2 POLYESTERS

Among the available biomacromolecules that can be found in nature, four of them stand out from the others due to their viability. They are proteins (peptides), nucleic acids (DNA and RNA), polysaccharides and polyesters (KOBAYASHI, 2015). In the past few years, the search for sustainable, environmentally friendly feedstocks and technologies has instigated the use of biodegradable materials from natural sources to replace the popular commodities from fossil oils. Thus, polyesters from non-fossil sources are a good alternative once they can be degraded when disposed in the environment (MILETIĆ; LOOS; GROSS, 2010; KOBAYASHI, 2015).

Polyesters are very useful as thermoplastics and eco-friendly materials due to their properties as biodegradability, biocompatibility, good mechanical properties and non-toxicity. Recently, they have been utilized as biomaterials for pharmaceutical and biomedical applications, such as sutures, screws, implants, artificial skin and as nanocarriers for controlled drug release (Figure 7) (ALBERTSSON, A-C.; VARMA, I. K.; SRIVASTAVA, 2009; KOBAYASHI, 2015).

Figure 7 - Polyesters application in biomedicine.



The addition of different functional groups in polyesters chains can alter their physical and biodegradability properties. Consequently, polymer characteristics as molecular weight, flexibility, crystallinity and orientation are also affected. In this case, functionalization processes allow the modification of polymer properties according to the desired application (ALBERTSSON; VARMA, 2003; COULEMBIER et al., 2006).

Poly lactides and ϵ -PCL are among the most commonly used polyesters for biomedical areas such as controlled drug release and contraceptives. Nowadays, aliphatic polyesters are produced in large scale for use as package materials and plastic commodities. On the other hand, a reduced number of high added value polyesters have been produced in pharmaceutical and biomedical fields. Aliphatic polyester synthesis can be carried out via different routes. Three different mechanisms can be used, such as ring-opening polymerization (ROP) of cyclic ketene acetals, step-growth polymerization of lactones and ROP of lactones.

2.3 POLYESTER SYNTHESIS

2.3.1 Polyester synthesis via ROP of lactones

ROP of lactones and cyclic monomers is an effective and simple way to prepare aliphatic polyesters when compared with methods as polycondensation. High molecular weight polymers with narrow dispersions and unique properties for biomedical applications can be obtained via this route. Several factors can affect the ROP of lactones such as monomer ring size, substituent position, number and nature of the ring substituents and reaction parameters (initiator concentration, catalyst, solvent, monomer concentration and temperature) (COULEMBIER; DUBOIS, 2009).

Distinct lactones can be used to synthesize aliphatic polyesters with different final properties, including chain size and mechanical properties. Over the past years, many groups reported ROP of lactones of small and medium chain whilst polyester synthesis making use of monomers with more constituents in the ring have been less explored. These materials with more units in the ring are popularly known as macrolactones and they have 12 or more atoms of carbon in their structure.

The angle and bond deformations are more pronounced in three and four-membered lactones, resulting in a higher ring strain. Conversely, cyclic monomers with more carbons in

the structure (macrolactones) are less strained leading to an increase in the entropy of the reaction (DUBOIS; COULEMBIER; RAQUEZ, 2009). Small cyclic lactones (4 to 7 members), that have high ring tension, are easily polymerized by organometallic catalysts. Alongside, when the same class of catalyst is used to polymerize macrolactones (12 or more members) slower kinetics are observed and polymers with low molecular weights are usually obtained. In this case, enzymatic ring-opening polymerization is more indicated (DUDA et al., 2002).

The difference in the reactivity is related to the size of the lactone/macrolactone. The ring strain is partially released in the transition state of the reaction in lactones (small units) during the chain growth and the polymerization is faster in chemical polymerizations. On the other hand, the rate limiting step of enzymatic ROP is the formation of the complex enzyme-monomer which is controlled by the hydrophobicity of the monomer, that is higher in macrolactones than in lactones (DUDA et al., 2002).

2.3.2 Macrolactones in ROP

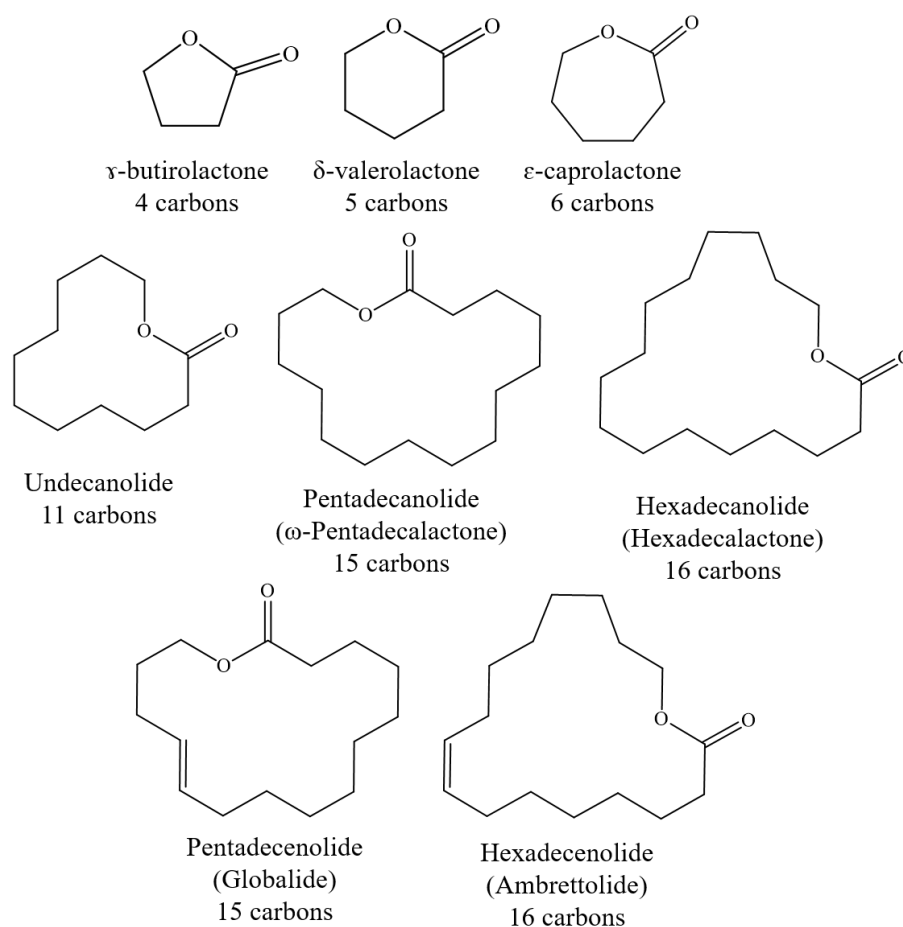
Macrolactones of 14-16 carbons are known to have musk-like odor. Pentadecanolide, also known as ω -pentadecalactone (ω -PDL), is one of the most used macrocyclic material as fragrance. Specifications as number of carbons and double bond position (in unsaturated macrolactones) are crucial to dictate their odor. The unsaturated macrolactone hexadecen-7-olide (ambrettolide), for example, has floral musk odor but its isomers do not possess the odor required for pharmaceutical applications being of interest just in academia (MUNRO; STANLEY, 1998).

In general, macrolactones are used to improve the odor of fragrances, or separately to contribute to the final aroma of detergents, disinfectants, air purifiers, shampoos, conditioners, skin lotions, deodorants and many others. In addition, some of them can be extracted from natural sources being an alternative to replace fossil monomers. ω -PDL, for example, can be extracted from the root of *Angelica archangelica* plant and its use as additive is approved by Food and Drug Administration. Besides, ω -PDL has natural occurrence in humans and it is one of the main pheromones produced by the male sudoriferous gland. Figure 8 shows the structure and the nomenclature of different lactones and macrolactones found in literature.

Aside of having unique odoriferous properties, macrocyclic musk's represent a small fraction in the market, from 3 to 4%, and in their majority are used in perfumery. Due to their intense odor, a minimal concentration is enough in the formulations and these compounds are considered eco-friendly once they degrade fast in the environment (HOMEM et al., 2015).

ROP of unsaturated macrolactones have been investigated in the last years and are a promising alternative to obtain polyesters with different functionalities. The double bond in the polymer backbone facilitates the addition of different functional groups via different chemical routes. Meulen and co-workers reported for the first time the use of the unsaturated macrolactones pentadecenolide and hexadecenolide, also known as globalide and ambrettolide. The authors obtained high molecular weight polymers via enzymatic ring-opening polymerization. Additionally, the polymers did not degrade over a period of 100 and 400 days due to the high hydrophobicity of these materials (MEULEN et al., 2008).

Figure 8 - Structure of lactones and macrolactones with different ring size.



2.3.3 Polyester synthesis via enzymatic ROP of lactones and macrolactones

Organometallic catalysts are widely used in polymer chemistry. Many drawbacks are associated to their use, such as metal toxicity for the environment and metal residues in the final material, what restricts polymer application in the biomedical field. Likewise, these materials are highly sensitive to moisture and impurities, and drastic reaction conditions are usually employed to obtain high molecular weight polymers (MONTANIER et al., 2017).

In face of this, enzymes are drawing attention in polymer synthesis due to their versatility. Aspects as high selectivity, high catalytic activity and possibility to react in mild reaction conditions (more favorable temperature, pressure and pH conditions when compared with organometallic catalysts) turn its use very attractive. In addition, no side products are formed during the reaction and no toxic traces can be found in the final material. Aside of having excellent properties, when enzymes are immobilized on solid supports, they are easily recovered after the reaction and are usually used in new reaction cycles without losing the catalytic activity.

All these advantages make the use of enzymes in polyesters synthesis an environmentally friendly process when compared to polymerizations using chemical catalysts. Besides, enzymes are stable in organic solvents that are commonly used for ROP, such as toluene, heptane, dichloromethane and chloroform. Furthermore, it is possible to use less toxic and harmful solvents such as water, supercritical carbon dioxide and ionic liquids (DUBOIS; COULEMBIER; RAQUEZ, 2009; LOOS, 2010; MILETIĆ; LOOS; GROSS, 2010; KOBAYASHI, 2015).

Final polymer properties as molecular weight and yields are strongly related to the macrolactone ring size, type of solvent, class of enzyme, water concentration in the medium and polymerization temperature (ALBERTSSON, A-C.; VARMA, I. K.; SRIVASTAVA, 2009; ZHANG et al., 2014). Solution polymerizations are widely used to obtain high molecular weight aliphatic polyesters from lactones and macrolactones.

Lactones with small rings were the first ones to be used in polyester synthesis via enzymatic ring-opening polymerization (e-ROP). Knani and co-workers studied ϵ -CL polymerization via e-ROP in solution using porcine pancreatic lipase as catalyst. The authors evaluated the influence of two different nucleophiles to initiate the reaction (methanol and 6-

hydroxyhexanoate (Me-6-HHX)) and polymers with molecular weights from 300 to 2,000 g mol⁻¹ were produced in long reaction times (624 h) at 45 °C (KNANI; GUTMAN; KOHN, 1993). Uyama and co-workers evaluated the copolymerization of ϵ -CL and δ -valerolactone (δ -VL) in bulk using *Pseudomonas fluorescens* as biocatalyst. The obtained molecular weights stayed in a range of 7,000 g mol⁻¹ (85% yield) and 2,100 g mol⁻¹ (91% yield) after 10 days of reaction at 60 °C. After this study, the authors concluded that the enzyme in the medium induced lactone ring-opening and the water molecules on the enzyme surface were essential to initiate the polymerization (UYAMA; TAKEYA; KOBAYASHI, 1993).

Regarding macrolactones use in e-ROP, structures composed of 12 (dodecanolide) and 15 (pentadecanolide, ω -PDL) members were the first ones to be used in this type of system. Interestingly, some studies showed higher molecular weight polymers making use of macrolactones rather than lactones in e-ROP systems (UYAMA et al., 1995; UYAMA; TAKEYA; KOBAYASHI, 1995). Kobayashi group obtained ω -PPDL, poly(dodecanolide) (PUDL) and ϵ -PCL with molecular weights of 16,200; 25,200 and 1,800 g mol⁻¹, respectively. The reactions were performed in bulk at 60 °C for 2 h using *Candida cylindracea* lipase (UYAMA et al., 1996).

Duda and co-workers used lactones and macrolactones with different ring sizes to evaluate its influence in e-ROP. For this, monomers containing from 6 to 17 members were used and the polymerizations were performed in bulk using zinc 2-ethylhexanoate/butyl alcohol at 100 °C. Then, the authors compared the obtained results with previous reactions conducted under the same conditions but in a lipase-catalyzed system. The authors observed significant differences in monomers reactivity according to ring size. The ring-strain, that is higher in small lactones, is partially released in the transition state of the elementary reaction of polyester chain growth. In this case, the propagation is faster in monomers with high ring-strain for systems where chemical catalysts are used. Conversely, the rate determining step in e-ROP involves the formation of the enzyme-monomer complex. This step is promoted by monomer hydrophobicity which is higher in larger lactone rings (macrolactones) (DUDA et al., 2002).

In tandem with other studies, these investigations in lactone/macrolactone e-ROP encouraged the use of these cyclic monomers in polymer chemistry. The use of unsaturated macrolactones (as globalide and ambrettolide) is also very promising in biomedical areas, once the unsaturation allows the addition of different functional groups in the polymer chain and materials with different architectures can be designed.

2.4 ENZYMES IN POLYESTER SYNTHESIS

Enzymes have a broad spectrum of potential applications in pharmaceutical, biomedical and food industry. Recently, lipases have been utilized in polyester synthesis via polycondensation or enzymatic ring-opening polymerization without the need for a co-catalyst (HEISE; DUXBURY; PALMANS, 2009; MILETIĆ; LOOS; GROSS, 2010). Enzymatic catalysis is a good approach to produce useful materials for use in different areas, including natural and synthetic polymers production to form well-defined materials with superior characteristics to those obtained by conventional chemical catalysis (HEISE; DUXBURY; PALMANS, 2009; KADOKAWA; KOBAYASHI, 2010; MILETIĆ; LOOS; GROSS, 2010).

Lipases are soluble in water and catalyze the hydrolysis of long chain triglycerides to diacylglycerides, monoacylglycerides, glycerol and fatty acids. This reaction is reversible, and they can catalyze esters synthesis and transesterification reactions in systems containing low water concentrations, making polyester synthesis feasible. In contrast to other classes, lipases are very selective and are easily found in plants, animals, microorganisms, bacteria, fungi and yeasts (MILETIĆ; NASTASOVIĆ; LOOS, 2012).

Lipases of *Candida antarctica*, *Candida rugosa*, *Pseudomonas fluorescens*, *Pseudomonas cepacia* and porcine pancreas have been used in polyester synthesis via e-ROP. Among them, *Candida antarctica* B (CALB) is the most popular for poly(macrolactones) synthesis and this enzyme is usually found in immobilized preparations (YANG et al., 2011). The most famous CALB immobilized preparation is commercialized by Novozymes and is also known as Novozym 435 (NVZ 435). NVZ 435 is immobilized in an acrylic porous resin of poly(methyl methacrylate-co-butyl-methacrylate) (MILETIĆ; LOOS; GROSS, 2010; SHODA et al., 2016).

2.4.1 Enzymatic ring-opening mechanism

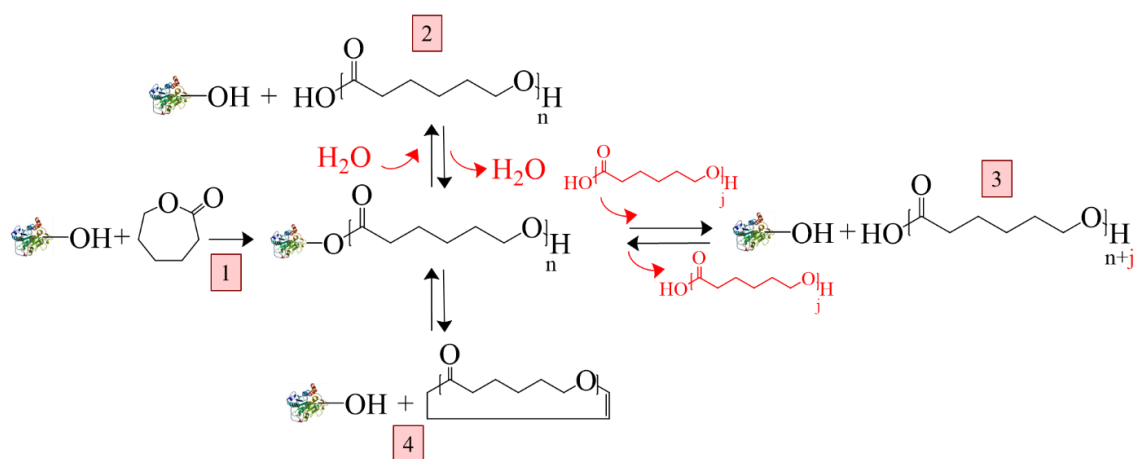
The main role of the initiator (nucleophile) in e-ROP is the ring-opening and the lipase active site regeneration. Different molecules can play the initiator role in e-ROP as water, alcohol, amines or thiols. Characteristics as molecular weight control and the functionalization of terminal chain can be easily tailored by the addition of different classes of initiators in

substitution to conventional water (KNANI; GUTMAN; KOHN, 1993; ZHONG; DIJKSTRA; FEIJEN, 2000). Thus, functionalized polyesters with unique properties can be designed.

Reaction kinetics and final polymer molecular weight in e-ROP are dictated by water concentration in the system. Basically, the water located on the enzyme surface initiates the polymerization. Thus, the ring-opening step is accelerated at high water contents leading to fast formation of a high number of polymer chains and consequently products of low molecular weight. However, a minimum water content is required to maintain lipase conformational flexibility which is primordial to the catalytic activity of the protein (GROSS; KUMAR; KALRA, 2001).

Johnson and co-workers built a kinetic model to describe e-ROP of ϵ -CL using NVZ 435 as biocatalyst in order to observe the molecular weight distribution over reaction time (JOHNSON; KUNDU; BEERS, 2011). Although it was developed for this specific system, the model is applicable to other e-ROP systems as lactones, macrolactones, lactams and cyclic carbonates. The proposed kinetic model pathway can be seen in Figure 9 and Johnson, Kundu and Beers developed the scheme based on the reaction pathways described by Mei, Kumar and Gross in 2002 (MEI; KUMAR; GROSS, 2002).

Figure 9 - Reaction mechanism in e-ROP of ϵ -caprolactone in the model proposed by Johnson.



Source: Adapted from Johnson et al. (2011).

According to the proposed model, three different chains can be formed during e-ROP. The first one corresponds to an 'enzyme-activated polymer chain' and in this case ϵ -PCL chain is connected to the lipase active site by an ester linkage. The second possible structure

corresponds to ϵ -PCL chain in solution containing both hydroxyl and carboxylic acid terminal groups. The third possibility is the formation of cyclic chains from intermolecular backbiting of an enzyme-activated polymer chain.

The first step in the model proposed by Johnson involves the enzyme-activated polymer chain formation. This step is irreversible once the formed chain is more stable thermodynamically than the cyclic ring. The second step has two kinetic pathways. When a water molecule is consumed in the 'enzyme-activated polymer chain', the ester bond between the polymer chain and the lipase is broken and consequently the active site is regenerated and a polymer chain in solution is formed. The reverse pathway leads to 'polymer-active site' formation by the ester linkage between active site and the terminal carboxylic acid from polymer chain, generating a water molecule.

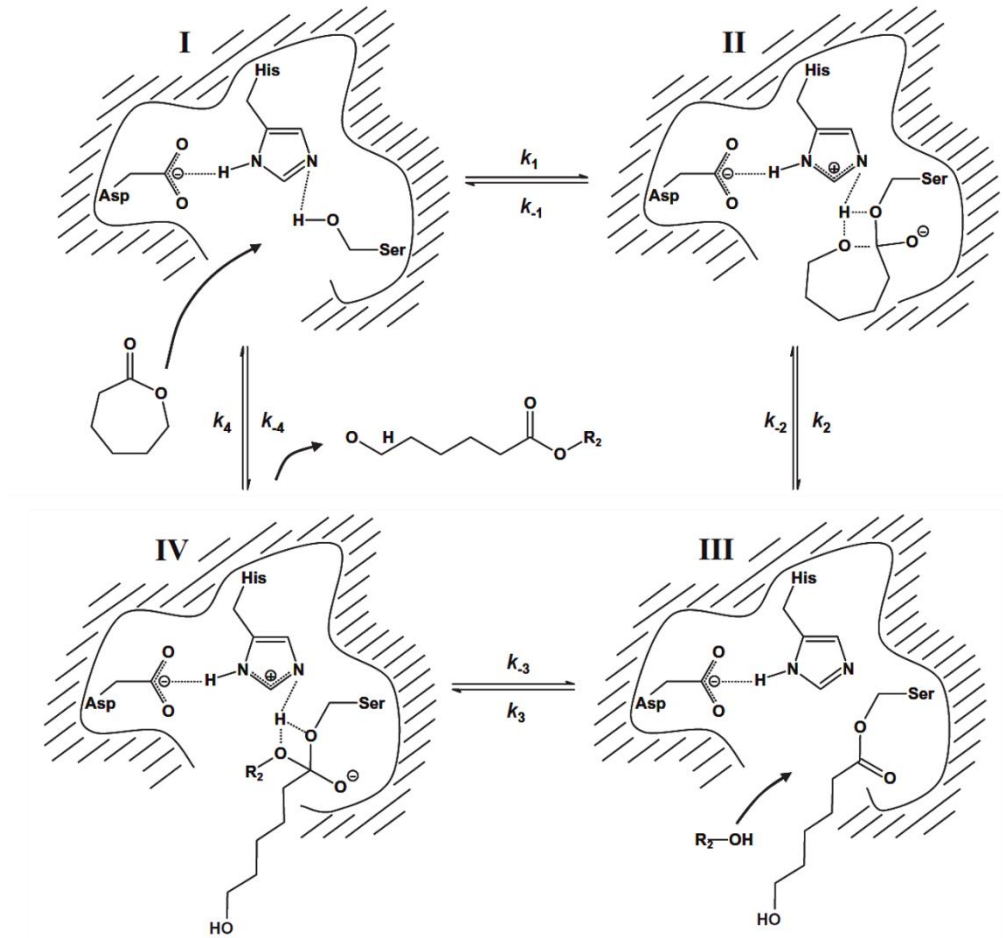
Enzymatic polycondensation reactions take place when an 'enzyme-activated polymer chain' reacts with the hydroxyl group from a linear chain in solution (step 3). Thus, the active site is regenerated and polymers with high molecular weights are formed. The reverse reaction consists in polymer chain (i+j) hydrolysis. The active site breaks the ester bond in a determined position of the polymer chain resulting in a linear polymer chain in solution (low molecular weight) and an 'enzyme-activated polymer chain'. The fourth and last step corresponds to the equilibrium between 'enzyme-activated polymer chains' and cyclic chains in solution. Cyclic formation occurs when the polymer chain reacts on itself at the active site generating an ester bond and the active site. The reverse is the ring-opening of the cyclic ring.

The scheme presented in Figure 10 represents the same mechanism proposed by Johnson and co-workers, but it shows the reactions occurring at the enzyme active site. The lipase active site is composed of serine, histidine and aspartate, which are electronically stable. The first step involved in the mechanism is the electrophilic attack of the ester group (from the cyclic lactone/macrolactone) in the primary alcohol of serin (in the lipase active site). The original alkoxy group is released from the lipase intermediate species (step II) generating the enzyme-activated monomer (EAM - step III). Subsequently, a nucleophile (e.g., water, alcohol or amine) can attack the activated monomer (EAM) by new intermediate species (stage IV) and then the final product is released, and the active site regenerated.

During the propagation, the complex EAM is attacked by the terminal hydroxyl group from a polymer chain to produce the polymeric chains and the steps of initiation and

propagation involve lipase deacetylation. As previously mentioned, the rate limiting step is the EAM formation and the transesterification reactions need to be considered in the process once lipase does not discriminate between the ester groups in the monomer and in the polymeric chain (HEISE; DUXBURY; PALMANS, 2009; YANG et al., 2011).

Figure 10 - Schematic representation of the mechanism involved between the lipase active site and ϵ -CL during e-ROP.



Source: Heise et al. (2009).

2.5 POLYESTER DEGRADATION

Biodegradable polymers are a good alternative in substitution to plastic materials with slow degradation or that are non-biodegradable such as polyethylene, polypropylene and polystyrene. Usually, biodegradable polymers can be degraded by living organisms via

hydrolysis when they are disposed in the environment (KOBAYASHI; UYAMA; TAKAMOTO, 2000).

The ester bonds in poly(lactones) and poly(macrolactones) are easy to be formed and to be degraded. Over the past years, some studies have shown the possibility to obtain high molecular weight polyesters via ϵ -ROP and its subsequent recycling using the same biocatalyst from the polymerization process (KOBAYASHI; UYAMA; TAKAMOTO, 2000; MATSUMURA; EBATA; TOSHIMA, 2000; SOEDA; TOSHIMA; MATSUMURA, 2005).

Kobayashi group studied ϵ -PCL (60,000 g mol⁻¹ molecular weight) degradation using lipase from *Candida antarctica* in toluene at 60 °C. After ϵ -PCL incubation in the enzymatic solution for 24 h, they observed the disappearance of the peak corresponding to polymer by GPC and only oligomeric compounds and monomer were detected. Interestingly, the authors used the monomer and lipase from degradation for a new synthesis of ϵ -PCL. Hence, the developed work opened up a new concept of an eco-friendly process enabling the starting materials recovery for their use in a new process (KOBAYASHI; UYAMA; TAKAMOTO, 2000).

Degradation studies of polyesters are essential to understand the chemical behavior of these materials for future use in biomedical applications. Biodegradable materials are of great interest for tissue engineering, sutures, drug release and several others. Poly(macrolactones) degradation have been studied in the last years in order to evaluate their use for this type of applications. Heise group studied ω -PDL, hexadecalactone (HDL), ambrettolide (Am) and globalide (Gl) macrolactones polymerization catalyzed by Novozym 435 lipase. The polymers did not show significant mass loss after incubation in enzymatic solution and it can be related to the high crystallinity of these materials which is around 60-70%.

Many strategies have been described to modify polymer structures in order to increase their biodegradability and cell adhesion allowing their use as biodegradable materials in biomedical areas (WEBB; HLADY; TRESKO, 1998).

2.6 POST-POLYMERIZATION FUNCTIONALIZATION OF POLYESTERS

Poly(macrolactones) modification can be conducted before and after polymerization by different techniques. Among the available techniques, the use of initiators containing

functional groups during the polymerization is a straightforward strategy to form polymers with functionalized terminations. Besides, different groups can be added in the polymer chain by copolymerization of different monomers (ZHANG et al., 2014).

Polymer modification by post-polymerization allows the preparation of functional polymers which could not be obtained by direct polymerization of the respective monomers. After the modification process, the physical and chemical properties of the polymers are usually modified like viscosity, solubility, adhesion, crystallinity, hydrophobicity and others. Moreover, more complex structures can be obtained.

Unsaturated polymers, as poly(globalide) (PGI), can undergo click reactions and different functional groups can be inserted in polymer unsaturation. In the past 11 years, different groups explored post-polymerization modification of PGI via thiol-ene click reactions. With the main goal of reducing PGI hydrophobicity, the studies reported the addition of hydroxyl, amide and poly(ethylene glycol) groups by thiol-ene reactions in PGI chain (ATES; THORNTON; HEISE, 2011; ATES; HEISE, 2014a; SAVIN et al., 2018; GUINDANI et al., 2019).

2.6.1 Click reactions

The concept of click chemistry was described by Barry Sharpless group in 2001 and several criteria were pointed to classify a system as “click”. According to them, the reactions must be “...modular, wide in scope, give very high yields, generate only inoffensive products that can be removed by nonchromatographic methods, and be stereospecific (but not necessarily enantioselective). The required process characteristics include simple reaction conditions (ideally, the process should be insensitive to oxygen and water), readily available starting material and reagents, the use of no solvent or a solvent that is benign (such as water) or easily removed, and simple product isolation. Purification, if required, must be by nonchromatographic methods, such as crystallization or distillation, and the product must be stable under physiological conditions” (KOLB; FINN; SHARPLESS, 2001).

The most common examples of click reactions comprehend cycloaddition of unsaturated species, nucleophilic substitution chemistry, carbonyl chemistry of the “non-aldol” type and additions to carbon-carbon multiple double bonds.

2.6.2 Thiol-ene click reactions

Thiol addition reactions (R-SH) to reactive carbon-carbon double bonds were described for the first time in literature in 1905, when the German chemist Theodor Posner showed that thiols and enes could react spontaneously or in acid presence (POSNER, 1905). Nevertheless, the investigation of the addition mechanism was only reported in 1938 by Kharasch. The first work to examine in an elucidative way the conjugation of thiols in olefins was reported in 1970 when photopolymerizable systems were studied (GRIESBAUM, 1970). Since then, thiol-ene chemistry has gained attention in organic and polymeric synthesis.

In its first applications, thiols were used in the fabrication of simple materials, such as films, protective coatings, electronic materials, among others (HOYLE; BOWMAN, 2010; CLAUDINO et al., 2012). The restriction in its applications was related to the fast change in the color of the coatings (from white/transparent to yellow) and this was being caused by the residual initiator in the material as well by weathering. However, these problems were related to the use of benzophenone (photo-initiator) and acrylate (low cost monomers) which implicated in the depreciation of thiol-ene chemistry at that time (HOYLE; LEE; ROPER, 2004; CLAUDINO et al., 2012). In the last years, thiol-ene reactions have been applied in the synthesis of high added value materials for biomedical applications.

Thiol-ene reactions are classified as “click” once they fit in the conditions described by Sharpless group. Among them, thiol-ene reactions present high yields and fast reaction kinetics, can be conducted in bulk or solution (using non-toxic solvents), are insensible to air, pure products are obtained, and a wide range of thiols is currently available. Besides, they can be conducted using thermal or photo-initiators (HOYLE; BOWMAN, 2010; KADE; BURKE; HAWKER, 2010).

The possibility of conducting these reactions in air makes this system very attractive. In a conventional polymerization of methacrylate's, for example, when oxygen is added to a radical of a growing chain this chain will terminate immediately by the alkyl peroxy radical formation, that does not have reactivity enough to add a new monomer chain. This problem does not happen in thiol-ene systems, since the peroxy radical abstracts a hydrogen atom from thiol generating a new thiyl radical, which can propagate the reaction (CLAUDINO, 2013).

Besides, the hydrogen atom from thiol is easily abstracted due to the weak covalent bond between sulfur-hydrogen (S-H). The facility to cleave S-H bond is not dependent of the radical group attached to the sulfur atom ($R = \text{Me, Et, Pr, and many others}$). Likewise, the cleavage can be induced via direct or indirect photolysis/thermolysis and subsequently initiator dissociation. The resulting thiyl radical (RS') can be added to a wide range of unsaturated compounds (rich or poor electron C=C bonds) to form new carbon C-C linkages. The thiyl addition to the double bond is an exothermic reaction and it forms a strong σ C-C bond (370 kJ/mol) that is stronger than the dissociation energy of π C=C bond (235 kJ/mol) (CLAUDINO, 2013).

Several factors dictate the success of thiol addition in unsaturated compounds (vinyl ethers, allyl ethers, vinyl acetates, methacrylates, and hydrocarbon alkenes). The type of the double bond (internal, terminal, conjugated, non-conjugated and substituted) has a strong influence. Particularly, in cyclic enes aspects as steric effects, stereoelectronics effects, ring-strain and the possibility of side reactions affect the reactivity. Roper and co-workers evaluated the structure of different alkenes in thiol-ene photopolymerizations using ethyl-3-mercaptopropionate as thiol. In general, the authors observed that terminal double bonds react faster than internal ones and in the last case lower conversions were observed (ROPER et al., 2004).

The mechanism of thiol-ene reactions is the radical step-growth polymerization where the thiyl addition to the double bond is followed by chain transfer to thiol. To achieve high conversions, a molar proportion of thiol and ene should be used. When the same stoichiometry is used, linear polymers are obtained and in order to obtain crosslinked materials, at least one of the reactants should present a functionality greater than two (e.g., dithiol or trithiol) (ROPER et al., 2004).

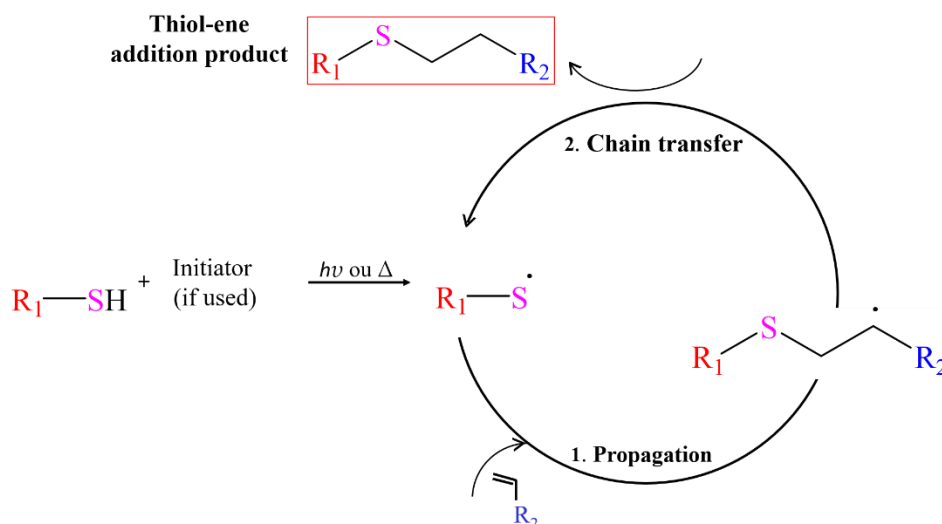
2.6.2.1 Thiol-ene polymerization mechanism

Thiol-ene polymerization follows the same mechanism as chain-growth polymerizations including initiation, propagation and termination steps. The initiation corresponds to thiyl radical formation RS' by the cleavage of the initiator/photo-initiator from thiol groups (R-SH). The propagation involves thiyl addition to C=C bond originating an intermediate β -carbon radical and is followed by chain transfer to a second molecule of thiol to

result in the product of thiol-ene addition. Aside of giving the product, a new thiyl radical is formed (MACHADO; SAYER; ARAUJO, 2017) (Figure 11).

The initiator keeps generating thiyl radicals allowing the reaction propagation as in a cycle until the depletion of thiol-ene species. Termination reactions involve the radical-radical coupling by the recombination of the radicals (thiyl or β -carbon). However, termination reactions are not so frequent when compared with propagation and chain transfer (LOWE, 2010; CLAUDINO, 2013). Thiol-ene reactions follow first order kinetics and parameters as propagation and chain transfer constants are the limiting steps and they control the polymerization (HOYLE; LEE; ROPER, 2004).

Figure 11 - Mechanism of thiol-ene addition via free radicals.



Source: Adapted from Claudino (2013).

2.6.3 Triazolinedione (TAD) in click reactions

Triazolinediones (TADs) are known to be the most reactive enophiles and dienophiles in organic chemistry. The first reports on TADs synthesis date from 1894 and 1912, when Thiele and Stolle obtained 4-substituted 1,2,4-triazoline-3,5-dione (PTAD) by 4-phenylurazole oxidation. In both cases, only low yield products were produced. Fifty years later, Cookson proposed the synthesis of the same compound by oxidation of 4-phenylurazole with t-butyl hypochlorite in dry acetone to obtain a high yield product (80%) (COOKSON; GILANI;

STEVENS, 1962). Besides, the authors showed Diels-Alder reaction from the synthesized TAD (COOKSON; GILANI; STEVENS, 1962, 1967). Cookson study is considered one of the cornerstones of TAD synthesis and since his research was published these compounds have been applied in many systems.

In 1979, Butler and Williams showed the modification of diene polymers and copolymers using PTAD and yields greater than 90% were reached at room temperature. The authors also observed the relation between the system reactivity and the group attached to the TAD molecule, once Phenyl-TAD (PhTAD) reacted 50% faster than Methyl-TAD (MeTAD) under the studied conditions (BUTLER, 1980). Mallakpour and co-workers showed the reaction of N-methylpyrrole with 4-substituted-1,2,4-triazoline-3,5-diones (4R-TADs) with MeTAD or PhTAD and the reactions were very fast at room temperature and without any catalyst (MALLAKPOUR; BUTLER, 1987).

Despite the improvement in TADs synthesis to obtain high-standard products and high yields, its use in click/modern polymer chemistry only started being explored in the last decade. Besides all advantages, the low availability of commercial TAD reagents is one of the limitations of the use of this technique. For this, many strategies have been described to obtain urazoles from different starting materials and their oxidation to obtain high pure TADs (DE BRUYCKER et al., 2016). Also, some TADs can be stored for months after their synthesis but in some cases more attention should be given once they can easily decompose. In this case, they should be used right after preparation.

2.6.3.1 TAD synthesis

Commonly, TADs are synthesized from their respective urazoles. The modern urazole synthesis is usually performed in two steps where the intermediate corresponds to a semicarbazide, such as **a** in Figure 12. In this case, they can be obtained from different starting materials, such as isocyanates, amines or anilines (DE BRUYCKER et al., 2016).

Semicarbazides can be synthesized by mixing isocyanates with ethyl carbazate and many protocols have been published in literature. Little and co-workers described novel 4-substituted TAD (urazoles) from isocyanates, amines, anilines and carboxylic acids. When the semicarbazide synthesis was performed from isocyanate (**1** in Figure 12) and ethyl carbazate (**2** in Figure 12), high yields were found after purification (above 90%). Then, the urazole (product

b in Figure 12) was formed upon semicarbazide cyclization under strong basic conditions (LITTLE et al., 2002).

Urazoles are usually oxidized to the respective triazolinedione (TAD) (Figure 13). Many available protocols relate urazole oxidation to convert its moieties into bright colored azo compounds and the change in color is an easy way to identify TAD formation (ZOLFIGOL et al., 2000, 2001; HAJIPOUR; MALLAKPOUR; ADIBI, 2001; ZOLFIGOL; GHAEMI; NIKNAM, 2008). This step is of great importance in the process and the main drawback is related to the high sensitivity of TADs to oxidizers/reaction medium. Thus, the choice of the oxidizer is primordial to obtain pure TAD compounds and avoid side products formation, that can destroy TAD or make its isolation unfeasible (ZOLFIGOL et al., 2000, 2001; HAJIPOUR; MALLAKPOUR; ADIBI, 2001; ZOLFIGOL; GHAEMI; NIKNAM, 2008).

Figure 12 - Urazole synthesis from isocyanates.

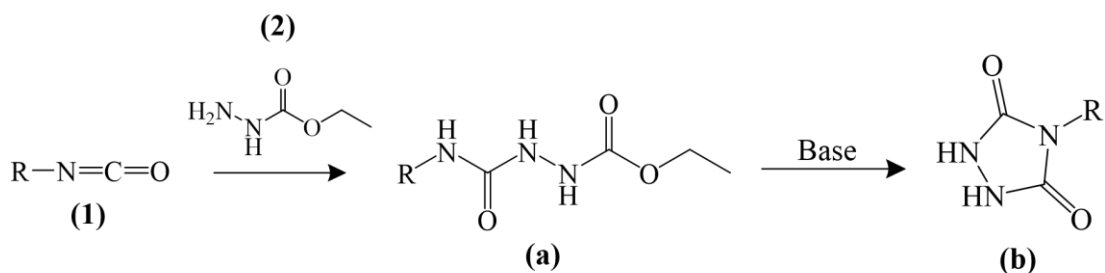
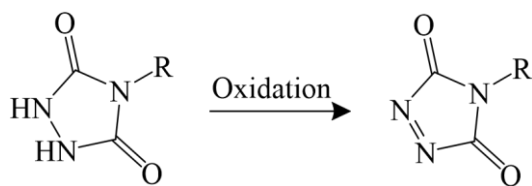


Figure 13 - TAD synthesis via urazole oxidation.



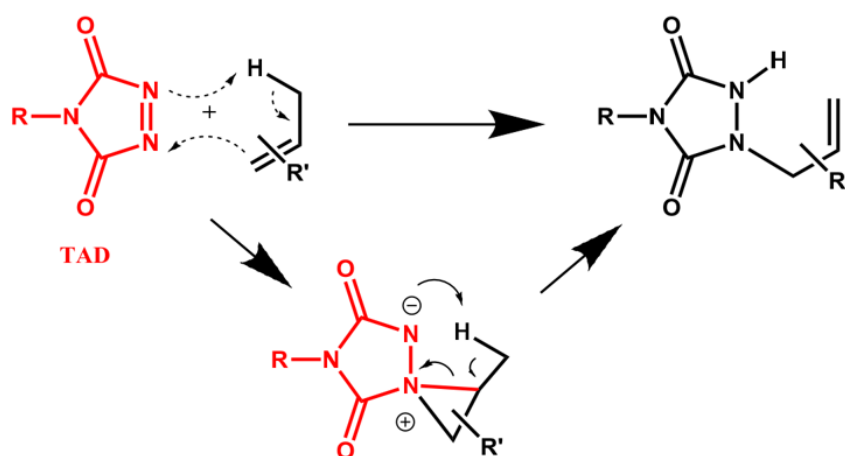
The use of silica-supported nitric acid in solvent to oxidize urazoles is a promising alternative and the silica can be filtrated after the reaction. Water traces in the oxidation step can decompose TAD, especially if the water gets concentrated after solvent evaporation. For this reason, magnesium sulphate should be used prior to solvent evaporation to eliminate water traces (GHORBANI-CHOGHAMARANI; CHENANI; MALLAKPOUR, 2009).

2.6.3.2 Reactions involving TAD

TADs can undergo Diels-Alder, Alder-ene, electrophilic aromatic substitution and cycloaddition reactions. Aside of having high selectivity with these systems, other reaction pathways are possible, but they are much slower and less selective (DE BRUYCKER et al., 2016). Alder-ene systems correspond to a reaction between an alkene and a double bond (enophile) and this type of reaction was reported for the first time by Alder and co-workers (ALDER; PASCHER; SCHMITZ, 1943). Despite the TAD-ene mechanism still generating discussion, a route involving the formation of a zwitterion aziridinium imide is well accepted, but the subsequent hydrogen transfer is not so clear. Besides, studies suggest that the mechanism is solvent-dependent and TAD reactivity is associated to the solvent polarity and its ability to donate protons to reagents (ACEVEDO; SQUILLACOTE, 2008; VOUGIOUKALAKIS et al., 2008; SYRGIANNIS et al., 2009).

In TAD systems, carbon-carbon double bonds are not consumed during the reaction but shifted along the chain as showed in Figure 14. Thus, additional functional groups can be added to the polymer chain via different chemical routes or either via a second TAD addition, although the urazole moieties from first addition can limit the second modification due to steric hindrance (TÜRÜNÇ et al., 2015).

Figure 14 - Alder-ene reaction between TAD and a substituted alkene.



Source: Türünç et al. (2015).

The double bond position in the substrate will dictate the kinetics of TAD chemistry and alkenes with higher substitution degrees are usually more reactive. Ultra-fast conversions are easily obtained at room temperature and without any catalyst. Besides, the reaction progress can be easily monitored by the system discoloration from pink/red (characteristic of TADs) to transparent which turns this chemistry very attractive and easy to follow (TÜRÜNÇ et al., 2015; DE BRUYCKER et al., 2016).

When TADs are used to modify unsaturated compounds, the physical properties of the modified material are susceptible to change. The addition of high polar pending groups to polymer chains allows inter- and intramolecular hydrogen bonding interactions between urazole moieties and this can be associated with differences in polymer elasticity, solubility, thermal behavior and tensile strength (BUTLER, 1980; DE BRUYCKER et al., 2016). In order to complement Sharpless criteria about click reaction definition, Barner-Kowollik proposed three further conditions for a process to be classified as click chemistry, such as equimolarity, scalability and high reaction rates (BARNER-KOWOLLIK et al., 2011). After some years of extensive research in its synthesis, TADs molecules with tailored functionalities could be produced to obtain high value materials in click chemistry.

Türünç and co-workers studied TAD conjugation in unsaturated vegetable oils, and they confirmed the ultra-fast TAD reactions utilizing oils with double bonds at different positions. As stated previously in literature, authors confirmed the lack of reactivity of TAD with terminal double bonds. Gelation occurred from 2 to 8 min and when soybean oil was used, a gelation time around 1 min and 45 s was observed. In addition, 30 min after gelation the dark pink/red color from MDP-bisTAD had disappeared (TÜRÜNÇ et al., 2015).

Vlaminck and co-workers described PTAD conjugation in unsaturated polymers obtained via ADMET reactions and full conversion was obtained within 6 h. Also, they showed the polymers crosslinking by the addition of different amounts of bifunctional TAD. Gelation occurred in 15 min at high methylene diphenyl bis-TAD (MDP-bisTAD) concentrations and the red color from MDP-bisTAD disappeared overnight (VLAMINCK et al., 2016a).

Hannay and co-workers showed the crosslinking of tryptophan (Trp) containing polypeptides with distinct ratios of benzyl-L-glutamate (BLG) and N α -(carbobenzyloxy)-L-lisine (Z-lys) by the reaction with hexamethylene-bisTAD (HM-bisTAD). After deprotection

of the organogels, the authors obtained biocompatible hydrogels in human mesenchymal stem cells (hMSCs).

In tandem with the mentioned works, many reports make use of TADs to modify unsaturated polyesters (VANDEWALLE et al., 2016; VLAMINCK et al., 2016a), crosslink vegetable oils (WANG et al., 2015, 2016; CHATTOPADHYAY; DU PREZ, 2016) and fibers (HEIJDEN et al., 2015, 2017), films preparation (HANAY et al., 2017a) and hydrogels (ABSIL et al., 2016; HANAY et al., 2017b, 2018).

2.6.4 Poly(globalide) post-polymerization modification

The first study relating the use of the unsaturated macrolactone globalide was reported in 2008 by Heise group. The authors performed e-ROP of different macrolactones in solution using Novozym 435 and obtained polymers with number average molecular weights around 24,000 g mol⁻¹. Also, they observed the high crystallinity of these polymers (above 60%) and no considerable hydrolytic and enzymatic degradation over a period of 100 days (MEULEN et al., 2008).

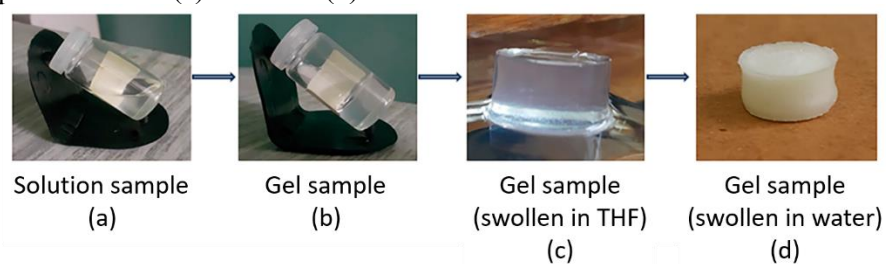
Since then, the same research group has studied PGI modification in order to obtain degradable materials aiming biomedical applications. As mentioned in previous chapters, the macrolactone globalide has 15 carbons and an unsaturation in its chain (position 11-12, isomers mixture) and can be polymerized via e-ROP to form a linear alkene polymer. The unsaturation in monomer/polymer backbone enables the modification of this compound via different chemical routes, such as thiol-ene and alder-ene routes, that were previously reviewed. Besides, globalide monomer is derived from fatty acid, is non-toxic and is usually employed in fragrances, shampoos, cosmetics and cleaning products. Hence, globalide is shown to be an excellent alternative in substitution to monomers from fossil sources (MEULEN et al., 2008; DE GEUS et al., 2010; ATES; THORNTON; HEISE, 2011).

Ates and co-workers studied the conjugation of amines and hydroxy groups in PGI backbone via thiol-ene reactions. High coupling yields were found (70-90%) when the concentration of the initiator and thiol was raised and the most successful results were accomplished when 11 times more thiol in relation to ene was used, due to the poor reactive double bonds in PGI chain (ATES; THORNTON; HEISE, 2011).

Meulen and co-workers copolymerized globalide with ϵ -CL, 4-methyl-caprolactone (4MeCl) and 1,5-dioxepan-2-one (4MeCl) to increase PGI degradability. Then, the authors used dicumyl peroxide to crosslink poly(Gl-co-4MeCl). Oliveira and co-workers produced crosslinked PGI electrospun fibers via *in-situ* electrospinning. A solution containing PGI, dithiol and photo-initiator was spun in dichloromethane and the fibers were crosslinked by UV irradiation inside of the electrospinning apparatus. After that, the crosslinked fibers were able to swell up 14% in organic solvent. Indomethacin was entrapped in the swelled fibers and the drug release profile from PGI fibers was evaluated.

Savin and co-workers reported for the first time the coupling between two polymers via photopolymerized thiol-ene reactions. For this, the authors used PGI and poly(ethylene glycol-co-thiomalate) (PEG-SH) to obtain polymeric gels (Figure 15).

Figure 15 - PGI-PEG materials (a) before and (b) after thiol-ene photopolymerization and after purification in (c) THF and (d) water.

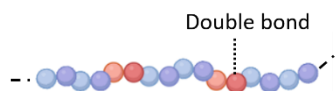


Source: Savin et al. (2018).

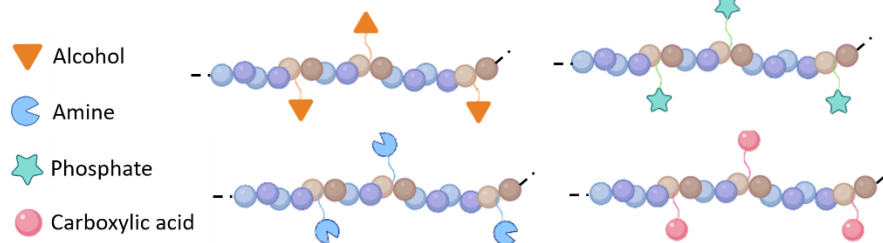
Overall, only a few works using PGI were described in literature and distinct routes and functionalities can be adopted to modify final PGI properties. As mentioned before, the unsaturation in the PGI chain allows a direct modification that is not possible in alkanes and usually in this last case many reaction steps are required in order to add unsaturations in the polymer chain, as in ϵ -PCL, for example (BASKO et al., 2017). Due to this, many functional groups can be easily added to the PGI chain via click reactions, as alcohols, amines, phosphates and many others (Figure 16).

Figure 16 - Post-polymerization modification of unsaturated polymers with distinct functional groups.

✘ Before post-polymerization modification



✘ After post-polymerization modification



2.6.5 Phosphoesters use in polymer modification

Phosphoesters (PEs) are a great alternative for polymer modification in order to prepare biodegradable materials. Although the first reports of its use are as flame retardants, PEs use as biomaterial for biomedical applications gained attention in the last years. They are hydrophilic materials of easy functionalization, biodegradable, biocompatible and similar to biomacromolecules as nucleic acids (DU et al., 2006; SHAO et al., 2012; DAS; KAR; GUPTA, 2013).

Recently, poly(phosphoesters) (PPEs) use is being directed to the following areas: PPEs synthesis to obtain polymers with controlled molecular weight and dispersity, copolymers synthesis, PEEs nanoparticles for drug and gene (DNA and siRNA) delivery and PEEs scaffolds for tissue engineering (WANG et al., 2009).

Many authors developed materials for use in tissue engineering using PPEs once the bonds present in their chain can be cleaved by water in physiological conditions and the degradation products consist of phosphate, alcohol and diol (WANG et al., 2001; SONG et al., 2008; MARSICO et al., 2012a; GAO et al., 2015). Polycondensation, polyaddition, transesterification and ring-opening polymerization can be used to synthesize PPEs (WANG et al., 2009).

Phosphodiesterase I hydrolase is capable to degrade compounds containing phosphate, as phosphoesters (PEs) and PPEs. This enzyme can be found in subcellular regions of human cells (BENDER, 2006). The enzymatic degradation by this hydrolase can facilitate the

intracellular release of drugs in cancer cells (in case of PPEs NPs use in drug delivery) (WANG et al., 2009). Wang and co-workers synthesized triblock copolymers composed of poly(ethyl ethylene phosphate) (PEEP) and ϵ -PCL with different chain lengths. When in aqueous solution, the polymers were able to form micelles of hydrophobic core (ϵ -PCL) and hydrophilic shell (PEEP). After incubation in a medium containing *Pseudomonas cepacia* or phosphodiesterase I, the authors observed the reduction in polymer peaks (by GPC) after 18 h (WANG et al., 2008). Another enzyme of interest in PEs/PPEs degradation is the alkaline phosphatase. This enzyme is produced in distinct organs and tissues, such as bones and hepatic cells and degrades PEs in tissues and cartilages (WANG et al., 2009).

In this context, materials containing PEs/PPEs can be degraded by enzymes present in the organism which make them interesting for *in vivo* use and there is no accumulation in the organism. To date, there are no reports in literature corresponding to poly(macrolactones) functionalization with phosphoester compounds.

2.7 FINAL CONSIDERATIONS

Many works have been described over the past few years involving polyester synthesis via e-ROP. Macrolactone globalide has shown great potential to be explored in different polymerization techniques, e.g. solution and miniemulsion. In this scenario, the current work has two different approaches. The first approach aims to study globalide e-ROP polymerization in solution and miniemulsion and show the flexibility of e-ROP polymerization and monomer to obtain either polymer films or nanoparticles for use in different fields of medicine. Secondly, the main goal of this work is the post-polymerization modification of PGI via click-like chemistry either via thiol-ene (making use of thiols containing phosphoester groups) and alder-ene reactions (making use of highly reactive triazolinediones).

The marriage of polymers, such as PGI, and phosphoesters is an attractive strategy to design novel polymers and as far as we know no works were described in literature in this context. Regarding lactones and macrolactones use in TAD click chemistry, ϵ -PCL was already used in this type of system. Unlike PGI (focus of this work), ϵ -PCL does not have readily available double bonds in its backbone. Therefore, several reaction steps are required to add unsaturation in α,ω ϵ -PCL backbone for a further modification. To the best of our knowledge,

modification and crosslinking of unsaturated poly(macrolactones), as PGI polymer, by TADs click chemistry was never reported before.

CHAPTER III

3. POLYESTERS FROM UNSATURATED MACROLACTONE GLOBALIDE USING COMMERCIAL LIPASE NS 88011 AND NOVOZYM 435 AS BIOCATALYSTS

3.1 INTRODUCTION

A series of lactones and macrolactones has been studied to evaluate their use in biomedical applications, including: ϵ -CL (UYAMA; TAKEYA; KOBAYASHI, 1993), δ -VL (KNANI; GUTMAN; KOHN, 1993), and macrolactones with 12 or more carbons in their structures (BISHT et al., 1997; MEULEN et al., 2008; POLLONI et al., 2016). The macrolactones globalide and ω -pentadecalactone, analogs having 15 carbons in their main backbones, are unsaturated and saturated, respectively, being very attractive for the synthesis of aliphatic polyesters with potential use in chemical, pharmaceutical and biomedical industries (MEULEN et al., 2008).

The macrolactone globalide is used in the fragrance industry because of its musky scent and its ability to release the aroma slowly for long periods of time (KRAFT; EICHENBERGER, 2004). Globalide contains an unsaturation in its structure and is a mixture of two different constitutional isomers with the double bond at position 11 or 12 (MEULEN et al., 2008). Due to the presence of the double bonds, globalide allows modification by post-polymerization inserting different functional groups in its main backbone, according to the desired application.

Cyclic lactones (4 to 7-membered) are easily polymerized by organometallic catalysts whereas for macrolactones (12 or more members) the polymerization using this type of catalyst is usually not so efficient due to the lack of ring tension, resulting in products with lower molecular weight (DUDA et al., 2002). Although recent studies show that catalysts based on aluminum-salen present good catalytic activity and can be used to generate high molecular weights products, this kind of catalyst requires manipulation under inert atmosphere (VAN DER MEULEN et al., 2011a).

Enzymes are highly selective, can catalyze polymerizations under mild conditions and are stable at different pH, temperature and pressure ranges, thus the enzymatic synthesis of polyesters is an environmentally friendly process when compared to polymerizations using

chemical catalysts. In addition, polymerization reactions using lipases can be conducted in organic and environmentally friendly solvents, such as water, supercritical carbon dioxide and ionic liquids (DUBOIS; COULEMBIER; RAQUEZ, 2009; LOOS, 2010; KOBAYASHI, 2015; POLLONI et al., 2016).

Lipases from *Candida antarctica*, *Candida rugosa*, *Pseudomonas fluorescens*, *Pseudomonas cepacia* and porcine pancreas have been used in the synthesis of polyesters via e-ROP (YANG et al., 2011). Among these lipases, the most reported one for polyester synthesis is *Candida antarctica* lipase B (CALB), which can be found immobilized in different supports. The CALB lipase physically adsorbed onto macroporous resin and commercially known as Novozym 435 from Novozymes (MILETIĆ; NASTASOVIĆ; LOOS, 2012; SHODA et al., 2016) stands out from the others and is used in the synthesis of high molecular weight polymers.

Immobilized enzymes have several advantages when used in biocatalytic processes such as the ease of recovery and reuse in another catalytic cycle, which is very important for industrial processes, since it results in cost-cutting processes (YANG et al., 2011). The major drawback of the industrial use of immobilized CALB is associated with the high cost of the currently available immobilized catalyst preparations Novozym 435 (Novozymes) and Chirazyme L-2 (Roche Molecular Biochemicals). Thus, immobilized preparations in more economical supports open up new possibilities of applications, like in the synthesis of aliphatic polyesters for use in pharmaceutical and food industries (KIRK; CHRISTENSEN, 2002). In this scenario, a new enzymatic preparation consisting of CALB immobilized on a hydrophobic polymeric resin (NS 88011) was formulated by Novozymes to provide a more economic support for production of compounds on an industrial scale.

Few reports can be found in literature regarding NS88011 use and all of them correspond to the synthesis of short chain esters, as geranyl cinnamate, cetostearyl stearate, ethylene glycol monostearate, benzyl propionate and benzyl butyrate (ZANETTI et al., 2016; HOLZ et al., 2018; PEREIRA et al., 2018; SÁ et al., 2018; DE MENESES et al., 2019). On the other hand, NS88011 was never reported as biocatalyst for polymer synthesis as proposed in this work.

In view of this, the aim of this work was to investigate the catalytic activity of commercial immobilized lipase NS 88011 in the solution e-ROP of globalide, evaluating its influence on the properties (polymerization yield, molecular weight, dispersity and thermal

properties) of the polyesters and to compare with results obtained under the same polymerization conditions, but using commercial Novozym 435 lipase as catalyst.

3.2 MATERIALS AND METHODS

3.2.1 Materials

Globalide (97%) was kindly provided by Symrise Aromas e Fragrâncias LTDA. Immobilized commercial lipases from *Candida antarctica* sp (NS 88011 and Novozym 435) were kindly supplied by Novozymes S/A, Brazil. Dichloromethane (DCM, 99.8%, VetecQuímica), Chloroform (99.8%, Panreac) and Toluene (99.8%, Sigma-Aldrich) were used as received. Molecular sieves (4Å) were purchased from Sigma-Aldrich.

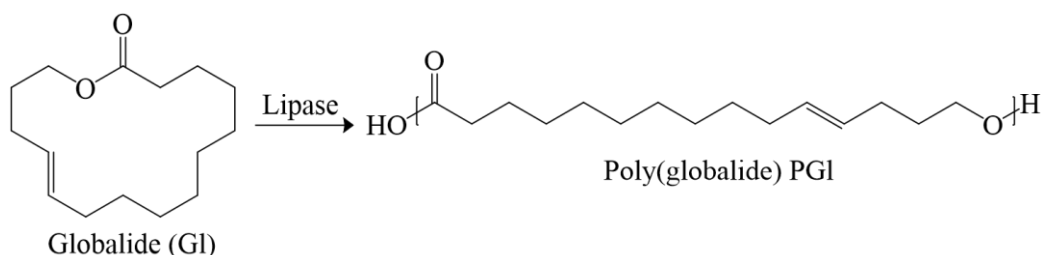
3.2.2 Methods

3.2.2.1 Enzymatic ring-opening polymerization of globalide

Before each polymerization reaction, the enzyme was dried in a vacuum oven at 40 °C and 0.4 bar for 24 h in the presence of molecular sieves. The effect of enzyme concentration (2, 6 and 10 wt.% in relation to monomer) in e-ROP was evaluated and reactions were conducted using destructive experiments, without sampling, in times of 10, 30, 60, 120, 240 and 360 min. For the polymerizations, the toluene solution of monomer (containing 33.3 wt.% of globalide) was mixed with the enzyme under N₂ atmosphere. Solution ring-opening polymerizations proceed in a water bath under magnetic stirring at 60 °C. This temperature was chosen once *Candida antarctica* B has the highest activity at this condition (KAMAL et al., 2013).

After reaction, dichloromethane was added to the final mixture and the enzyme was removed by filtration. The polymer was precipitated in cold methanol and dried during 24 h at 60 °C to remove residual solvent. Reaction yield was determined gravimetrically (mass of final polymer in relation to mass of monomer used in the reactions). Figure 17 shows a schematic representation of globalide e-ROP.

Figure 17 - Schematic representation of PGI synthesis via e-ROP.



3.2.3 Characterization

3.2.3.1 Molecular Weight Distribution

Molecular weights were determined by gel permeation chromatography (GPC) in a high-performance liquid chromatograph (LC 20A, Shimadzu) equipped with a refraction index detector (RID-10A), a pre-column (PLgel 5 μm MINIMIX-C guard, 50 x 4mm, Agilent, USA) and a 250 x 4.6 mm column set of two columns in series (PLgel 5 μm MiniMIX-C, Agilent, USA). Molecular weight distributions, weight average (M_w) and number average (M_n) molecular weights were calculated against polystyrene standards in a range from 580 to 3,000,000 g mol^{-1} . Chloroform was used as eluent at a flow rate of 0.3 mL min^{-1} . Polymeric samples were dissolved overnight in chloroform at 40 $^{\circ}\text{C}$ and the solutions with concentrations of 0.5 wt.% were filtered (0.450 μm Nylon filter) before injection.

3.2.3.2 Thermal Properties

Thermal analyzes of poly(globalide) were performed by differential scanning calorimetry (DSC) measurements in a Perkin-Elmer JadeDSC calibrated with zinc and indium, using approximately 9.0 mg of dried polymer. Samples were first heated from -30 $^{\circ}\text{C}$ up to 150 $^{\circ}\text{C}$ at a heating rate of 20 $^{\circ}\text{C min}^{-1}$ under nitrogen flow at 20 mL min^{-1} , to eliminate their thermal history. Then samples were cooled to -30 $^{\circ}\text{C}$ at a cooling rate of 20 $^{\circ}\text{C min}^{-1}$, maintained at this temperature for 1 min and heated again to 150 $^{\circ}\text{C}$ at a heating rate of 10 $^{\circ}\text{C min}^{-1}$. Melting enthalpies and temperatures were determined from the second heating run.

3.2.3.3 Crystallinity properties

Crystallinity characterization was performed by X-ray diffraction (XRD) using a PANalytical X'PERT X-ray system $\lambda=1.5406 \text{ \AA}$ Cu $K\alpha_1$ radiation at 2θ 10 - 60 ° range, employing a scanning rate of 2,5 °/min.

3.2.3.4 Enzyme activity

The enzymatic activity was measured by esterification reaction between lauric acid and propanol. The lipase activity was quantified by the lauric acid consumption during the esterification reaction under the same conditions reported by Oliveira and co-workers (OLIVEIRA et al., 2006) using a molar ratio of 3:1 (acid to alcohol) at 60 °C for 40 min and with 5 wt.% of lipase. The reaction was initiated by the addition of the lipase to the reaction medium and lauric acid content was determined by titration with sodium hydroxide until pH 11. Aliquots were collected from the reaction medium at time zero (without enzyme) and after 40 min of reaction and diluted in acetone-ethanol (1:1). One unit of activity (U) was defined as the amount of enzyme necessary to consume 1 μmol of lauric acid/min at the established experimental conditions.

3.3 RESULTS AND DISCUSSION

In contrast to well-known studied lactones and macrolactones, as ϵ -PCL and ω -PPDL, there are only a few works in literature regarding globalide polymerization. Polymerization kinetics of the macrolactone globalide, aiming to evaluate the effect of different types of enzymes or/and different enzyme concentrations during the reaction, was never investigated in the literature. Meulen and co-workers evaluated the conversion of globalide in polymer at different reaction times using a constant concentration of 2 wt.% of Novozym 435 lipase at 60 °C. The authors observed a fast conversion even in the initial minutes of the reaction (MEULEN et al., 2008).

To investigate the relation between enzyme concentration, yield and molecular weight, the effect of different enzyme concentrations: 2, 6 and 10 wt.% was evaluated in the solution e-

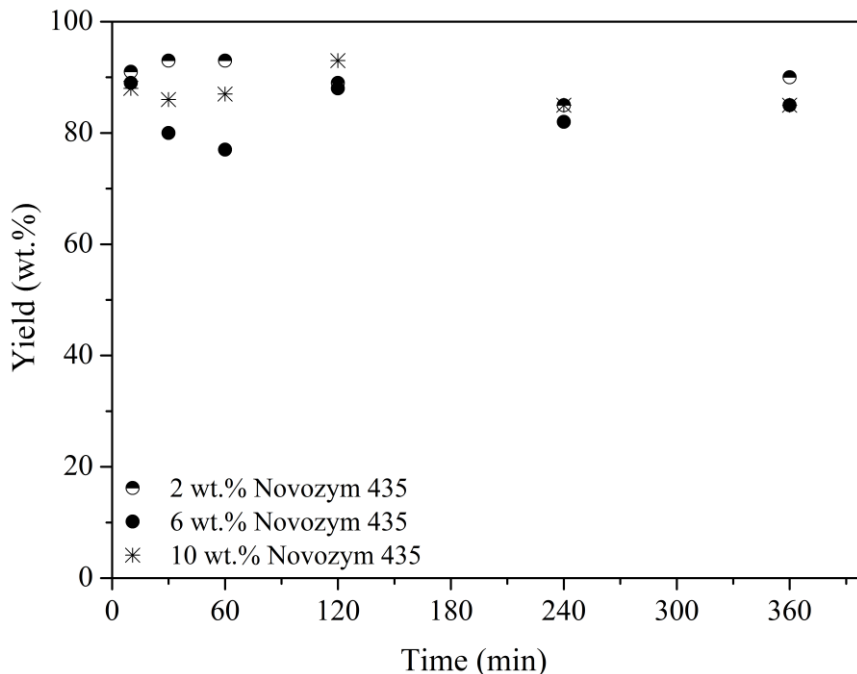
ROP of globalide at 60 °C, using toluene as solvent, in a 2:1 (toluene to monomer) mass ratio. Two different lipases were used to conduct the polymerization reactions. Before each reaction, the enzyme activity was measured and expressed in terms of U g⁻¹. The activity found for the immobilized lipase preparations were 35 (± 3.5) U g⁻¹ and 38 (± 1.7) U g⁻¹ for Novozym 435 and NS88011, respectively.

3.3.1 e-ROP of globalide using different lipases

3.3.1.1 Yield of PGI as a function of reaction time

Figure 18 shows the reaction yields in different times at 60 °C using different concentrations of Novozym 435. As can be seen, high yields (between 85-93%) were reached in only 10 min of reaction for all enzyme concentrations. Thus, the monomer consumption is almost complete in the first minutes even at the lowest enzyme concentration tested.

Figure 18 - Yield of poly(globalide) after different reaction times at 60 °C using different Novozym 435 lipase concentrations (2, 6 and 10 wt.%) and toluene as solvent (solvent to monomer mass ratio 2:1).

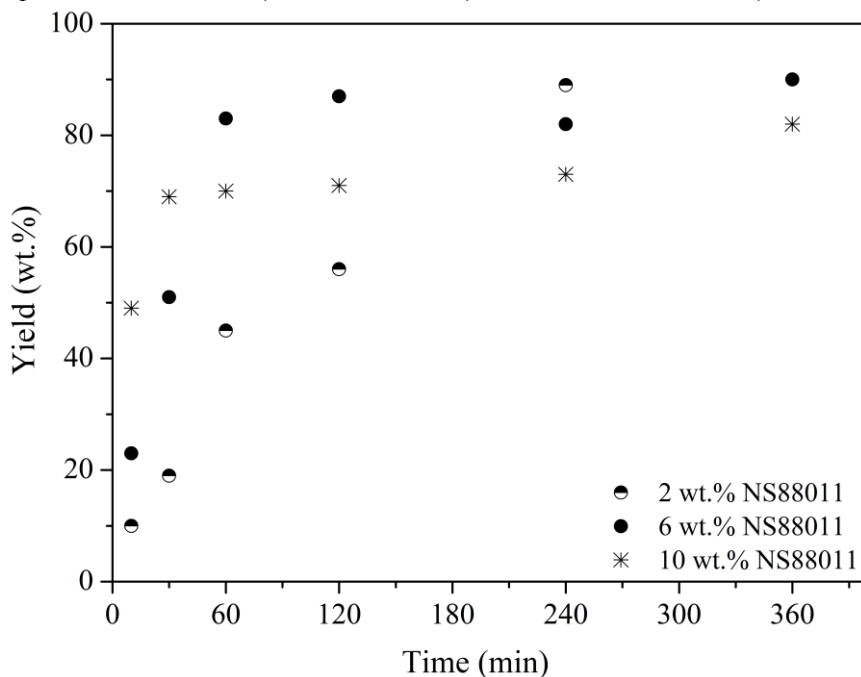


The slight shift of the yield during the reaction time can be attributed to the variation of water in each system and to external factors such as air moisture. The water plays an important role in polymerization kinetics and molecular weight in e-ROP systems once it acts as an initiator (nucleophile) (MEI et. al., 2003). Measurements of lipase esterification activity after 360 min of reaction showed that Novozym 435 remained stable without losing its catalytic activity (esterification activity: $31 (\pm 1.6) \text{ U g}^{-1}$) after polymerization.

Meulen and co-workers studied globalide conversion upon time and they followed the conversion by $^1\text{H-NMR}$ during 200 min using a globalide:toluene mass ratio of 1:1 and a fixed amount of Novozym 435 (2 wt.%). The authors observed high yields (around 90%) after 35 min of reaction and complete conversion of GI after 3 h. This data corroborates the obtained results in the present work, indicating the fast reaction kinetics of macrolactones when polymerized via enzymatic route.

Figure 19 shows the yield of globalide e-ROP when the effect of NS88011 concentration was evaluated. The experiments were performed as those reported using Novozym 435. It can be seen in Figure 19 that, unlike the behavior found for Novozym 435 lipase, when the NS 88011 lipase was used, yield increased gradually during the reaction time. In 10 min of reaction, yields of 10, 23 and 50 wt.% were obtained using 2, 6 and 10 wt.% of enzyme, respectively. For the same enzyme concentrations, after 360 min, yields have reached 72, 90 and 88 wt.%. Also, measurements of lipase esterification activity after 360 min of reaction showed that NS 88011 remained stable without losing its catalytic activity (esterification activity: $35 (\pm 1.9) \text{ U g}^{-1}$) after polymerization.

Figure 19 - Yield of poly(globalide) after different reaction times at 60 °C using different NS88011 lipase concentrations (2, 6 and 10 wt.%) and toluene as solvent (solvent to monomer mass ratio 2:1).



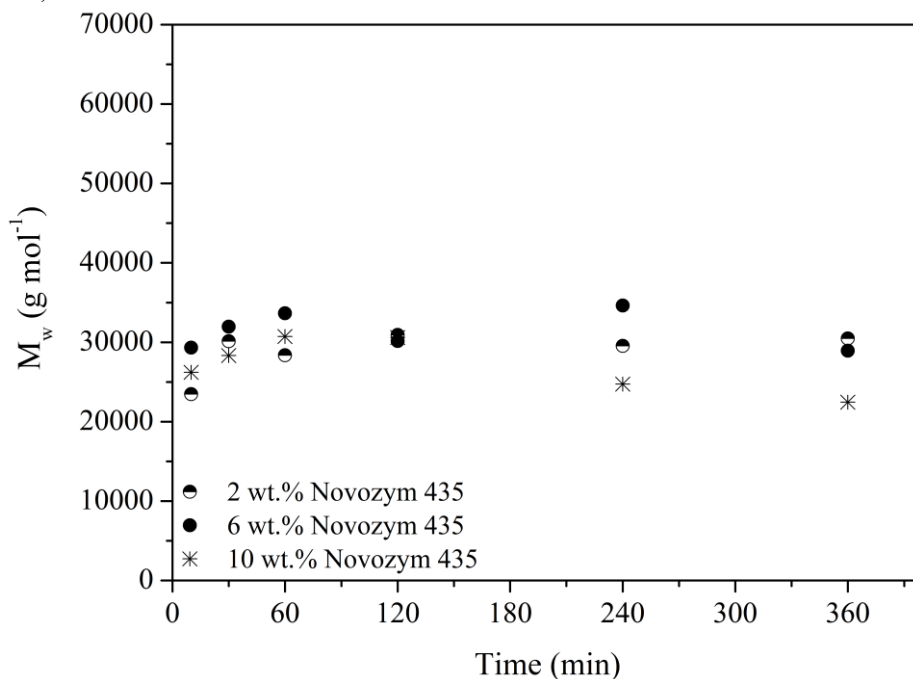
3.3.1.2 PGI molecular weight as a function of reaction time

Weight average molecular weights of PGI obtained via e-ROP using Novozym 435 or NS88011 are shown, respectively, in Figures 20 and 21. When Novozym 435 was used, it is possible to observe that molecular weights in similar ranges were reached when different enzyme concentrations were used. At 30 min of reaction, M_w of 30,100; 31,900 and 28,300 g mol^{-1} were obtained for enzyme concentrations of 2, 6 and 10 wt.%, respectively. During the reaction, it was possible to observe an increase in the viscosity due to the polymer formation, considerably reducing the magnetic stirring and the diffusion of the ‘enzyme-activated polymer chains’ through the system, which hinders the increase of molecular weight with longer reaction times. The same phenomenon was previously reported (CAI et al., 2010; POLLONI et al., 2016) in the study of e-ROP of ω -PDL macrolactone at 70 °C in toluene using Novozym 435 commercial lipase as catalyst.

Additionally, the increase in the system viscosity leads to an increase in the water concentration at the enzyme’s surface. Thus, hydrolysis reactions in the polymer chain can occur under the action of the enzyme, leading to chain degradation and consequent molecular weight reduction (DE GEUS et al., 2010). Reasonable dispersity values (\mathcal{D}) were found in all

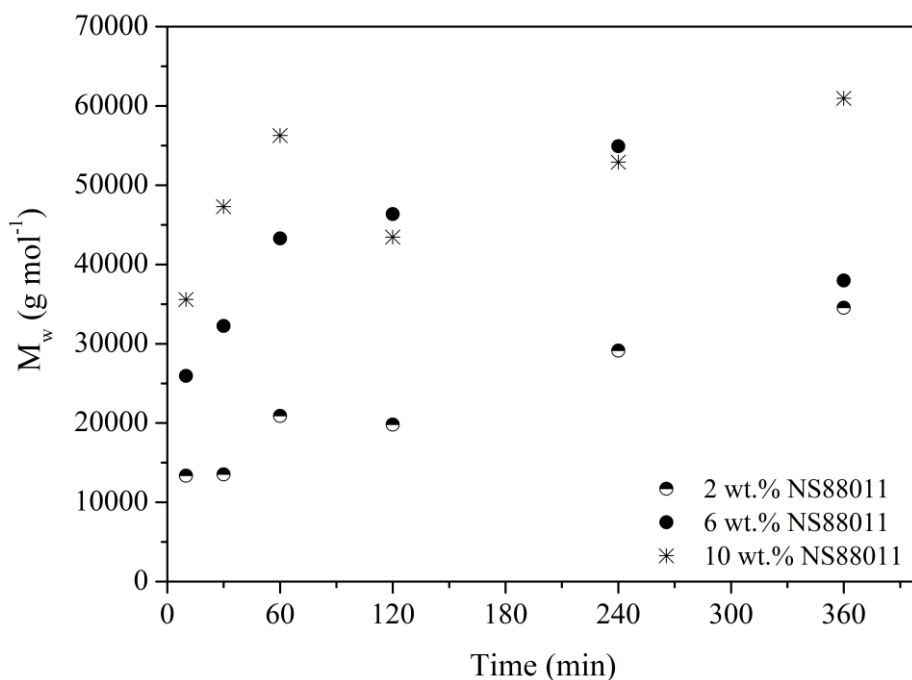
tested conditions in a range from 2.0 to 3.0 and these values are in accordance to previous works reported in literature for e-ROP of globalide catalyzed by Novozym 435 (MEULEN et al., 2008; ATES; THORNTON; HEISE, 2011).

Figure 20 - Weight average molecular weights of poly(globalide) produced at 60 °C with different Novozym 435 concentrations (2, 6, and 10 wt.%) and toluene as solvent (solvent to monomer mass ratio 2:1) in function of reaction time.



Weight average molecular weight of poly(globalide) samples produced using NS 88011 lipase as catalyst are shown in Figure 21, where it is possible to observe an increase in M_w during the reactions and with the increase of the enzyme concentration, contrary to the behavior found for Novozym 435 lipase. In 30 min, M_w of 13,400; 25,900 and 35,600 g mol^{-1} were obtained for 2, 6 and 10 wt.% of enzyme, respectively. For the same enzyme concentrations (2, 6 and 10 wt.%), M_w of 34,500; 38,000 and 61,000 g mol^{-1} were reached after 360 min, much higher than those obtained after 360 min using 2, 6 and 10 wt.% of Novozym 435 lipase (M_w of 30,500, 28,900 and 22,500 g mol^{-1} , respectively). In addition, using lipase NS 88011 led to somewhat higher dispersities (\mathcal{D}) than using Novozym 435, varying from 2.5 to 7.0. The increase of the dispersity can be attributed to a series of factors, such as the increase of system viscosity, which triggers a chain mobility decrease and the formation of regions with higher concentrations of water, favoring the formation of cyclic oligomers.

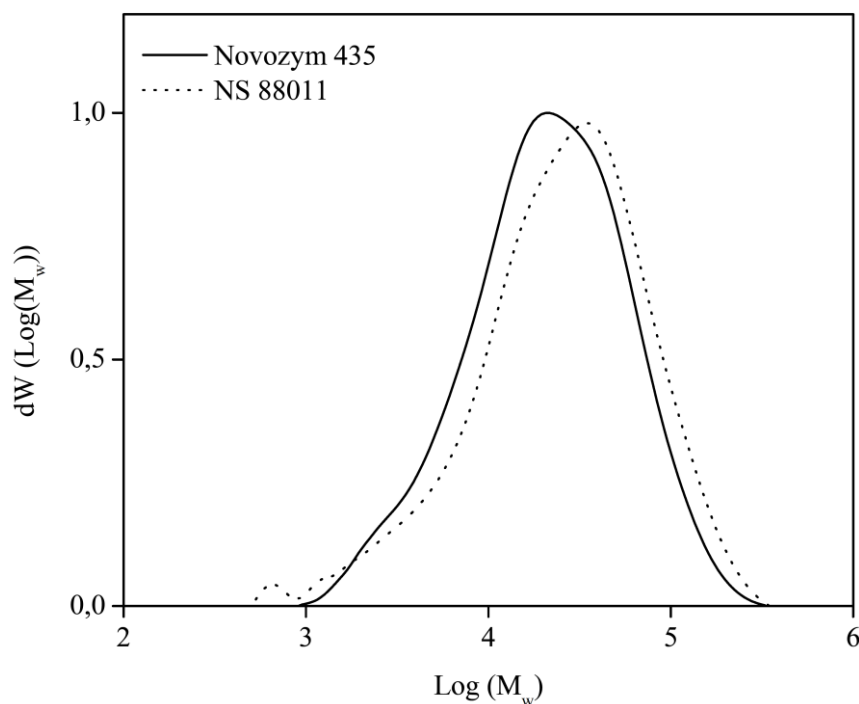
Figure 21 - Weight average molecular weights of poly(globalide) produced at 60 °C with different NS88011 concentrations (2, 6, and 10 wt.%) and toluene as solvent (solvent to monomer mass ratio 2:1) in function of reaction time.



Unlike Novozym 435, the use of NS88011 lipase as a catalyst for polymerization in polyester synthesis was never reported in literature. Interestingly, poly(globalide) obtained via e-ROP using NS88011 as catalyst reached higher molecular weight, up to 61,000 g mol⁻¹ when compared with Novozym 435 (maximum M_w of 34,900 g mol⁻¹) under the tested conditions. These differences can be associated to many factors and one of them is related to the enzyme and, more specifically to the support where the lipase is immobilized. Differences in support porosity can affect the diffusion of ‘enzyme-activated polymer chains’ through the pores (where the enzyme is adsorbed) and consequently to the active site. In this case, the higher the pores inside the support the faster is the macrolactone ring-opening and consequently higher yields and lower molecular weights are obtained. Sá and co-workers characterized Novozym 435 and NS88011 supports and Novozym 435 showed larger surface area (78.69 m²/g), total pore volume (0.2837 cc/g) and average pore diameter (144.2 Å) than NS88011 (15.16 m²/g, 0.02613 cc/g and 68.96 Å, respectively) (SÁ et al., 2018). The data reported by Sá and co-workers corroborates the behavior observed for both lipases in the current work.

Figure 22 shows the molecular weight distribution for poly(globalide) produced using both lipases as catalysts. As can be seen in the reaction conducted using NS 88011 lipase as catalyst, the distribution was shifted towards higher molecular weights and also presented a low molecular weight tail, that is responsible for the higher values of the dispersities.

Figure 22 - Molecular weight distribution of poly(globalide) produced using toluene as solvent (solvent to monomer mass ratio 2:1) at 60 °C, in 30 min of reaction and using 10 wt.% of lipase.



3.3.1.3 Thermal and crystalline properties

Thermal analysis of poly(globalide) produced using both Novozym 435 or NS 88011 lipases as catalysts was conducted and the DSC curve of PGI obtained using NVZ435 can be seen in Figure 23. The values found for ΔH_m were 59.9 (for NVZ435) and 61.1 J g⁻¹ (for NS88011). Also, melting temperatures (T_m) around 49 °C were found for both tested enzymes. These values are in accordance with those reported previously by Meulen and co-workers (MEULEN et al., 2008) for poly(globalide) synthesized via e-ROP using Novozym 435 in solution (2 wt.%) and toluene as solvent (ΔH_m of 77.4 J g⁻¹ and T_m of 46.2 °C). PGI T_m is lower than the one found for its analogue ω -PPDL (around 96 °C) due to PGI unsaturations, which

are responsible for a more irregular and less packed structure than that of the highly crystalline ω -PPDL.

X-ray diffraction was performed in order to evaluate the crystalline properties of the polymer. Reflection values in $2\theta = 21.2$ and 23.2 were found indicating a semi-crystalline polymer as reported before in literature for PGI (MEULEN et al., 2008) (Figure 24). When NS88011 was used in the polymerizations, the same thermal and crystalline behaviors were found.

Figure 23 - DSC curve of PGI obtained from e-ROP using 10 wt.% of Novozym 435.

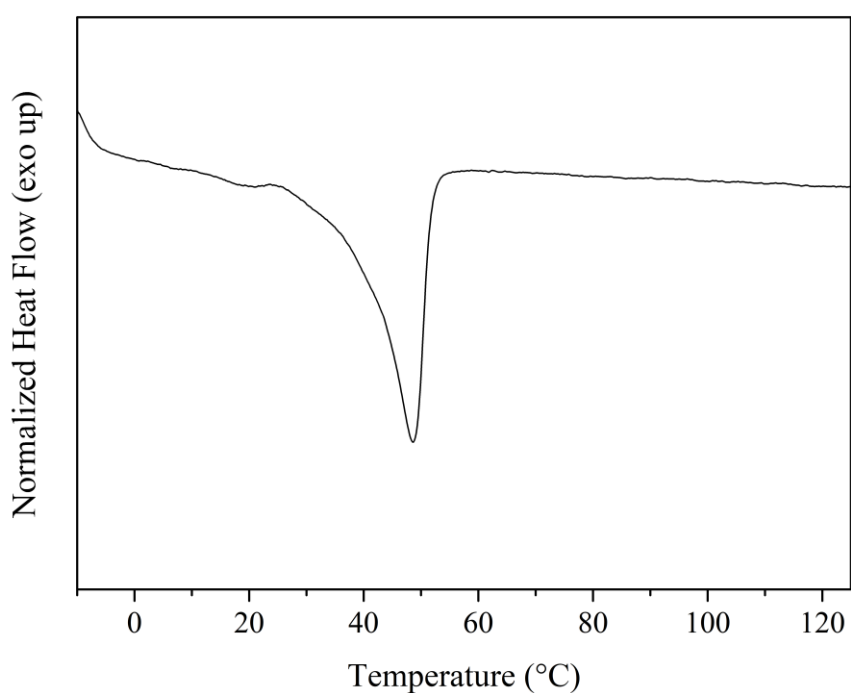
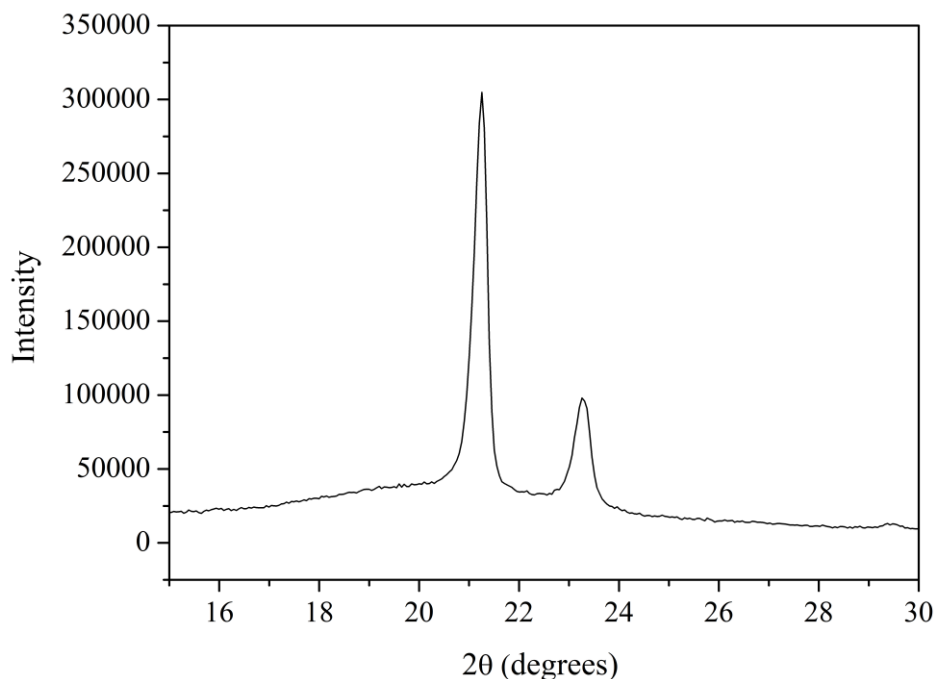


Figure 24 - X-ray diffraction spectra of PGI obtained from e-ROP using 10 wt.% of Novozym 435.



3.4 CONCLUSIONS

In order to overcome the high cost related to the use of traditional biocatalysts in the synthesis of polyesters, in this chapter we have reported the use of immobilized commercial lipase NS 88011 in the e-ROP of unsaturated macrolactone globalide. Reactions conducted using NS88011 as catalyst resulted in high yields of 80 to 90 wt.% and weight average molecular weights up to $61,000 \text{ g mol}^{-1}$. These molecular weights are above those found when the enzyme Novozym 435 was used as catalyst. Regarding the effect of the NS88011 enzyme concentration in polymerization, it was noted a strong influence of the amount of catalyst in yield and molecular weights. Finally, thermal properties of poly(globalide) synthesized using NS 88011 lipase as catalyst are in agreement with literature data. An alternative and cheaper route to synthesize new polyesters by e-ROP was shown in this work using the NS88011 lipase. This immobilized enzyme preparation, available commercially, has a low cost when compared to Novozym 435, and our group is conducting experiments to evaluate the stability of this biocatalyst to different pH and temperature as well as reuse experiments in order to determine the viability of this enzyme in the large-scale production of biodegradable polymers. The results

presented in this chapter were published in *Applied Biochemistry and Biotechnology Journal*, 184, 659-672, 2018.

CHAPTER IV

4. POLYESTER NANOPARTICLES FROM UNSATURATED MACROLACTONE GLOBALIDE VIA MINIEMULSION ENZYMATIC RING-OPENING POLYMERIZATION

4.1 INTRODUCTION

Aliphatic polyesters have been used in the last years in biomedical applications including sutures, screws, scaffolds for tissue engineering and nanoparticles (NPs) for drug delivery (SEYEDNEJAD et al., 2011; KUMAR; SAWANT, 2013; STEMPFLE et al., 2014; SHADI; KARIMI; ENTEZAMI, 2015; SAMANTA et al., 2017). The advantages of these materials comprehend their biocompatibility, biodegradability and non-toxicity (KOBAYASHI, 2010; SEYEDNEJAD et al., 2011; ULERY; NAIR; LAURENCIN, 2011). This class of polymer can be synthesized by two main methods: polycondensation and ring-opening polymerization (ROP) of cyclic esters (lactones and macrolactones) (KOBAYASHI, 1999, 2010; KADOKAWA; KOBAYASHI, 2010; SEYEDNEJAD et al., 2011; MILETIĆ; NASTASOVIĆ; LOOS, 2012). Several lactones and macrolactones can be used in ROP polymerization to obtain biodegradable polyesters. In recent years, macrolactones (12-17 carbons) investigation was increased due to their biological and medicinal properties. These materials are used commonly in pharmaceutical and cosmetic industry as odoriferous compounds, deodorants, shampoos and flavoring (ALBERTSSON; SRIVASTAVA, 2008; MCGINTY; LETIZIA; API, 2011). Globalide (GI), a 16-membered macrolactone, has attracted attention recently due to the presence of an unsaturation in its backbone, allowing crosslinking and functionalization of double bonds after polymerization (ATES; THORNTON; HEISE, 2011; DE OLIVEIRA et al., 2017b).

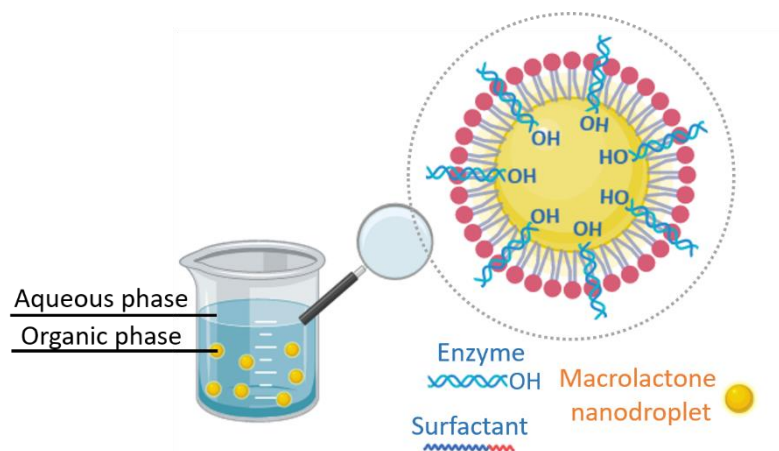
Polyester synthesis via ring-opening polymerization of macrolactones using enzymes as catalysts has several advantages in relation to ROP performed with chemical catalysts, once enzymes are specific for a large range of substrates and are considered natural catalysts (KOBAYASHI, 1999; SEYEDNEJAD et al., 2011; YANG et al., 2014). Thus, this method has

been the most used in the last years to synthesize high molecular weight polymers under mild reaction conditions (ATES; THORNTON; HEISE, 2011; ZHANG et al., 2014).

Despite most works regarding polyester synthesis being conducted by ROP solution polymerization using different catalysts (BOUGARD et al., 2007; MEULEN et al., 2008; VAIDA; KEUL; MOELLER, 2011; ZHOU; HONG, 2013), biodegradable and biocompatible polyester nanoparticles (NPs) synthesis has shown potential for biomedical applications, including drug delivery systems. The drug release from the polymeric matrix is controlled by polymer biodegradation, which is related to polymer properties such as crystallinity, hydrophobicity, among others (TADEN; ANTONIETTI; LANDFESTER, 2003). Besides that, the high surface area of the nanoparticles can provide a faster degradation of these materials. Meulen and co-workers accessed the hydrolytic and enzymatic degradation of PGI and ω -PPDL films and the authors did not observe mass loss after 100 days (MEULEN et al., 2008). On the other hand, Oliveira and co-workers studied the hydrolytic degradation of PGI microfibers (from 5 to 11 μm) and after 90 days the mass loss was in a range of 30% (DE OLIVEIRA et al., 2017b).

Miniemulsion polymerization is a versatile technique to obtain a wide variety of polymeric NPs without using toxic solvents, once the reaction occurs in water. Additionally, it is a simple process and it is possible to control the NPs diameter (ASUA, 2002). Generally, direct miniemulsions consist of a dispersion of two immiscible liquids: an organic phase (containing a hydrophobic monomer and a co-stabilizer to minimize diffusion degradation) and an aqueous phase (containing water and a surfactant to retard coalescence). When used, the initiator can be added either to the dispersed or to the continuous phase, depending on its hydrophilic/lipophilic nature. For nanodroplets formation, both phases are miniemulsified in a high-shear equipment. The formed nanodroplets act as nanoreactors for polymerization reactions and, consequently, for NP preparation (ASUA, 2002). When the polyester synthesis is conducted via enzymatic ring-opening polymerization in miniemulsion, the enzyme (amphiphilic character) is adsorbed on the surface of the monomer nanodroplets (Figure 25). Due to this, ring-opening, propagation and transesterification reactions take place at the nanodroplets interface - where the enzyme is adsorbed - and inside the nanodroplets. Once the reaction is conducted in water, it is not possible to limit the water content (reaction initiator) (GROSS; KUMAR; KALRA, 2001; POLLONI et al., 2016) in the reaction medium as in solution polymerization, which may affect the polymer properties, mainly molecular weight.

Figure 25 - e-ROP in aqueous miniemulsion - nanodroplets before polymerization.



Usually, the works described in literature involving polyester NPs or microspheres preparation from lactones uses ϵ -CL as cyclic monomer and the methods for NPs preparation do not include miniemulsion polymerization. In contrast to lactones, macrolactones have already been used for polyester NPs synthesis via miniemulsion polymerization. Taden and co-workers (TADEN; ANTONIETTI; LANDFESTER, 2003) were the first group to investigate polyester NPs synthesis from macrolactones via miniemulsion in water. The authors produced ω -PPDL NPs with particle sizes around 100 nm using hexadecane as co-stabilizer, Lutensol AT50 as surfactant and *Pseudomonas cepacia* as biocatalyst. A few years later, the group of Målberg and co-workers (MÅLBERG; FINNE-WISTRAND; ALBERTSSON, 2010) studied the synthesis of ω -PPDL, and poly(hexadecanolide), P(HDL) NPs using *Burkholderia cepacia* and *Pseudomonas fluorescens* as biocatalysts and Brij 58 and hexadecane as surfactant and co-stabilizer, respectively. The obtained polymer presented low molecular weight (below 2,000 g mol⁻¹) and high dispersity in long reaction times (from 5 to 22 h). The only work found in literature for NP synthesis from the macrolactone globalide was reported by Pascual and co-workers (PASCUAL; LEIZA; MECERREYES, 2013b). The authors studied the miniemulsion ROP of ambrettolide (Am), Gl and ω -PDL using acid catalysts. The obtained molecular weights remained in a range from 800 to 1,660 g mol⁻¹ - which corresponds to 6 or 7 macrolactone units - after 24 h of reaction at 80 °C.

The works mentioned previously are the only reports in literature covering polyester synthesis in miniemulsion from macrolactones until now. The enzymatic polyester synthesis of

cyclic macrolactones in miniemulsion involves a series of reactions at the droplet/water interphase, including ring-opening and polycondensation. Once this kind of system is not so well explored in literature, new detailed investigations are required to understand the polymerization behavior of macrolactones in aqueous media. Besides that, few works are described in literature regarding the unsaturated macrolactone globalide and this compound has become of great interest in the last years due to its properties and ease of functionalization (DE OLIVEIRA et al., 2017a; SAVIN et al., 2018; GUINDANI et al., 2019).

In this scenario, the aim of this work was to synthesize poly(macrolactones) NPs via enzymatic ring-opening polymerization in miniemulsion using non-conventional monomers and biocatalyst. For this, globalide (GI) - unsaturated 16-membered macrolactone - was chosen as monomer for the ring-opening and the enzymes free *Candida antarctica* B lipase (free CALB) and *Thermomyces lanuginosus* (NS40116) were used in the reactions as biocatalysts. To the best of our knowledge, this is the first work that shows the use of these lipases for e-ROP of macrolactones in miniemulsion.

4.2 MATERIALS AND METHODS

4.2.1 Materials

Globalide (GI, 97% purity) was a kind gift of Symrise. Lutensol AT50 (with a polyethylene glycol, PEG, chain of 2000 g mol⁻¹) was provided by BASF and used as surfactant. Hexadecane (VETEC, HD, 99% purity, CAS: 544-76-3) and crodamol GTCC (Alfa Aesar) - a fully saturated triglyceride mainly consisting of caprylic acid (C8) and capric acid esters (C10) obtained from coconut oil - were used as co-stabilizers. Sorbitol solution of free *Candida antarctica* B (Novozymes NZL-102, CALB) and NS40116 were donated by Novozymes Latin América Ltda (Araucária, PR, Brazil) and used as biocatalysts.

4.2.2 Methods

4.2.2.1 Enzyme concentration

To eliminate undesirable components in the enzymatic broths provided by Novozymes (sorbitol solution of CALB and NS40116), a purification step reported previously for this class of enzyme was conducted (CIPOLATTI et al., 2014; CHIARADIA et al., 2016; BRESOLIN et al., 2019). In short, free lipase in sorbitol solution was concentrated by dialysis of the enzymatic broth using cellulose membrane (for free CALB) or collagen membrane (for free NS40116) in sodium phosphate buffer 0.05 M (pH 7.0) during 24 h. After dialysis, the concentrated enzyme was lyophilized for 24 h and stored under refrigeration prior to use.

4.2.2.2 Enzyme catalyzed miniemulsion polymerization of unsaturated macrolactone

Polymerizations of G1 were based on miniemulsion enzymatic ring-opening polymerization (miniemulsion e-ROP) described by Taden and co-workers (TADEN; ANTONIETTI; LANDFESTER, 2003) to synthesize ω -PPDL NPs using *Pseudomonas cepacia* lipase. The organic phase was prepared using monomer (G1) and co-stabilizer (hexadecane or crodamol - 4.16 wt.% in relation to monomer). The aqueous phase was prepared using water and Lutensol AT50 (1, 2.5 and 5 wt.% in relation to water). All miniemulsion reactions were prepared using 10 mL of water and polymerization temperatures of 45 and 60 °C were studied. When CALB was used as biocatalyst, a concentration of 0.5 wt.% in relation to monomer was used. On the other hand, when NS40116 was used, 2.5 wt.% of this enzyme was used once in lower concentrations no polymerization was observed. The formulations used in miniemulsion e-ROP of G1 with free CALB lipase are shown in Table 1.

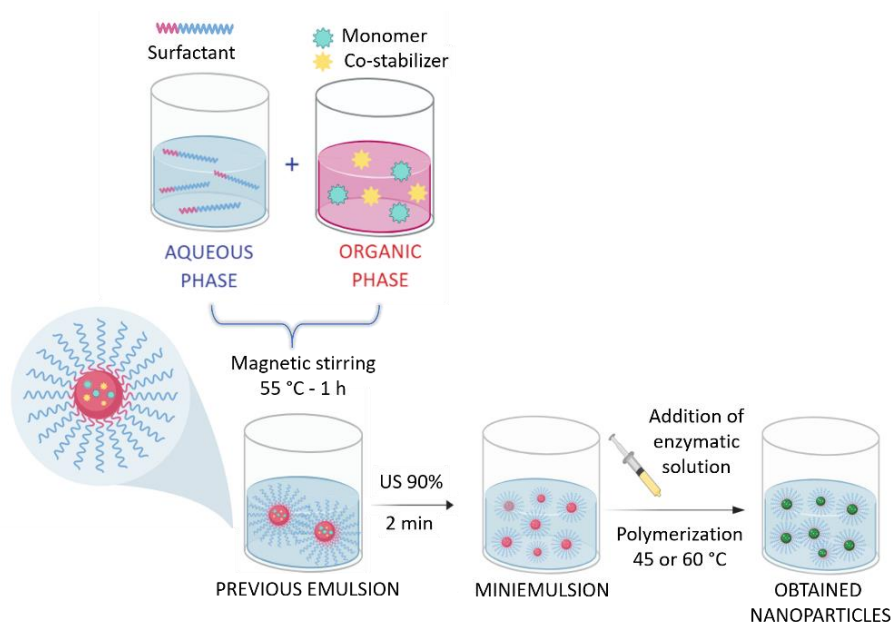
At the same time, crodamol was used as co-stabilizer for CALB formulations and the reactions are named from GC7 to GC8. The aqueous phase (water and surfactant) and the organic phase (monomer and co-stabilizer) were mixed in a water bath at 55 °C with magnetic stirring for 1 h. Then, the formed coarse emulsions were sonified using an ultrasonic probe (Fischer-Scientific-Ultrasonic Dismembrator 500, 400 W) for 120 s at 90% amplitude. Finally, an aqueous solution containing surfactant and enzyme (0.5 or 2.5 wt.% in relation to monomer)

was added to the formed miniemulsions and the polymerizations were conducted under magnetic stirring at different temperatures (45 or 60 °C) during 5 h, as shown in Figure 26. Subsequently, sodium hydroxide (NaOH, pH 14) was added to the latexes to stop the reaction by enzyme denaturation.

Table 1 - Formulations of miniemulsion e-ROP using CALB as biocatalyst.

Reactants and conditions	GC1	GC2	GC3	GC4	GC5	GC6
Globalide (g)	2.4	2.4	2.4	2.4	2.4	2.4
Hexadecane (g)	0.1	0.1	0.1	0.1	0.1	0.1
Lutensol AT 50 (g)	0.1	0.25	0.5	0.1	0.25	0.5
CALB (g)	0.012	0.012	0.012	0.012	0.012	0.012
Temperature (°C)	45	45	45	60	60	60

Figure 26 - Procedure for macrolactone e-ROP in aqueous miniemulsion.



4.2.3 Characterization

4.2.3.1 Chemical characterization

¹H-NMR spectra were recorded on a Varian Mercury Plus AS400 spectrometer at 400 MHz. Chemical shifts were reported in parts per million (ppm) from 0.00 ppm using

tetramethylsilane (TMS) - 0.01% (v/v) ($\delta = 0.00$) - as internal standard and the dried samples (without any purification) were solubilized in CDCl_3 ($\delta = 7.26$). The degree of monomer conversion was determined comparing the relative intensities of the peaks originating from the resonance peaks from the ester methylene of the monomer (4.15 ppm) and the ester methylene of the polymer (4.05 ppm).

4.2.3.2 Morphology and particle size

Transmission Electron Microscopy (TEM, JEM 1011 TEM) at 100 kV was used to verify the NPs morphology. One drop of the diluted latex was placed on a carbon coated grid and dried overnight at room temperature. The intensity average diameters of polymer particles (D_p) were measured by dynamic light scattering (DLS; Zetasizer Nano S, from Malvern). Latexes were diluted in distilled water (1:10) and the diameters (nm) were the average of two runs.

4.2.3.3 Molecular Weight Distribution

The polymer molecular weight was evaluated by gel permeation chromatography (GPC) using a high-performance liquid chromatograph (LC 20A, Shimadzu) equipped with a refraction index detector (RID-10A), a pre-column (PLgel 5 μm MINIMIX-C guard, 50 x 4 mm, Agilent, USA) and a set of two 250 x 4.6 mm columns in series (PLgel 5 μm MINIMIX-C, Agilent, USA). Molecular weights were determined against polystyrene standards in a range from 580 to 3,000,000 g mol^{-1} . For the GPC analyses, the samples were dried in a forced convection oven at 60 °C. After this, the samples were purified under vigorous stirring in cold ethanol to remove residual components (surfactant, lipase, NaOH, monomer). After the purification step, the dried polymer was dissolved in chloroform (JT Baker) at 40 °C during 24 h. The obtained solutions with a concentration of 0.5 wt.% (polymer to chloroform) were filtered (0.450 μm , Nylon filter) before the injection.

4.2.3.4 Thermal analysis

Thermal analysis of the dry polymer (after purification in ethanol) was conducted in a Perkin-Elmer Jade DSC calibrated with zinc and indium, using approximately 9.0 mg of dried purified polymer. Temperature profiles from -10 °C to 120 °C with heating and cooling rate of 10 °C/min were applied. The melting temperature was determined by the second heating.

4.3 RESULTS AND DISCUSSION

4.3.1 Poly(globalide) nanoparticles obtained via miniemulsion e-ROP

4.3.1.1 Nanoparticles synthesis using hexadecane as co-stabilizer

PGI nanoparticles were first synthesized using free *Candida antarctica* B as biocatalyst, Lutensol AT 50 as surfactant (to minimize droplets coalescence) and hexadecane as co-stabilizer (to reduce diffusional degradation). The intensity average diameter (D_p) and dispersity (PDI) of the PGI NPs, as well as the respective weight (M_w) and number (M_n) average molecular weights and dispersities (\mathcal{D}) are shown in Table 2.

The resulting D_p of PGI NPs was affected by surfactant concentration, decreasing from 91 nm (1 wt.% of surfactant) to 87 nm (2.5 wt.% of surfactant) and 78 nm (5 wt.% of surfactant) at 45 °C and from 283 nm (1 wt.% of surfactant) to 229 nm (2.5 wt.% of surfactant) and 215 nm (5 wt.% of surfactant) at 60 °C. In general, PGI NPs presented low PDI values, especially in the reactions carried out at lower temperature (45 °C), indicating the formation of narrow particle size distributions (PSDs) as shown in Figure 27. For reactions at 60 °C, besides the formation of bigger particles, the PSD also became somewhat less narrow (Figure 28). It is worth mentioning that this temperature (60 °C) is above the melting temperature of the polymer PGI (between 40 and 48 °C) (MEULEN et al., 2008). Thus, the formed NPs were more susceptible to coalescence events.

Målberg and co-workers (MÅLBERG; FINNE-WISTRAND; ALBERTSSON, 2010) prepared poly(hexadecalactone) NPs by miniemulsion e-ROP using *Pseudomonas cepacia* lipase with D_p varying from 113 to 534 nm, depending on the surfactant content. When the

authors used lipase from *Pseudomonas fluorescens*, NPs obtained under most polymerization conditions did not present quality criteria by DLS analysis due to their high PDI values.

Table 2 - e-ROP in miniemulsion of GI using free CALB as lipase and hexadecane as co-stabilizer.

Entry	Surf. wt. %	Temp °C	Dp nm ^a	PdI ^a	M _n ^b	M _w ^b	Đ ^b
GC1	1	45	91±0.2	0.13±0.01	5,300	10,000	1.89
GC2	2.5	45	87±0.2	0.15±0.02	5,600	13,500	2.41
GC3	5	45	78±0.1	0.11±0.01	9,800	23,200	2.37
GC4	1	60	283±1.2	0.23±0.01	4,100	6,800	1.66
GC5	2.5	60	229±0.6	0.17±0.01	7,400	14,800	2.00
GC6	5	60	215±0.6	0.20±0.02	8,200	16,300	1.99

Reactions were carried out using 0.5 wt.% of enzyme in relation to monomer during 5 h.

^a Intensity average diameter (Dp) and dispersity (PdI) measured by DLS.

^b Number average (M_n) and weight average (M_w) molecular weights in g mol⁻¹ and, dispersity measured by GPC.

Figure 27 - Particle size distribution of P(GI) NPs obtained by miniemulsion e-ROP using free CALB and hexadecane as co-stabilizer at different surfactant concentrations (1, 2.5 and 5 wt.%) at 45 °C (Table 1, entries GC1 to GC3).

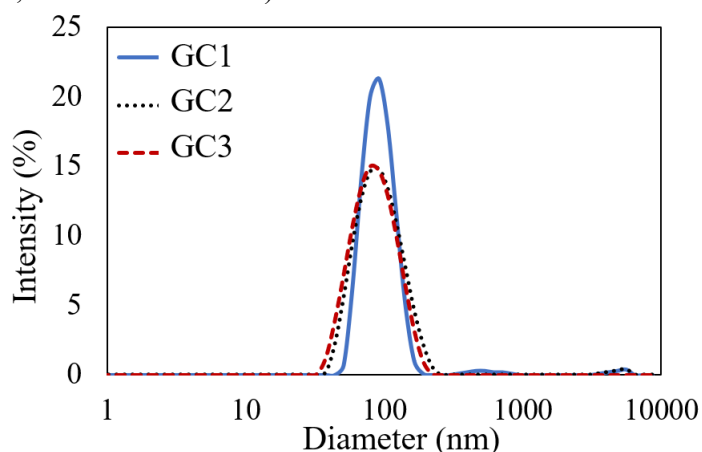
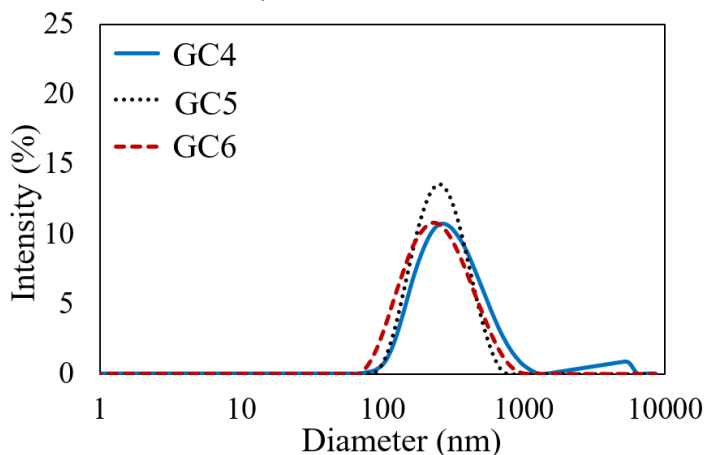
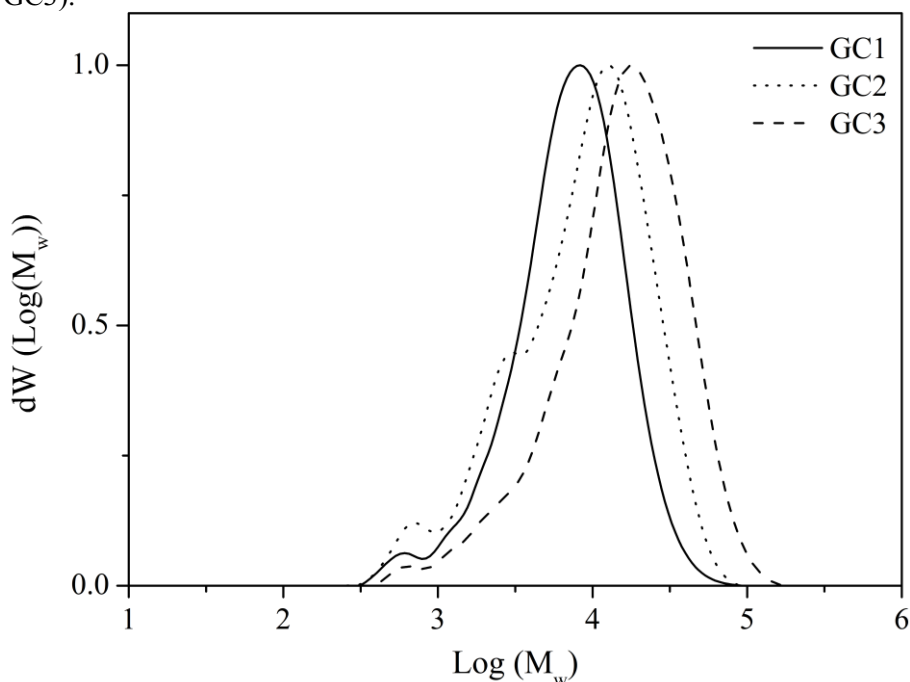


Figure 28 - Particle size distribution of P(GI) NPs obtained by miniemulsion e-ROP using free CALB and hexadecane as co-stabilizer at different surfactant concentrations (1, 2.5 and 5 wt.%) at 60 °C (Table 1, entries GC4 to GC6).



Molecular weights of PGI NPs were measured by GPC using chloroform as eluent (Table 2). For PGI NPs, higher molecular weight values were reached when higher surfactant concentrations were used and when the polymerization was conducted at 45 °C (Figure 29). M_w of 10,000 g mol⁻¹, 13,500 g mol⁻¹ and 23,200 g mol⁻¹ were obtained for polymerizations using 1, 2.5 and 5 wt.% of surfactant, respectively. The obtained molecular weights (M_w) for NPs synthesized at 60 °C using 1, 2.5 and 5 wt.% of surfactant were 6,800 g mol⁻¹, 14,800 g mol⁻¹ and 16,300 g mol⁻¹, respectively. At 60 °C temperature was above the melting point of PGI leading to some coalescence events and, consequently, to the reduction of total surface area of the NPs. It is important to note that the reaction occurs at the NPs interface thus, characteristics as droplet and particle diameter affect directly the polymer properties.

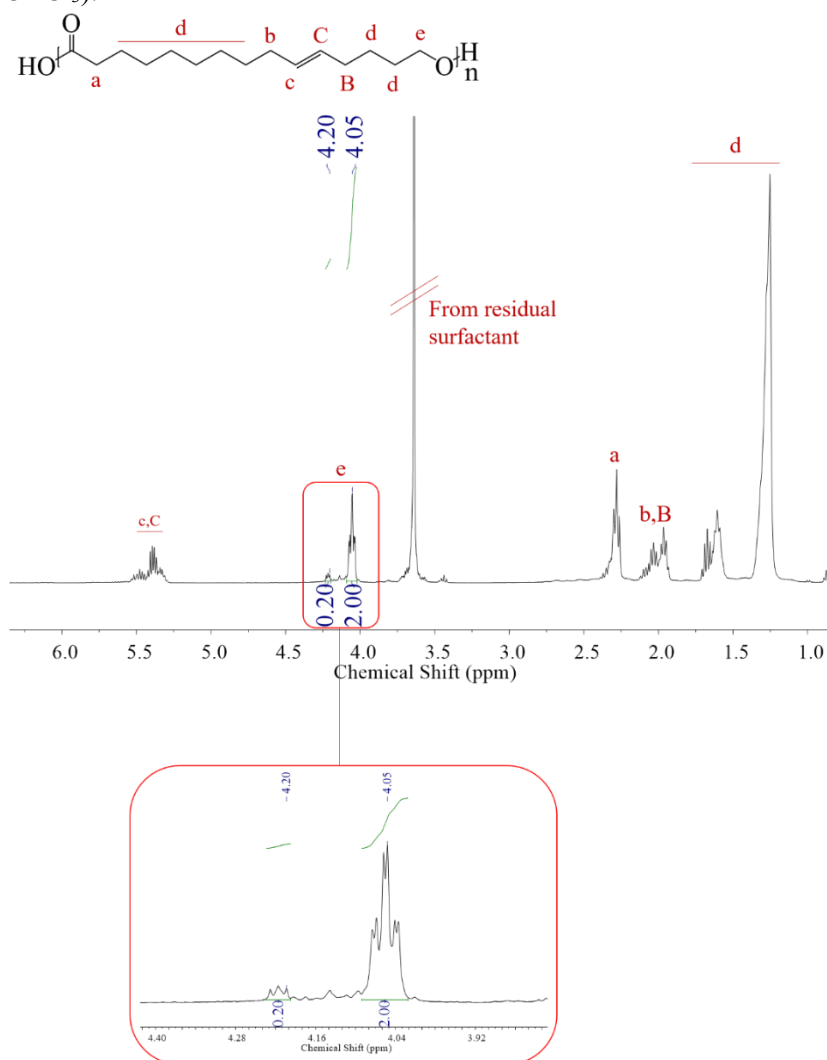
Figure 29 - Molecular weight distribution of P(GI) NPs produced using free CALB and hexadecane as co-stabilizer at different surfactant concentrations (1, 2.5 and 5 wt.%) at 45 °C (Table 2, entries GC1 to GC3).



P(GI) nanoparticles were also synthesized using NS40116 as biocatalyst under the same conditions as those reported to free CALB in exception to enzyme concentration (2.5 wt.% in relation to monomer). Molecular weights from 6,950 to 14,620 g mol⁻¹ were obtained and these values are considerably lower than those obtained using CALB as biocatalyst. In contrast to CALB, non-stable nanoparticles were formed when NS40116 was used and only larger particles without quality criteria in DLS were found (bimodal distributions).

Overall, the obtained molecular weight values are promising when compared with the literature for e-ROP of macrolactones to obtain ω -PPDL and poly(hexadecanolide) (PHDL) (TADEN; ANTONIETTI; LANDFESTER, 2003; MÅLBERG; FINNE-WISTRAND; ALBERTSSON, 2010). Besides, monomer conversions above 90% were found in all tested conditions. The conversions were measured comparing the peak areas of signals corresponding to the ester methylene group present in the monomer (δ , 4.20 ppm) and polymer (δ , 4.05 ppm). After 5 h of reaction, only a small peak corresponding to methylene group from monomer was observed in the NMR spectrum as observed in Figure 30.

Figure 30 - $^1\text{H-NMR}$ spectrum of PGI nanoparticles obtained via miniemulsion e-ROP (400 MHz in CDCl_3).



4.3.1.2 Nanoparticles synthesis using crodamol as co-stabilizer

Caprylic and capric acid triglycerides (crodamol GTCC) are medium chain triglycerides (MCT) derived from coconut oil. This class of oil is considered toxicologically and dermatologically innocuous and classified as GRAS (generally recognized as safe) by FDA. Besides, MCT has been used in pharmaceutical formulations as carriers for active ingredients, including drugs for diseases treatment. Considering the crodamol benefits, the miniemulsion was carried out using this component in order to replace hexadecane, once this last can limit NPs application in biomedical area and is the only co-stabilizer reported to date for

miniemulsion ROP (TADEN; ANTONIETTI; LANDFESTER, 2003; MÅLBERG; FINNE-WISTRAND; ALBERTSSON, 2010; PASCUAL; LEIZA; MECERREYES, 2013b).

Table 3 shows the intensity average diameter (Dp) and polydispersity index (PDI) measured by DLS. NPs in a similar range that PGI-hexadecane NPs were obtained, from 75 to 212 nm. Molecular weight of PGI NPs synthesized using Crodamol was measured by GPC (Table 3). Lower molecular weights were found when PGI polymerization was carried out at 60 °C (M_w of 7,550 g mol⁻¹), as observed previously for the ones prepared with hexadecane as co-stabilizer. The high molecular weight of PGI NPs (12,000 g mol⁻¹) was found at 45 °C.

Table 3 - e-ROP in miniemulsion of macrolactones GI using free CALB as lipase and crodamol as co-stabilizer.

Entry	Surf. wt. %	Temp °C	Dp nm ^a	PDI ^a	M_n ^b	M_w ^b	\bar{D} ^b
GC7	5	45	75±0.3	0.17±0.01	5,000	12,000	2.40
GC8	5	60	212±1.0	0.17±0.01	3,600	7,550	2.10

Reactions were carried out using 0.5 wt.% of enzyme in relation to monomer during 5 h.

^a Intensity average diameter (Dp) and dispersity (PDI) measured by DLS.

^b Number average (M_n) and weight average (M_w) molecular weights in g mol⁻¹ and, dispersity measured by GPC.

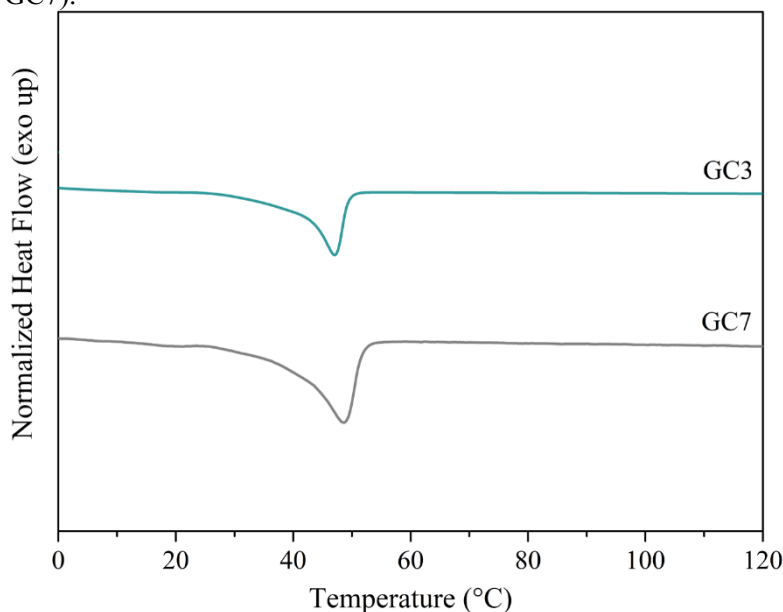
4.3.2 Thermal analysis of PGI NPs obtained by miniemulsion e-ROP

Thermal analysis of synthesized NPs was conducted by DSC. Table 4 shows the fusion enthalpy (ΔH_m), melting temperature (T_m) and crystallization temperature (T_c) of the materials. PGI NPs synthesized using hexadecane and crodamol presented melting points (T_m) of 47 °C and 49 °C and the fusion curves can be visualized in Figure 31.

Table 4 - Thermal properties of NPs obtained by miniemulsion e-ROP using different co-stabilizers.

Entry	Co-stabilizer	Temperature (°C)	ΔH_m (J/g)	T_m (°C)	T_c (°C)
GC3	Hexadecane	45	89	47	30
GC7	Crodamol	45	60	49	30

Figure 31 - DSC traces of NPs obtained via miniemulsion e-ROP (Table 3, entry GC3 and Table 4, entry GC7).

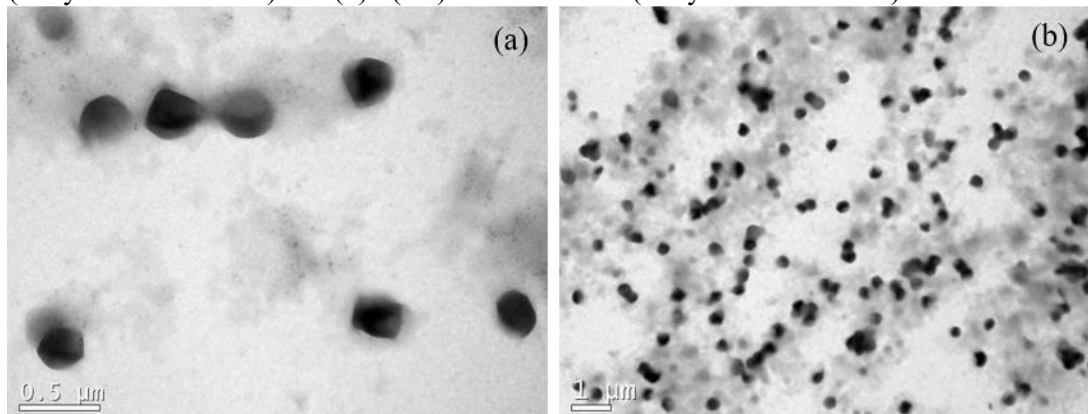


The obtained values of fusion enthalpy, melting temperature and crystallization temperature are in agreement with those reported in the literature for solution e-ROP of GI using toluene as solvent and immobilized lipase (Novozym 435) as biocatalyst (FOCARETE et al., 2001; MEULEN et al., 2008, 2011; CAI et al., 2010).

4.3.3 Morphology of PGI NPs

PGI NPs were characterized by Transmission Electron Microscopy (TEM) to evaluate particle morphology. TEM images of NPs synthesized using hexadecane and crodamol are shown in Figure 32 (a) and (b), respectively. It is possible to observe stable NPs after polymerization in the same range diameter of DLS analysis, (200-260 nm for reactions GC6 and GC8), without aggregates formation. According to Taden and co-workers (TADEN; ANTONIETTI; LANDFESTER, 2003), the ‘lemon-shaped’ morphology of these materials occurs due to low crystallization temperature (T_c) of poly(macrolactones) NPs in aqueous dispersion. Thus, the NPs crystallization occurs after polymerization (45 or 60 °C) and cooling leads to non-spherical NPs.

Figure 32 - TEM images of PGI NPs obtained via miniemulsion e-ROP. (a) P(G1) with hexadecane (entry GC6 in Table 3) and (b) P(G1) with crodamol (entry GC8 in Table 4).



4.4 CONCLUSIONS

Polymers obtained from macrolactones via enzymatic polymerization are potential for biomedical applications due to its properties, such as biocompatibility and biodegradability. In this work, unsaturated macrolactone was investigated by miniemulsion enzymatic ring-opening polymerization to produce biodegradable nanoparticles for future drug delivery applications. Nanoparticles with diameters from 70 to 280 nm were obtained and the diameter was affected by surfactant concentration. GPC analysis confirmed macrolactones polymerization, once molecular weights from 6,800 to 23,200 g mol⁻¹ were reached. Nanoparticles synthesis from unsaturated macrolactones, as globalide, allows to obtain functional latexes by polymeric chain crosslinking and/or functionalization with different compounds. Thus, this work showed a promising alternative way to produce biodegradable and biocompatible nanoparticles by organic solvent-free e-ROP, using the miniemulsion versatile technique. The results presented in this chapter were published in *Colloid and Polymer Science Journal*, 296, 861-869, 2018.

CHAPTER V

5. POST-POLYMERIZATION MODIFICATION OF POLY(GLOBALIDE) WITH PHOSPHOESTER GROUPS VIA THIOL-ENE CHEMISTRY

5.1 INTRODUCTION

Aliphatic polyesters as poly(lactones) and poly(macrolactones) are biodegradable, non-toxic and hydrophobic polymers. The high hydrophobicity and crystallinity of these materials limit their application in the biomedical field - specially for applications where the polymers need to be degraded, e.g. sutures, drug delivery and tissue regeneration - due to low cell adhesion and proliferation (NARAYANAN et al., 2016; SAGITHA et al., 2018). Different strategies have been reported in literature to increase poly(lactones) and poly(macrolactones) hydrophilicity including copolymerization (RODRIGUES et al., 2013; FERNÁNDEZ et al., 2014, 2017; BANSAL et al., 2015; WILSON et al., 2015a, 2015b; FERNÁNDEZ; ETXEBERRIA; SARASUA, 2016) or blending methods (NAKANE et al., 2008; PAWAR et al., 2015; ZIEMBA et al., 2018).

Amongst the variety of hydrophilic materials available to modify the structure of hydrophobic polymers, phosphoesters (PEs) has drawn attention since they are biocompatible, biodegradable, similar to biomacromolecules - as nucleic acids - and they show reduction in protein adsorption when in the organism (MONGE et al., 2011b; SHAO et al., 2012; SETTANNI et al., 2017b). Although first reports of phosphorous-based polymers were focused on flame-retardant application (JOSEPH; TRETSAKOVA-MCNALLY, 2011; VAN DER VEEN; DE BOER, 2012) these compounds are of great interest for biomedical field as biomaterials. Also, materials containing PEs groups have shown good bone adhesion and are indicated as promising supports for bone regeneration (MONGE et al., 2014; BAUER et al., 2017).

Compounds containing PEs groups and polyesters can be cleaved by water in physiological conditions and this reaction can be catalyzed by enzymes such as phosphodiesterase and lipase. Usually, these enzymes can be found in human cells. Hence, the enzymatic degradation from these hydrolases may facilitate the intracellular release of

encapsulated drugs (e.g., PEs nanoparticles in cancer cells (BENDER; BEAVO, 2006; WANG et al., 2009)). Another enzyme that degrades phosphate groups is alkaline phosphatase - produced for instance in bone and liver cells (WANG et al., 2005, 2008; STEINBACH; ALEXANDRINO; WURM, 2013). Copolymers composed of polyesters and phosphate groups were already reported in literature and in most cases polymers as ϵ -PCL (DU et al., 2006; SONG et al., 2008; WANG et al., 2008; ZHU et al., 2011; SHAO et al., 2012) and poly(D,L-lactide) (WEN; KIM; LEONG, 2003; YANG et al., 2009) were used, once they are recognized as safe by Food and Drug Administration (FDA). But differently from the present work, only copolymers with phosphoester groups in the polymer main chain were described and not in the side chain.

Besides the use of ϵ -PCL and PLLA as biomaterials, in the past few years the poly(macrolactone) poly(globalide), PGI, has attracted great attention for biomedical applications. The saturations in PGI backbone allow the easy functionalization and/or crosslinking via click chemistry-based reactions, such as diels-alder and thiol-ene addition. As mentioned above, the high crystallinity of PGI is one of the main issues limiting its application in the biomedical area. Furthermore, studies showed that PGI films are not susceptible to degradation even over periods of more than one year (MEULEN et al., 2008). In this context, several works showed the reduction in PGI crystallinity by simple copolymerization with less hydrophobic materials (GUINDANI et al., 2017), copolymerization followed by crosslinking (MEULEN et al., 2011; PASCUAL; LEIZA; MECERREYES, 2013b) and by addition of functional thiols in PGI chain via thiol-ene reactions (ATES; THORNTON; HEISE, 2011; DE OLIVEIRA et al., 2017a; SAVIN et al., 2018), and also the combination of different approaches (CLAUDINO et al., 2012; ATES; HEISE, 2014b). Consequently, modified PGI polymers presented different rates of degradation depending on the pendant group attached to the chain and depending on the morphology of the final polymer (films or fibers).

Moreover, high surface area of fibers favors polymer degradation once the medium can interpenetrate the porous structure and degrade the polymeric matrix. Considering the methods described in literature to produce polymeric fibers, electrospinning is a versatile and simple technique where fibers ranging from nanometers to micrometers can be obtained (AGARWAL; WENDORFF; GREINER, 2008). The unique properties, such as high surface area to volume ratio, porosity and similarity to the fibrillar structure of the collagen fibers enable these materials to mimic the natural extracellular matrix (ECM). Thus, polymeric fibers can improve

100

cell attachment, drug loading and mass transfer properties and these materials have been studied for biomedical areas, especially in tissue regeneration and regenerative medicine once they can be used as a support to regenerate damaged tissues (KALAOGLU-ALTAN; SANYAL; SANYAL, 2015; DUQUE SÁNCHEZ et al., 2016; SAGITHA et al., 2018).

Herein, we report the modification of PGI chain adding pendant phosphoester groups via thiol-ene coupling in PGI double bonds. To the best of our knowledge, to date phosphoester groups have not been applied to the modification of poly(macrolactones). In this context, thiols containing phosphate groups were first synthesized and characterized for further addition in the polymer backbone. The materials were then evaluated in terms of double bond conversion and thermal properties. Also, selected modified polymer was used to prepare fibers via electrospinning method. Here, we show the possibility of tuning PGI properties by changing different parameters in thiol-ene coupling and we believe that these materials are very attractive candidates for tissue engineering applications to support human fibroblasts attachment and proliferation.

5.2 MATERIALS AND METHODS

5.2.1 Materials

Diethyl chlorophosphate and diphenyl 6-mercapto-1-hexyl phosphate were dried under 4 Å molecular sieves. 2-mercaptoethanol and 6-mercapto-1-hexanol were dried under vacuum at 50 °C and pyridine was distilled from calcium hydride under inert conditions. Dried toluene was used as solvent. All reactants used for thiol-phosphoester synthesis were purchased from Sigma-Aldrich. Globalide (GI, 97% purity) was provided by Symrise and immobilized lipase B from *Candida antarctica* (Novozym 435) was purchased from Novozymes S/A. Tetrahydrofuran (THF) and chloroform (CHCl₃) were used as received. Phosphate-buffered saline (PBS) was purchased from Sigma-Aldrich and azobisisobutyronitrile (AIBN, Fluorechem) was recrystallized before use.

5.2.2 Methods

5.2.2.1 Synthesis of thiols containing phosphoester groups (PEs-SH)

Three different thiol phosphoesters were synthesized, denoted as TF1 (diethyl 2-mercaptoethyl phosphate), TF2 (diethyl 6-mercapto-1-hexyl phosphate) and TF3 (diphenyl 6-mercapto-hexyl phosphate). Syntheses were adapted from a literature procedure (CLOUET; KNIPPER, 1987).

Argon was purged in a dried 250 mL Schlenk flask equipped with a dropping funnel. Then a toluene solution of diethyl chlorophosphate (P1) (14.5 mL, 0.1 mol) - for syntheses 1 (TF1) and 2 (TF2) - and a toluene solution of diphenyl phosphoryl chloride (P2) (20.72 mL, 0.1 mol) - for synthesis 3 (TF3) - was added to the experimental apparatus and cooled to 0 °C in an ice bath. After reaching the specified temperature, pyridine (0.1 mol), the respective thiol (2-mercaptoethanol (T1) or 6-mercapto-1-hexanol (T2)) (0.1 mol) and toluene were added via syringe to the dropping funnel and slowly dropped (30 min) into the solution containing P1 or P2. After the addition was completed, the reaction was stirred overnight at room temperature. The solution was filtered, washed with 10% hydrochloric acid and dried over magnesium sulfate. The toluene was removed under reduced pressure and the product was purified by silica gel column using hexane:ethyl acetate (70:30). The respective R_f values for the final products were 0.2, 0.3 and 0.7 for TF1, TF2 and TF3, respectively. The reactional schemes for each thiol-phosphoester are represented in Figures 33, 34 and 35.

Figure 33 - Synthesis of diethyl 2-mercaptoethyl phosphate (TF1).

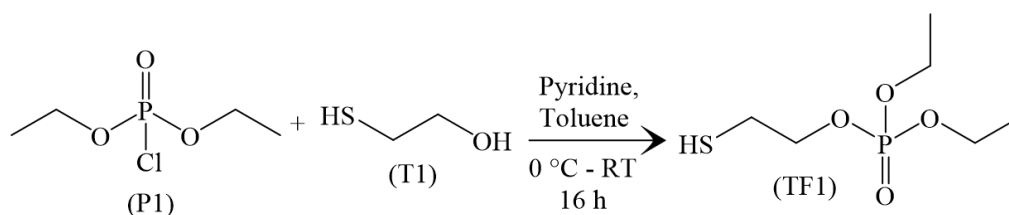


Figure 34 - Synthesis of diethyl 6-mercapto-1-hexyl phosphate (TF2).

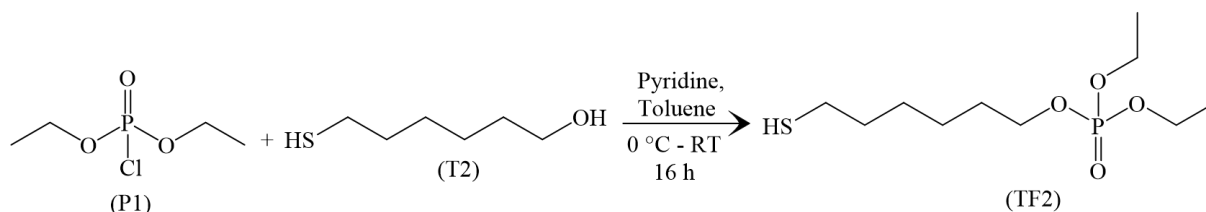
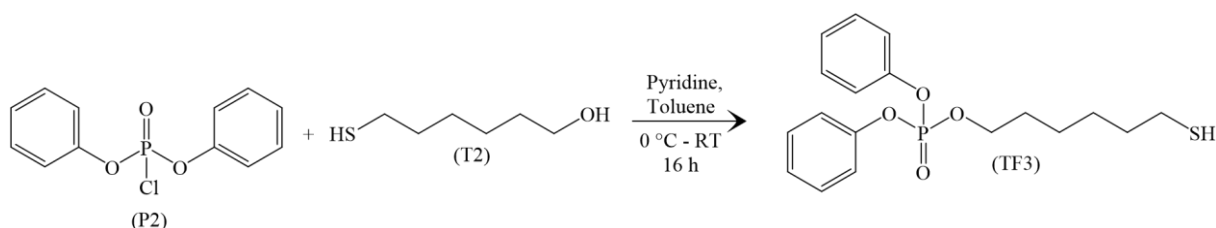


Figure 35 - Synthesis of diphenyl 6-mercapto-hexyl phosphate (TF3).



Synthesis of TF1 (diethyl 2-mercaptoethyl phosphate): Yield: 64%. $^1\text{H-NMR}$ (400 MHz, CDCl_3): δ (ppm) = 4.04-3.95 (m, 6H, $-\text{CH}_2\text{O}$), 2.70-2.61 (m, 2H, $-\text{CH}_2\text{S}$), 1.50-1.42 (t, 1H, $-\text{SH}$), 1.25-1.15 (t, 6H, $-\text{CH}_3$).

Synthesis of TF2 (diethyl 6-mercapto-1-hexyl phosphate): Yield: 72%. $^1\text{H-NMR}$ (400 MHz, CDCl_3): δ (ppm) = 4.08-3.92 (m, 6H, $-\text{CH}_2\text{O}$), 2.49-2.40 (m, 2H, $-\text{CH}_2\text{S}$), 1.65-1.50 (m, 8H, $-\text{CH}_2$), 1.55-1.50 (t, 1H, $-\text{SH}$), 1.30-1.25 (t, 6H, $-\text{CH}_3$).

Synthesis of TF3 (diphenyl 6-mercapto-1-hexyl phosphate): Yield: 60%. $^1\text{H-NMR}$ (400 MHz, CDCl_3): δ (ppm) = 7.27 (t, 4H), 7.19 (d, 4H), 7.14 (t, 2H), 4.21-4.12 (m, 2H, $-\text{CH}_2\text{O}$), 2.45-2.37 (m, 2H, $-\text{CH}_2\text{S}$), 1.68-1.58 (m, 8H, $-\text{CH}_2$), 1.54-1.44 (t, 1H, $-\text{SH}$).

5.2.2.2 Synthesis of PGI homopolymer

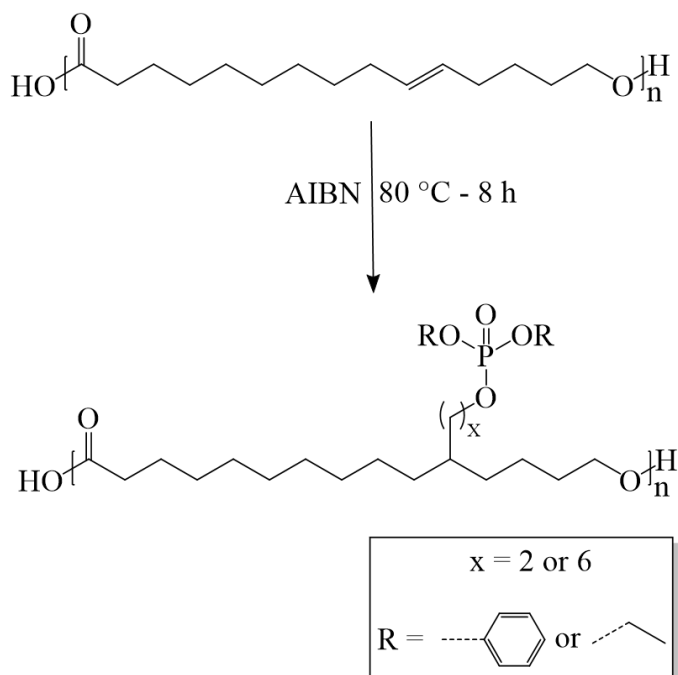
Poly(globalide) homopolymer was synthesized according to previous works (MEULEN et al., 2008; POLLONI et al., 2018) and as described in Chapter 3 of this thesis. The synthesis was conducted in toluene using a globalide:toluene mass ratio of 1:2 and 6 wt.% of Novozym 435 in relation to monomer. The reaction proceeded for 4 h at 60 °C. Then, dichloromethane was added, and the final solution was filtered and precipitated in cold methanol. The precipitate was dried under vacuum at room temperature to result in a polymer with a number average molecular weight (M_n) of 20,000 g mol^{-1} (dispersity (\mathbb{D}) of 3.5).

Poly(globalide) polymer: Yield: 80%. ¹H-NMR (400 MHz, CDCl₃): δ (ppm) = 5.55-5.30 (m, CH=CH), 4.10-4.02 (m, CH₂O(C=O)), 2.32-2.25 (m, CH₂(C=O)O), 2.12-1.92, 1.72-1.55, 1.38-1.20 (m, CH₂).

5.2.2.3 Post-polymerization modification of PGI

The synthesized phosphoesters containing thiol group (TF1, TF2 and TF3) were attached to PGI backbone via thiol-ene reactions and the effect of parameters as thiol:ene ratio and initiator concentration was evaluated. For each thiol-phosphoester, thiol to ene molar ratio of 0.5:1, 1:1 and 2:1 were tested varying AIBN concentrations of 1 and 5 mol% related to thiol. PGI and the respective thiol were placed in a vial until complete solubilization in THF. Then, the oil-soluble initiator AIBN was added and the mixture was stirred for 8 h at 80 °C. Subsequently, samples were dialyzed against ethanol to remove unreacted thiol using a 10 kDa MWCO membrane. For all experiments, the amounts of PGI for the desired thiol:ene molar ratios were calculated based on the number average molecular weight of PGI measured by GPC. A schematic representation of thiol-phosphoester addition in PGI chain can be seen in Figure 36.

Figure 36 - Modification of PGI with thiol-phosphoesters.



5.2.2.4 Electrospinning of PGI and PGI-phosphoester (PGI-PEs)

PGI (20,000 g mol⁻¹) and modified PGI were used to prepare fibers using a Spraybase electrospinning machine with a stationary collector at room temperature. The conditions for electrospinning were adapted from literature (DE OLIVEIRA et al., 2017a). Parameters as polymer concentration (25, 30 and 40 wt.% in relation to DCM) and voltage range (8, 10 or 12 kV) were evaluated. The flow rate (100 µL/min) and the distance from tip to collector (15 cm) were kept constant. The electrospun mats were collected on an aluminum foil for SEM analysis and on Teflon for biocompatibility tests.

5.2.2.5 Biocompatibility assays

Human fibroblasts (Detroit 551 - ATCC® CCL-110™) were selected to evaluate biocompatibility of pure and modified polymer. After electrospinning, the produced electrospun mats were cut into 8 mm disks, sterilized with 70% ethanol and washed with phosphate saline buffer - PBS. Subsequently, the fibers were incubated in regular growth medium - low Glucose ulbecco's modified Eagles's medium (DMEM) supplemented with 10% fetal bovine serum (FBS; Hyclone) and 1% penicillin/streptomycin (Sigma-Aldrich) for 30 min in humidified atmosphere with 5% CO₂ at 37 °C prior to cell seeding. After incubation, cells were seeded onto fibers at 2000 cells per sample (n=3). The seeded electrospun mats were kept in regular growth medium for up to 7 days. During this time the medium was changed twice. Cell viability was measured with AlamarBlue® reagent (Invitrogen) after 7 days of seeding. Cell proliferation was measured by DNA quantification after 1, 4 and 7 days of seeding using the PicoGreen assay (Quant-iT PicoGreen d₈DNA Assay Kit, Invitrogen). Fluorescence intensity was read on a plate spectrophotometer with excitation at 560 nm and emission at 590 nm for the AlamarBlue assay and excitation at 485 nm and emission at 538 nm for the PicoGreen assay. Statistical significance was evaluated by a two-way ANOVA with Bonferroni post-test. For a qualitative analysis of cell viability, seeded samples cultured for 7 days were stained with 4 mM calcein-AM (green = live) and 2 mM ethidium homidimero-1 (red = dead) in PBS for 15 min at 37 °C, protected from light (Live/dead viability/cytotoxicity assay,

Invitrogen). The samples were then analyzed in a confocal microscope at excitation and wavelengths of 515 and 615 nm, respectively.

5.2.3 Characterization

5.2.3.1 Chemical Characterization

Proton ^1H -NMR spectra were recorded using a Bruker spectrometer at 400 MHz. Chemical shifts were reported in parts per million (ppm) from 0.00 ppm using tetramethylsilane (TMS) - 1% (v/v) ($\delta = 0.00$) - as internal standard and the samples were solubilized in CDCl_3 ($\delta = 7.26$).

5.2.3.2 Thermal Properties

Thermal analysis of the modified polymers was conducted in a TA Instruments Q200 DSC, using approximately 9.0 mg of dried purified polymer. Temperature profiles from $-10\text{ }^\circ\text{C}$ to $120\text{ }^\circ\text{C}$ with heating and cooling rate of $10\text{ }^\circ\text{C}/\text{min}$ were applied under nitrogen atmosphere. The melting temperatures were determined by the second heating.

5.2.3.3 Molecular Weight Distribution

Gel permeation chromatography (GPC) was performed using a high-performance liquid chromatograph (Agilent 1200). All measurements were carried out using a Polymer Laboratories Gel $5\text{ }\mu\text{m}$ Mixed-C $300 \times 7.5\text{ mm}$ column at $40\text{ }^\circ\text{C}$ with DAD and RID detection. Molecular weights were determined against polystyrene standards (from 550 g mol^{-1} to $1.568 \times 10^6\text{ g mol}^{-1}$) using chloroform as eluent.

5.2.3.4 Fibers morphology

Fibers morphology was confirmed by scanning electron microscopy (SEM) with a Hitachi SU 6600 Fe-SEM instrument (Hitachi High Technologies Europe GMBH Whitebrook Park Lower Cookham Road Maidenhead SL6 8YA UK). Samples were placed on conductive

106

carbon stubs and coated with Pt/Pd using a Cressington HR sputter coater (Cressington Scientific Instruments Ltd. 4 Chalk Hill Watford WD19 4BX, England UK) giving a coating of 5 nm. An accelerating voltage of 2 kV, working distance of 10 mm, condenser lens of 21.0 and current of 20 μ A were used for all samples. Fiber size distribution was accessed by selecting randomly at least 70 fibers for each image using the software ImageJ and reported as number average fiber diameter.

5.3 RESULTS AND DISCUSSION

5.3.1 Synthesis of phosphoester containing thiol group (PEs-SH)

Aiming the chemical modification of PGI by the addition of a phosphoester at PGI unsaturations, different thiols containing phosphoester groups were synthesized. Syntheses were adapted from a literature procedure (CLOUET; KNIPPER, 1987) and conducted in toluene by slow addition of the respective thiol and pyridine to the chlorophosphate containing reaction medium over a period of 16 h.

The products were purified by silica gel chromatography to obtain high purity phosphoesters with yields greater than 60% and stored under refrigeration in a sealed container until use. The success of the syntheses as well as the purity of the compounds was accessed by $^1\text{H-NMR}$ spectroscopy (Figures 37, 38 and 39). Figure 38, for example, depicts the example of TF2 displaying characteristic peaks for the methylene groups adjacent to the thiol (b) and the phosphoester group (a). All integrated peak areas are in agreement with the expected values confirming the proposed structure of TF2.

Recently, several phosphoesters monomers have been synthesized for regenerative medicine applications once they have good cytocompatibility (MARSICO et al., 2012b). At the same time, polyesters derived from macrolactones are good alternatives for biomedical applications due to their biocompatibility and hydrolysable groups, but the high hydrophobicity of these polymers limits their application (MEULEN et al., 2008; SAVIN et al., 2018). This way, the combination of polyesters and phosphoesters might be an interesting solution to overcome the aforementioned problems (DU et al., 2006; SHAO et al., 2012).

Figure 37 - $^1\text{H-NMR}$ spectrum of diethyl 2-mercaptoethyl phosphate - TF1 (400 MHz in CDCl_3).

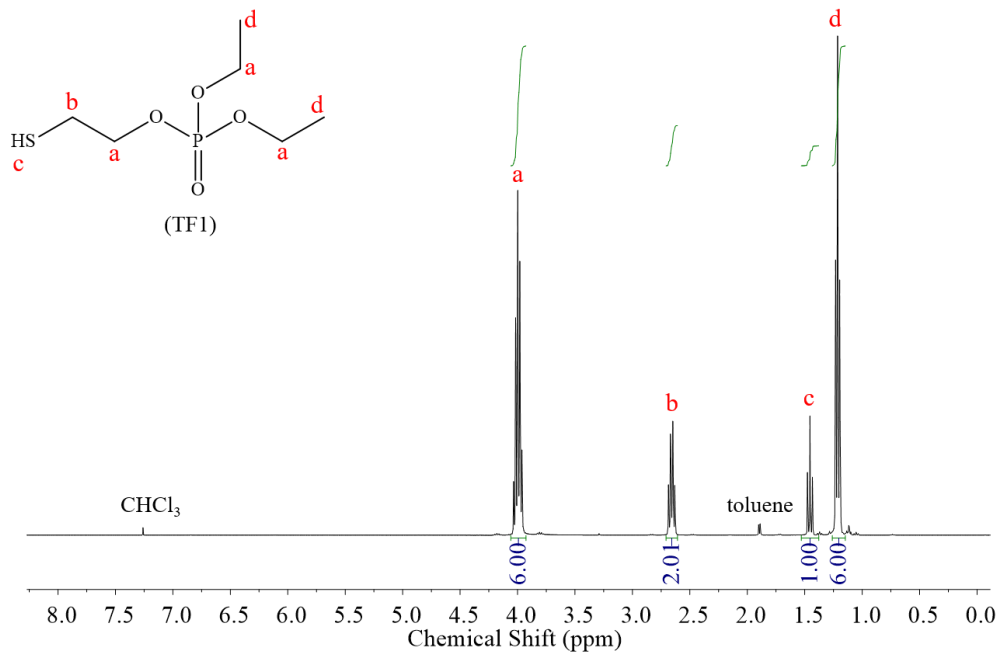


Figure 38 - $^1\text{H-NMR}$ spectrum of diethyl 6-mercapto-1-hexyl phosphate - TF2 (400 MHz in CDCl_3).

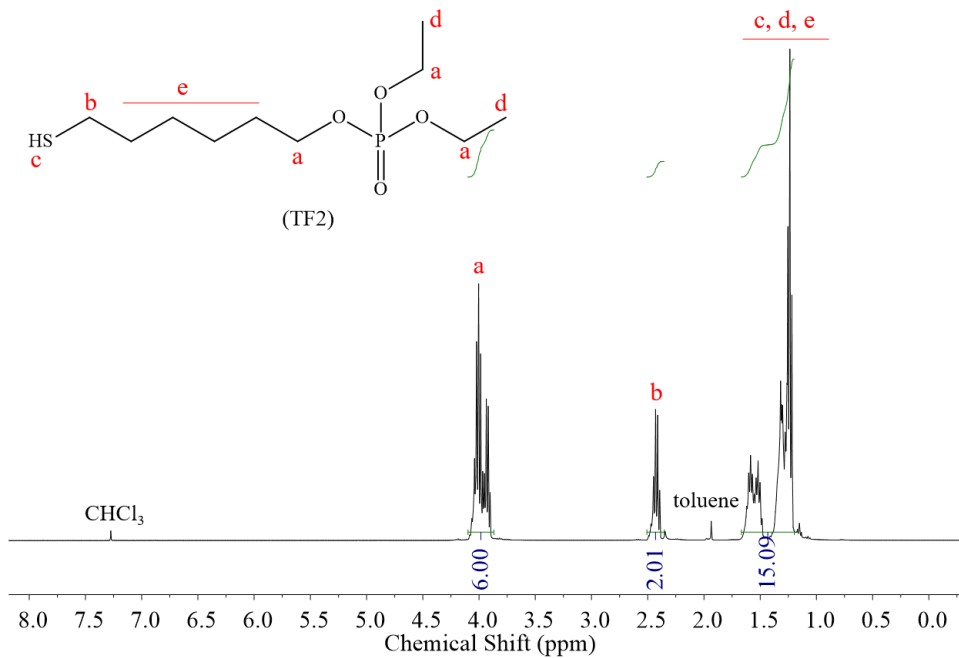
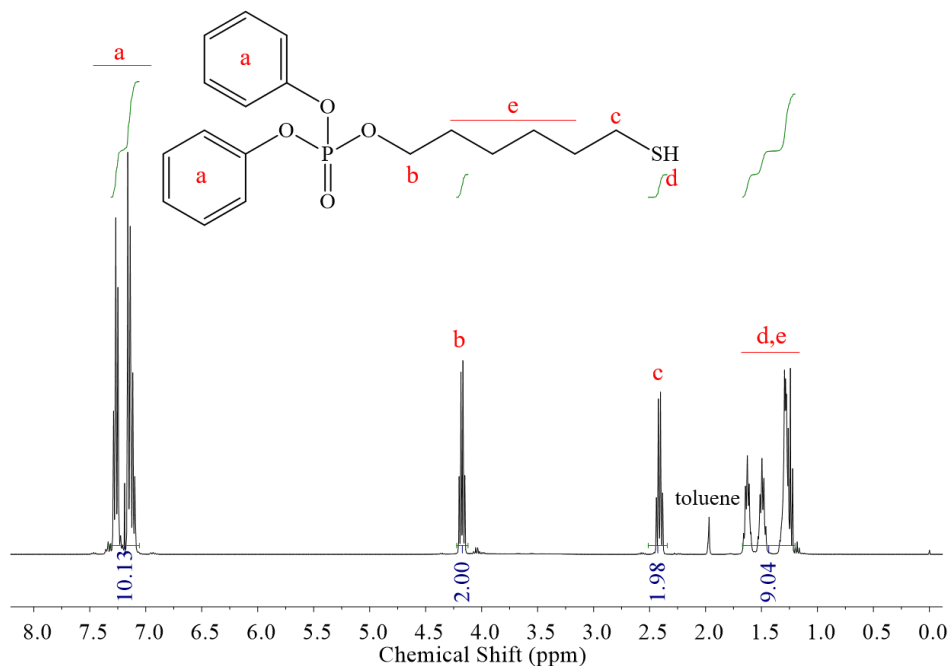


Figure 39 - $^1\text{H-NMR}$ spectrum of diphenyl 6-mercapto-1-hexyl phosphate - TF3 (400 MHz in CDCl_3).

5.3.2 Post-polymerization modification of PGI

PGI polymer with number average molecular weight of $20,000 \text{ g mol}^{-1}$ and dispersity of 3.6 was synthesized via enzymatic ring-opening polymerization using Novozym 435. The PGI molecular weight distribution and $^1\text{H-NMR}$ are shown in Figures 40 and 41. Subsequently, PGI chain was modified by adding phosphoesters groups in its chains via thiol-ene reactions.

Polymers with tunable thermal properties were prepared using different thiols and reactional conditions. The double bond conversion (DB%) was quantified by $^1\text{H-NMR}$ integrating peak areas corresponding to the double bond protons at 5.4 ppm and methylene groups at 4.05 ppm in case of polymers modified with TF1 and TF3. When TF2 was used, methylene peaks from thiol-phosphoester overlap methylene peak from polymer. In this case, conversions were estimated comparing double bond protons at 5.4 ppm and methylene groups near to carbonyl group at 2.3 ppm and a relation between the integrations in pure and modified polymer was used.

Figure 40 - GPC trace of PGI homopolymer.

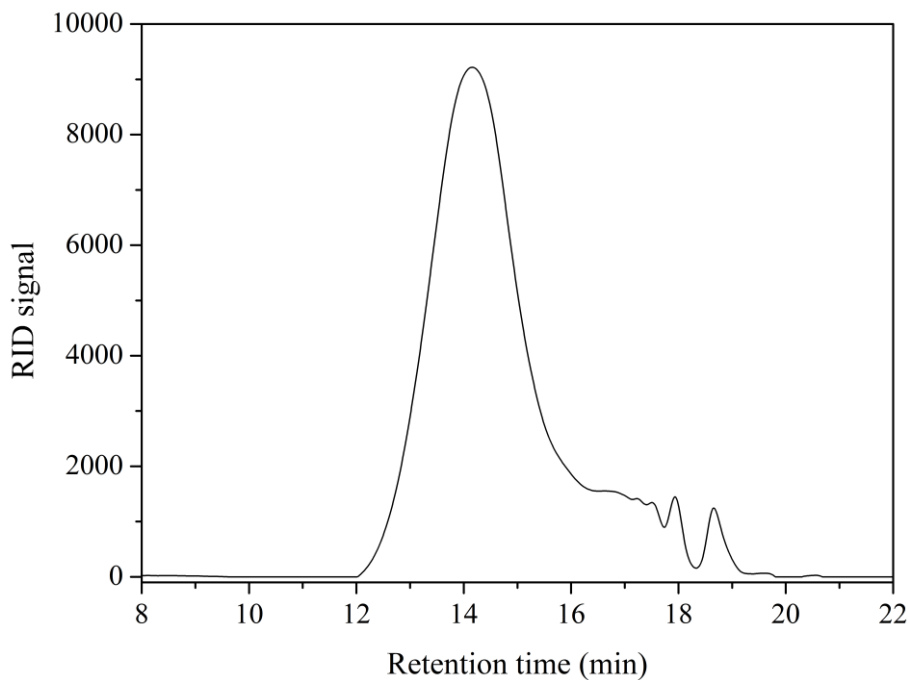
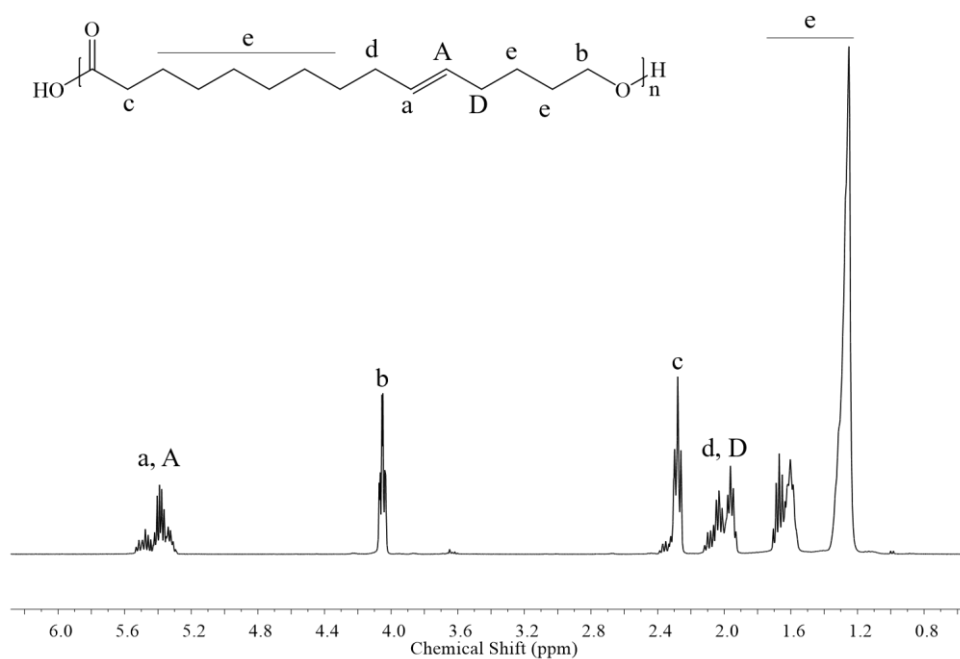


Figure 41 - $^1\text{H-NMR}$ spectrum of PGI homopolymer (400 MHz) in CDCl_3 .

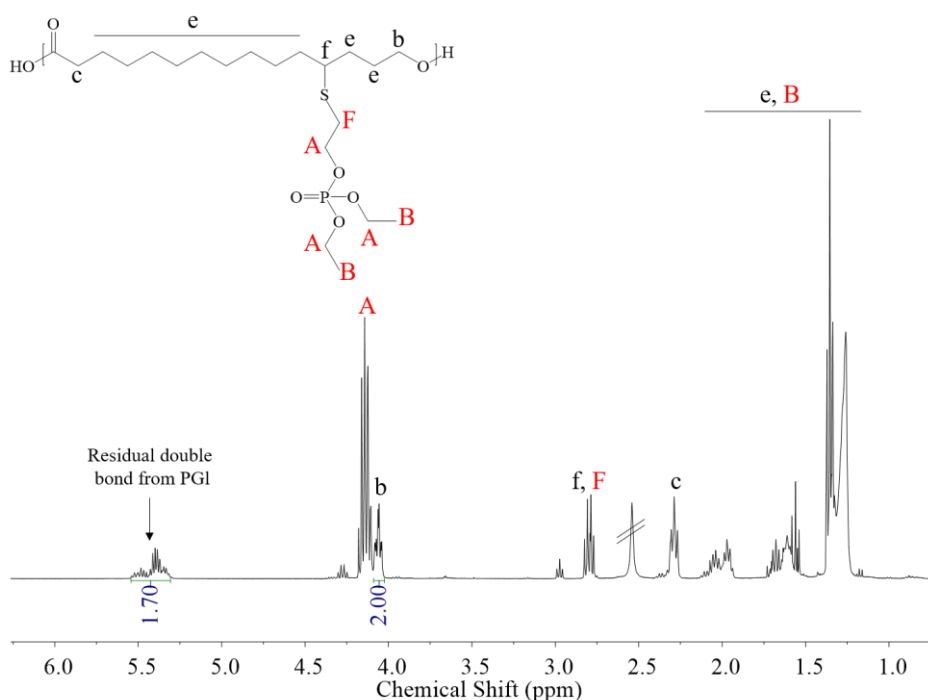


When PGI was modified with diethyl 2-mercaptoethyl phosphate (TF1), only low double bond conversions were observed. In a formulation consisting of 2:1 thiol:ene molar ratio and 5 mol% of AIBN a conversion of 15% was reached. This is presumably due to steric

110

hindrance caused by the short spacer. Figure 42 shows a $^1\text{H-NMR}$ spectrum of modified PGI with TF1 with a double bond conversion of 15%. It is possible to observe the presence of TF1 peaks confirming thiol addition in PGI backbone.

Figure 42 - $^1\text{H-NMR}$ spectrum of PGI modified with TF1 (400 MHz) in CDCl_3 .



DSC analysis showed the reduction in polymer melting point (T_m) and in enthalpy of fusion (ΔH_m) after TF1 addition in PGI chain (Figure 43) and the sample corresponds to polymer with 15% double bond conversion.

Meanwhile, double bond conversions in a range from 14 to 84% were achieved for PGI modified with diethyl 6-mercapto-1-hexyl phosphate (TF2) and all the characteristic peaks from TF2 were found in the final spectrum after thiol-ene coupling, as shown in Figure 44 for condition 6M6 (Table 5). As could be seen in Figure 44, only a small signal corresponding to double bond peaks (between 5.55 and 5.35 ppm) was observed when a molar ratio PGI:TF2 of 1:2 and AIBN concentration of 5 mol% were used, which confirms the consumption of the double bonds. Figure 45 shows the reduction in double bond signal in $^1\text{H-NMR}$ upon the increase of TF2 and AIBN concentrations in the formulation.

Figure 43 - Differential scanning calorimetry thermograms (second heating curve) before and after post-polymerization modification of PGI with diethyl 2-mercaptoethyl phosphate (TF1).

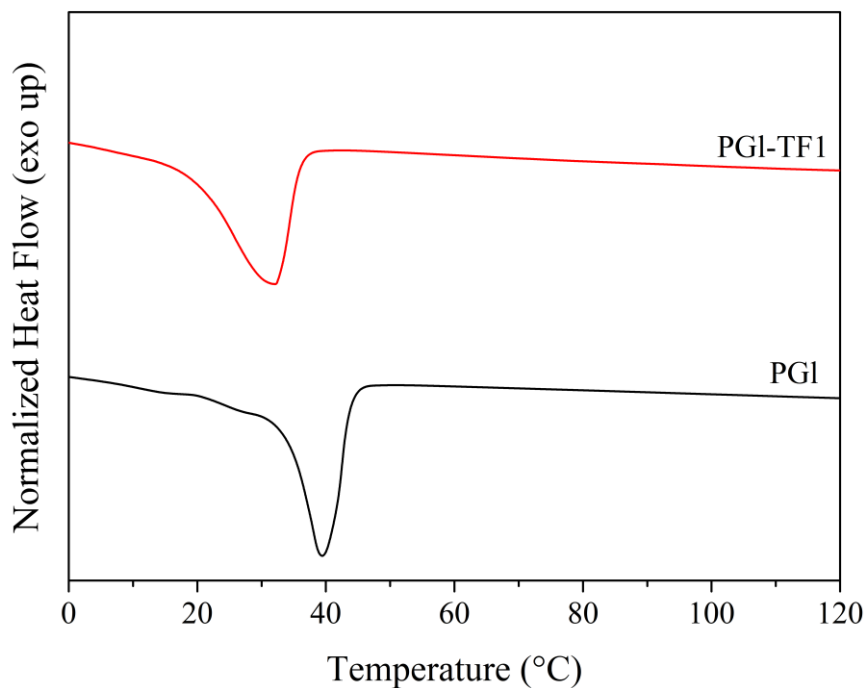


Table 5 - Poly(globalide) functionalization via thiol-ene reactions using TF2.

Entry	AIBN [mol%]	MR thiol:ene	DB ^a (%)	T _m ^b (°C)	ΔH _m ^b (Jg ⁻¹)
PGI	-	-	-	41.0	160.4
6M1	1	0.5:1	14	32.8	77.1
6M2	5	0.5:1	17	29.0	72.0
6M3	1	1:1	20	33.11	73.0
6M4	5	1:1	36	-	-
6M5	1	2:1	45	-	-
6M6	5	2:1	84	-	-

^a Double bond conversion % determined by ¹H-NMR.

^b Melting point determined by the second heating curve from DSC.

^c Enthalpy of fusion determined by integration of the second heating curve from DSC.

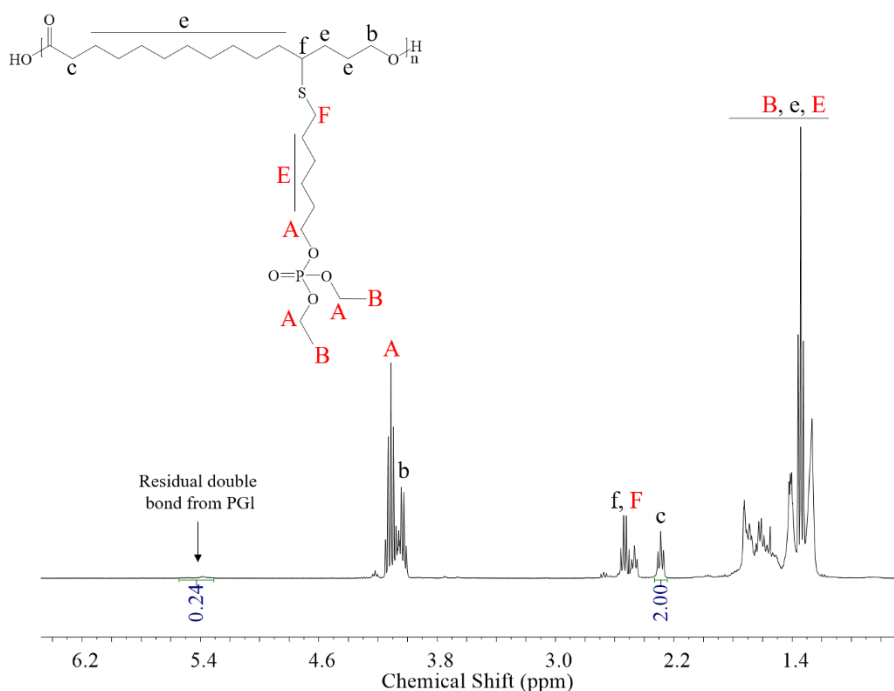
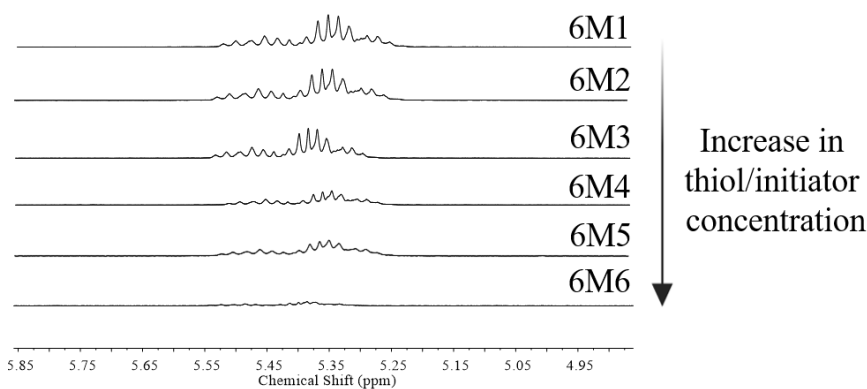
Figure 44 - $^1\text{H-NMR}$ spectrum of PGI modified with TF2 (400 MHz) in CDCl_3 (Entry 6M6 in Table 6).

Figure 45 - PGI double bond consumption after TF2 addition in PGI backbone.



Thermal analysis of PGI before and post-polymerization modification with TF2 was accessed by differential scanning calorimetry (DSC) and results are shown in Table 5. It is already known that PGI is a semi-crystalline polymer with a melting temperature (T_m) in a range of 40-48 °C (MEULEN et al., 2008; ATES; THORNTON; HEISE, 2011). The DSC melting temperature curves for PGI-TF2 polymers can be seen in Figure 46. It is possible to see the decrease in T_m after TF2 addition. In addition, completely amorphous polymers were obtained

for specific conditions. Figure 47 shows the clear difference between the polymers when TF2 concentration was raised in the formulation. PGI homopolymer is a white fluffy material and after TF2 addition in its chain, viscous and transparent amorphous polymers were obtained.

Figure 46 - Differential scanning calorimetry thermograms (second heating curve) before and after post-polymerization modification of PGI with diethyl 6-mercapto-1-hexyl phosphate (TF2).

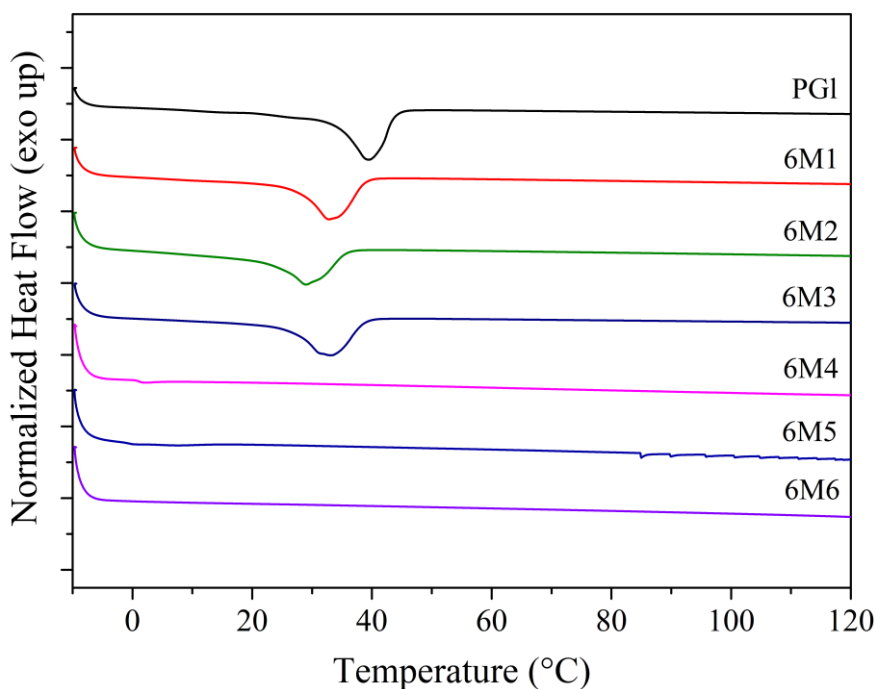
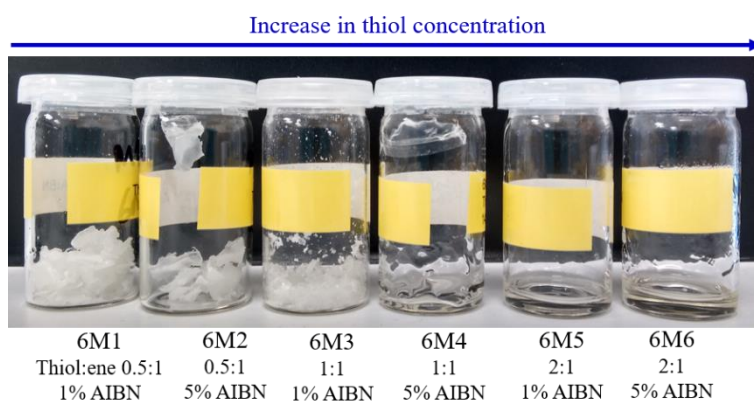


Figure 47 - PGI after modification with TF2 using different ratios of thiol:ene.



Results for PGI modification with diphenyl 6-mercapto-1-hexyl phosphate (TF3) showed a maximum double bond conversion of 28 % when a molar ratio thiol:ene of 2:1 was

used in 5 mol% AIBN concentration. When 0.5:1 thiol:ene ratio was used, TF3 did not conjugate in polymer chain. While TF3 also contains a hexyl spacer, it is speculated that the presence of the bulky benzyl rings could cause additional steric hindrance thus reducing the reaction efficiency. Double bond conversions can be seen in Table 6.

Table 6 - Poly(globalide) functionalization via thiol-ene reactions using TF3.

Entry	AIBN [mol%]	MR thiol:ene	DB ^a (%)	T _m ^b (° C)	ΔH _m ^b (Jg ⁻¹)
PG1	-	-	-	41.0	160.4
Ph3	1	1:1	4	28.3	112.3
Ph4	5	1:1	7	15.8	93.5
Ph5	1	2:1	17	16.1	37.5
Ph6	5	2:1	28	-	-

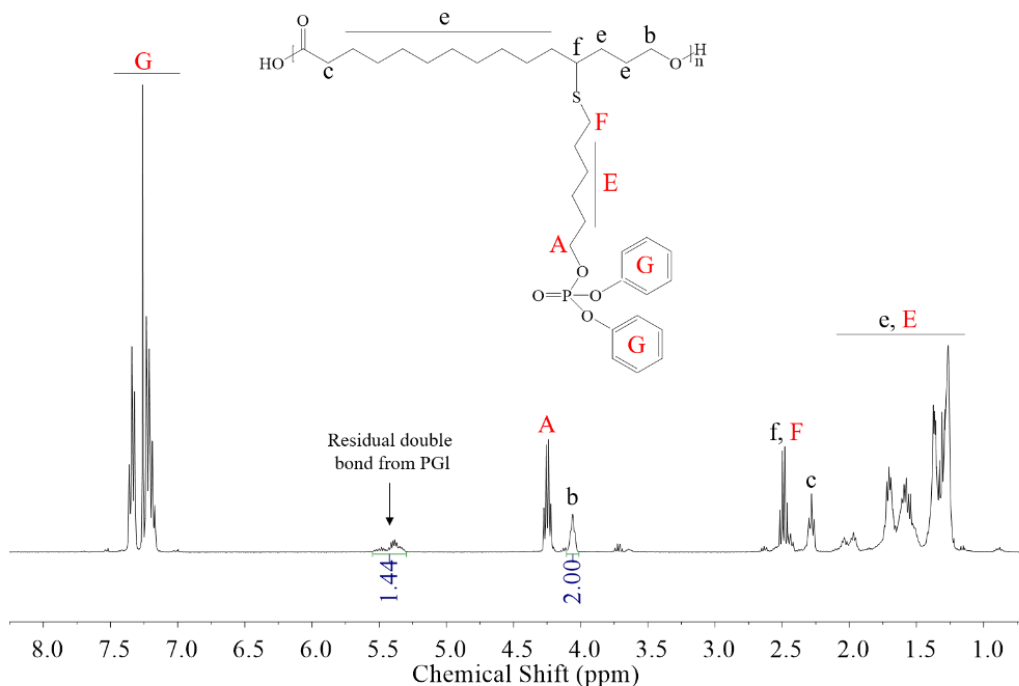
^a Double bond conversion % determined by ¹H-NMR.

^b Melting point determined by the second heating curve from DSC.

^c Enthalpy of fusion determined by integration of the second heating curve from DSC.

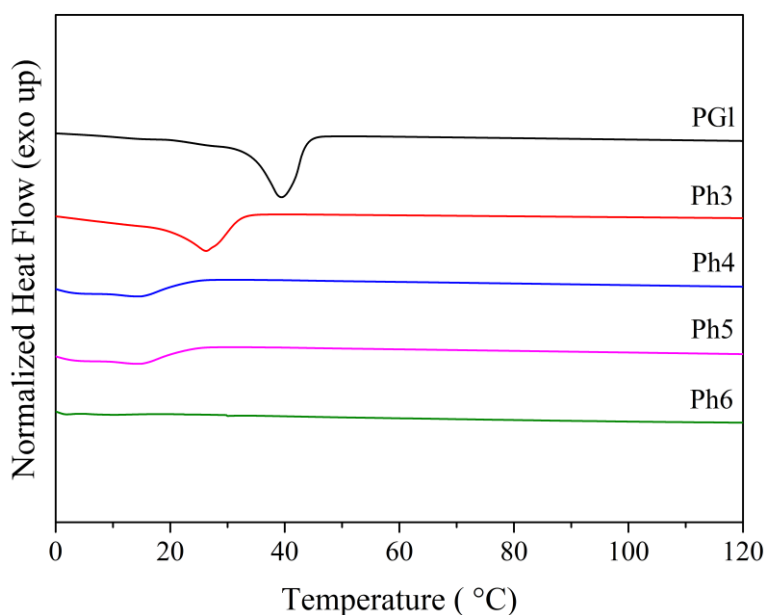
¹H-NMR shows the reduction in double bond signal after thiol addition and the appearance of TF3 peaks in the functionalized polymer spectra (Figure 48) with peaks corresponding to thiol - benzene ring peaks (7.4-7.1 ppm), methylene groups near to oxygen (4.28-4.20 ppm) and methylene groups near to sulfur atom (2.52-2.44 ppm).

Figure 48 - $^1\text{H-NMR}$ spectrum of PGI modified with TF3 (400 MHz) in CDCl_3 (Entry Ph6).



DSC melting temperature curves for PGI-TF3 polymers can be seen in Figure 49. It is possible to see the decrease in T_m after TF3 addition and the formation of amorphous polymers. DSC curves obtained for each polymer showed that the melting temperature and the enthalpy of fusion were dependent on the double bond conversion and the length of thiol-phosphoester chain. Therefore, the thermal properties of the polymers modified with longer chain thiols (with TF2 and TF3) were more affected after functionalization, once they led to a greater distance between polymer chains and consequently reduced the crystallinity of the final material. Additionally, when TF2 and TF3 were added to PGI backbone completely amorphous polymers could be obtained depending on the initiator concentration and thiol:ene ratio.

Figure 49 - Differential scanning calorimetry thermograms (second heating curve) before and after post-polymerization modification of PGI with diphenyl 6-mercapto-hexyl phosphate (TF3).



Generally, the coupling yield was affected by increasing the AIBN concentration and thiol:ene ratio. In addition, higher double bond conversions were obtained when thiols containing longer chains were used, as TF2 and TF3. Thiol-ene reactions have been reported in literature for PGI modification and crosslinking using thiols or dithiols containing different functional groups as alcohol and amines (ATES; THORNTON; HEISE, 2011; CLAUDINO et al., 2012). When PGI functionalization with *N*-acetylcysteamine (nACA) was reported, the authors reached double bond conversions in a range from 17 to 95% using molar thiol:ene ratios of 0.4:0.6 and 6.6:0.6, respectively and high conversions were only obtained in an excess of thiol in relation to double bonds (11 times more thiol than ene) (ATES; THORNTON; HEISE, 2011).

A similar approach was reported for the modification of a copolymer of PGI and ϵ -PCI using *N*-acetylcysteine as thiol. The authors tested different contents of unsaturation (from PGI) in the polymer backbone. When a 90/10 ratio of GI/CI was used in the formulation, a double bond conversion of 42% was observed (GUINDANI et al., 2018).

5.3.3 Electrospun PGI and PGI-PEs

Solid PGI-TF2 modified polymer, sample 6M1, with low double bond conversion (14%) was selected to prepare fibers by electrospinning. The crystalline structure of the polymer is affected even in low degrees of thiol-phosphoester addition to the polymer chain, as shown in Figure 46, and the creation of amorphous domains makes these new materials more susceptible to degradation.

Several parameters should be considered to obtain homogeneous and well-defined fibers. Among them, the choice of the appropriate solvent, polymer concentration, applied voltage, distance from electrode to collector and flow rate are the most important factors. Thus, the main parameters were chosen adapting from a procedure reported in literature (DE OLIVEIRA et al., 2017a). Distance from tip to collector and flow rate were kept constant in 15 cm and 100 $\mu\text{L}/\text{min}$, respectively and parameters as polymer concentration (25, 30 and 40 wt.% of polymers in relation to DCM) and voltage (8, 10 and 12 kV) were evaluated. The best conditions to prepare well defined fibers using different voltages and polymer concentrations are shown in Table 7. Furthermore, SEM micrographs and fibers size distribution of PGI and 6M1 fibers are presented in Figures 50 and 51.

Table 7 - Experimental conditions selected for the preparation of PGI and PGI-PEs fibers using a flow rate of 100 $\mu\text{L}/\text{min}$ and a distance from tip to collector of 15 cm.

Polymer	Polymer concentration (wt.%)	Voltage (kV)	Fiber diameter (μm)
PGI	30	12	8.3
6M1	30	8	11.4

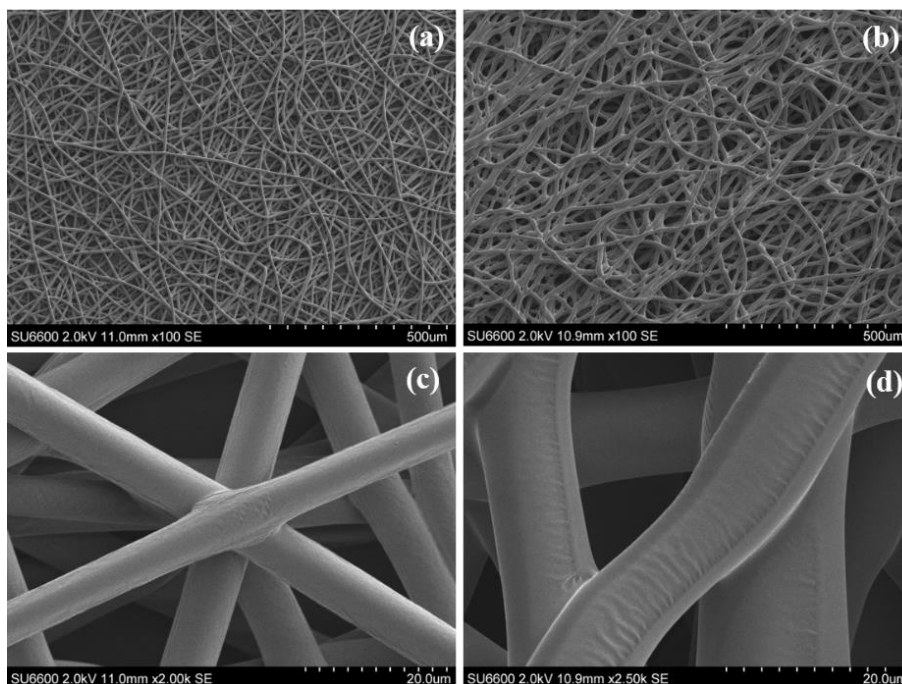
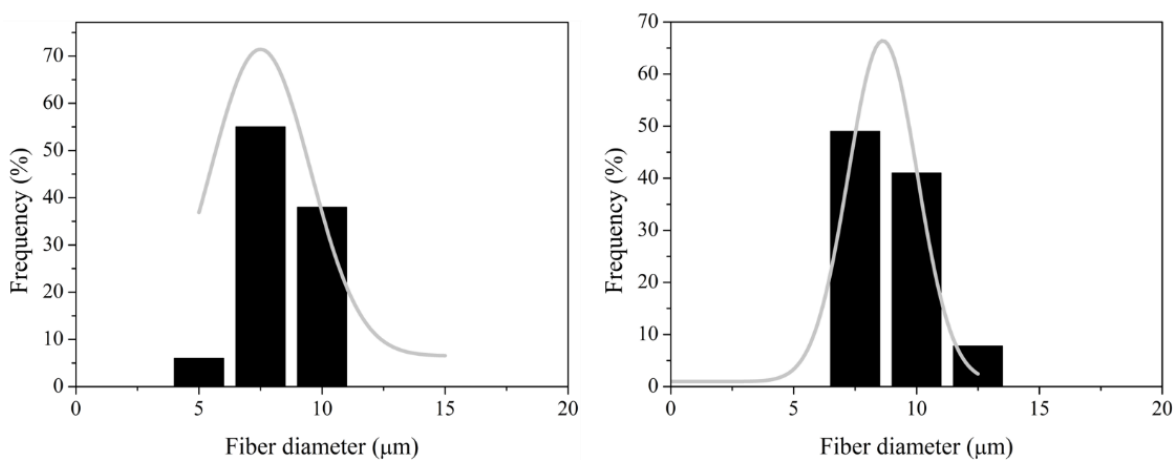
Figure 50 - SEM images of (a) PGI - 500 μm , (b) 6M1 - 500 μm , (c) PGI - 20 μm and (d) 6M1 - 20 μm .

Figure 51 - Fiber size distribution of (a) PGI and (b) 6M1 fibers.



Homogeneous and smooth fibers around 8-11 μm in diameter were obtained for both materials. Despite the low melting point of these polymers, we have shown that it is possible to produce fibers by this technique. Besides, after electrospinning these fibers can be crosslinked by means of the remaining double bonds in polymer chain to obtain amorphous polymers, allowing their use in body conditions.

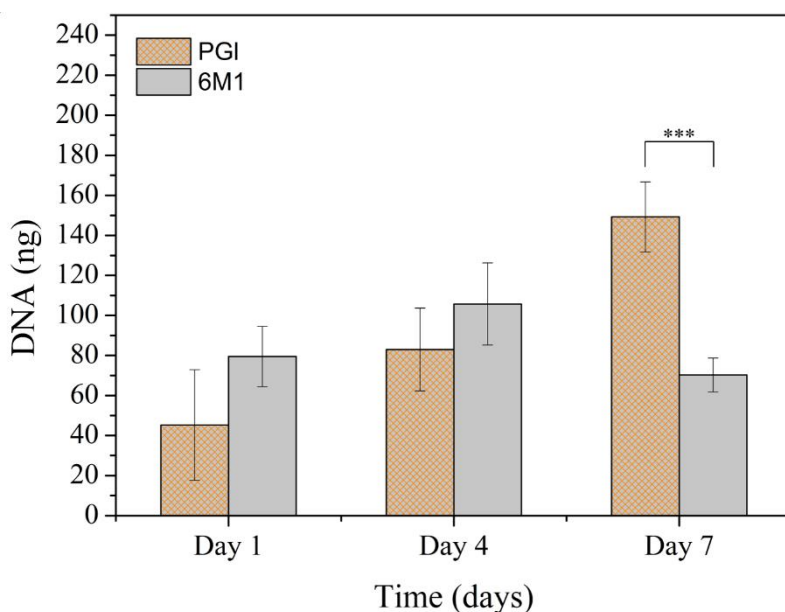
Oliveira and co-workers were the first group to report PGI fibers production by electrospinning and the authors obtained well defined fibers with an optimal diameter of 7.9 μm using PGI homopolymer with a similar molecular weight (DE OLIVEIRA et al., 2017a).

5.3.4 Biocompatibility of PGI and PGI-PEs fibers

In the last years, different studies have shown that PGI is a non-toxic material (MEULEN et al., 2008; DE OLIVEIRA et al., 2017a), which has drawn the attention of many researchers to investigate its use for biomedical applications. In the present work the biocompatibility of the modified PGI with TF2 (6M1) was accessed using human dermal fibroblast cells. Fibroblast cells in a concentration of 2000 cells/disc were seeded on PGI and 6M1 fibers to check the proliferation and metabolic activity.

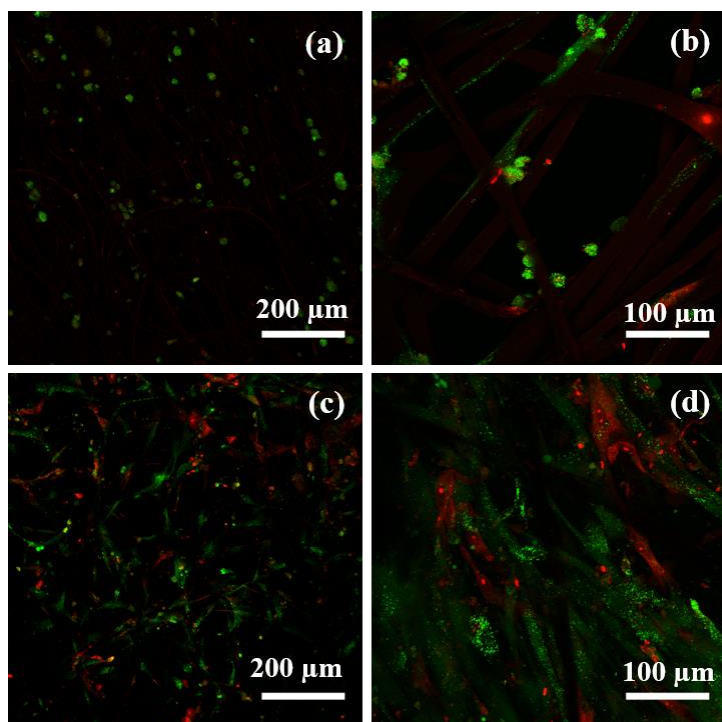
Cell proliferation was quantified by measuring DNA content by Pico Green assay on PGI and 6M1. DNA content evidenced that cells proliferated on the modified polymer from day 1 to day 4. From day 4 to day 7, however, there was a decrease in DNA content (Figure 52). Cell metabolic activity was investigated by AlamarBlue reduction after 7 days of culture. Metabolic activity for PGI and 6M1 after 7 days was 1 ± 0.66 and 0.82 ± 0.35 , respectively.

Figure 52 - Proliferation of cells seeded on PGI and 6M1 fibers at day 1, 4 and 7. Data is reported as mean \pm standard deviation, *** $p < 0.001$ (n=3).



Live/dead staining followed by confocal microscopy imaging was performed to qualitatively observe cell viability after 7 days of culture (Figure 53). For both polymers, a higher number of green cells (live) was detected when compared with red cells (dead).

Figure 53 - Live/dead images of cells at day 7 in PGI (a,b) and 6M1 (c,d).



5.4 CONCLUSIONS

In the present chapter, we have shown the synthesis of different phosphoesters containing thiol groups and the subsequent addition of these to the PGI main chain via thiol-ene reactions. Highly pure thiols containing phosphoesters with different chain lengths were synthesized. The efficiency of thiol addition was correlated with the thiol type and when TF1 was used only low conversions of the double bond were observed. When TF2 and TF3 were used to modify the PGI chain, double bond conversions up to 84% and 30% were found, respectively. Polymer thermal properties were changed by the insertion of pendant groups in polymer chain and polymers with lower melting points, as well as completely amorphous polymers were obtained. Solid polymer modified with TF2 (14% of double bond conversion) was selected to obtain fibers by electrospinning and homogeneous fibers with diameters around

11 μm were produced. Moreover, 6M1 showed to have similar cell metabolic activity when compared with non-modified polymer fibers. The data obtained from this study show the possibility to tune PGI properties by inserting different functional groups in its structure and turn PGI a good candidate for applications as degradable material in drug delivery and tissue regeneration.

CHAPTER VI

6. CLICK MODIFICATION AND CROSSLINKING OF POLY(GLOBALIDE) VIA ALDER-ENE REACTIONS

6.1 INTRODUCTION

Aliphatic polyesters are among the most widely used biodegradable polymers in biomedical applications including sutures, nanoparticles for drug delivery and scaffolds for tissue regeneration (SEYEDNEJAD et al., 2011). The ring-opening polymerization and the post-polymerization modification of the cyclic unsaturated macrolactone globalide (GI) has been studied in the last few years due to its properties as biocompatibility and non-toxicity (MEULEN et al., 2008; VAN DER MEULEN et al., 2011b; ATES; THORNTON; HEISE, 2011; CLAUDINO et al., 2012; PASCUAL; LEIZA; MECERREYES, 2013b; ATES et al., 2014; ATES; HEISE, 2014a; DE OLIVEIRA et al., 2017a; POLLONI et al., 2018; SAVIN et al., 2018; GUINDANI et al., 2019). PGI modification and crosslinking are very promising strategies once different functional groups can be added to the polymer chain. When crosslinked, the formed polymeric networks can be tuned in order to create a material with different release profiles in drug delivery systems. Additionally, it is possible to decrease polymer hydrophobicity and crystallinity favoring cell proliferation and adhesion (MEULEN et al., 2008).

Click-like reactions as thiol-ene have been described in literature in the last few years for polymer modification and crosslinking using alkenes and thiols/dithiols (TURUNC; MEIER, 2013; DURHAM et al., 2017; MACHADO; SAYER; ARAUJO, 2017). Some recent works described PGI modification and crosslinking via thiol-ene reactions in order to modify PGI crystallinity, add different functional groups in its structure and improve its mechanical properties (ATES; THORNTON; HEISE, 2011; CLAUDINO et al., 2012; ATES; HEISE, 2014a; DE OLIVEIRA et al., 2017a; SAVIN et al., 2018; GUINDANI et al., 2019). Thiol-ene reactions are highly selective and robust systems, although the double bond position (from monomer/polymer) can affect the system reactivity and usually internal double bonds are less

reactive than terminal ones and, in this case, a molar excess of thiol must be used in relation to ene (LOWE, 2014).

Triazolinediones (TADs) have recently become popular in polymer modification and crosslinking due to developments in TAD synthesis and their click-reactions at ambient temperature without any catalyst. This way, TADs have been used to modify unsaturated polymers (VANDEWALLE et al., 2016; VLAMINCK et al., 2016a), crosslink vegetable oils (TURUNC; MEIER, 2013; CHATTOPADHYAY; DU PREZ, 2016), preparation of films (HANAY et al., 2017a) and hydrogels (HANAY et al., 2017b, 2018). Besides, the reaction can easily be monitored by the color change as TADs distinctive red/pink color disappears upon reaction. The reaction can be conducted at room temperature via either diels-alder or alder-ene reactions without the need for a catalyst (DE BRUYCKER et al., 2016). Furthermore, the double bond is preserved after the reaction - shifted to the adjacent carbon - allowing the post-modification of polymer backbone with additional groups using the available unsaturation. Unlike, in thiol-ene systems the double bond from monomer/polymer is consumed during the radical addition in the chain.

Nanometric and micrometric fibers obtained from electrospinning are promising alternatives for tissue engineering applications due to their attractive properties such as large surface area, porosity and the fibrillar structure that is similar to collagen fibers. Besides, electrospun fibers can be used as a support to immobilize and entrap proteins, drugs and enzymes of interest (KALAOGLU-ALTAN; SANYAL; SANYAL, 2015; KHARAGHANI et al., 2018). Heijden and co-workers studied the post-treatment of styrene-butadiene-styrene (SBS) triblock copolymers fibers submerging the membranes in TAD solutions in order to improve fibers mechanical properties (HEIJDEN et al., 2015, 2017). Aside of tuning fiber properties, the process is eco-friendly once no energy is applied during the reaction.

ϵ -PCL is one of the most commonly used polyesters for biomedical applications and some recent work (BASKO et al., 2017; DEFIZE et al., 2017; VANDEWALLE et al., 2018) described ϵ -PCL modification and crosslinking by TAD click chemistry. Unlike PGL, ϵ -PCL does not have readily available double bonds in its backbone. Therefore, several reaction steps are required to add unsaturation in α,ω ϵ -PCL backbone for a further click reaction. To the best of our knowledge, modification and crosslinking of unsaturated poly(macrolactones), as PGL polymer, by TADs click chemistry was never reported. Herein, we showed the fast and selective

TAD chemistry to modify and crosslink PGI. Moreover, we investigated thermal and mechanical properties of TAD crosslinked fibers obtained via electrospinning.

6.2 MATERIALS AND METHODS

6.2.1 Materials

All chemicals were purchased from Sigma-Aldrich unless otherwise noted. Globalide (GI, 97% purity) was purchased from Symrise and immobilized lipase B from *Candida antarctica* (Novozym 435) was purchased from Novozymes S/A. Dry ethanol was purchased from Romil.

6.2.2 Methods

6.2.2.1 Synthesis of PGI

PGI homopolymer was synthesized according to previous works (MEULEN et al., 2008; POLLONI et al., 2018) and as described in Chapters 3 and 5. The synthesis was conducted in toluene using a globalide:toluene mass ratio of 1:2 and 6 (wt.)% of Novozym 435 in relation to monomer. The reaction proceeded for 4 h at 60 °C. Then, dichloromethane (DCM) was added and the final solution was filtered and precipitated in cold methanol. The precipitate was dried under vacuum at room temperature to result in a polymer with a number average molecular weight (M_n) of 20,000 g mol⁻¹ (dispersity (\bar{D}) of 3.5).

Poly(globalide) polymer: Yield: 80%. ¹H-NMR (400 MHz, CDCl₃): δ (ppm) = 5.55-5.30 (m, CH=CH), 4.10-4.02 (m, CH₂O(C=O)), 2.32-2.25 (m, CH₂(C=O)O), 2.12-1.92, 1.72-1.55, 1.38-1.20 (m, CH₂).

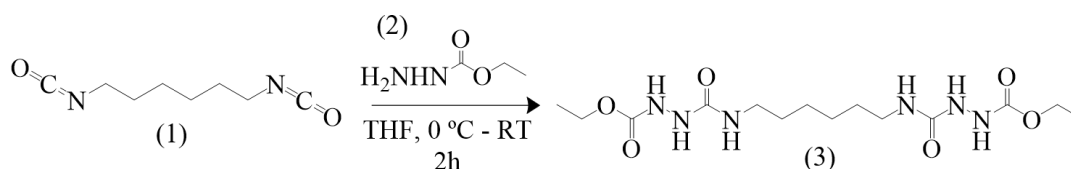
6.2.2.2 Synthesis of triazolinediones

4-phenyl-1,2,4-triazoline-3,5-dione (PTAD) was purchased from Sigma-Aldrich. On the other hand, hexamethylene bis-TAD (HM-bisTAD) and methylene diphenyl bis-TAD

(MDP-bisTAD) were synthesized in three steps as previously reported by Little and co-workers and a few years later by Hanay and co-workers (LITTLE et al., 2002; HANAY et al., 2017b).

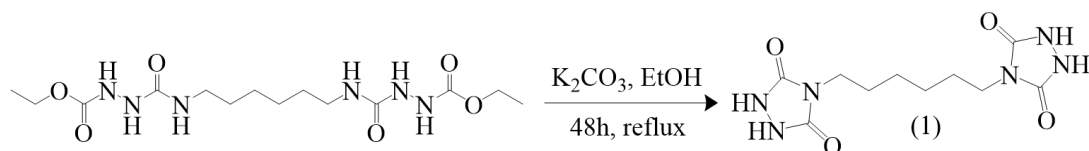
In the first step of HM-bisTAD synthesis, ethyl carbazate (2 in Figure 54) (10.4 g) was dissolved in 200 mL of anhydrous tetrahydrofuran (THF) under inert atmosphere in an ice bath. Then, hexamethylene diisocyanate (1 in Figure 54) (8 mL) was added dropwise in the previous solution. After addition, the reaction proceeded at room temperature during 2 h. The final mixture was filtrated, and the product (3 in Figure 54) (hexamethylene bishydrazine carboxylate) was washed with THF and dried overnight under vacuum to give a pure product with 95% yield.

Figure 54 - Hexamethylene bishydrazine carboxylate.



The product obtained in step 1 (5 g) and potassium carbonate (7.5 g) were suspended in 300 mL of pure ethanol under nitrogen atmosphere. The mixture was allowed to react for 2 days in reflux. After 2 days, the ethanol was evaporated, and the final material dissolved in a small amount of distilled water. Then, the pH was adjusted to 1.5 by the dropwise addition of concentrated hydrochloric acid (HCl) at 0 °C. The precipitated fraction was washed with distilled water and dried to give a pure product (hexamethylene bisurazole, 1 in Figure 55) with 87% yield.

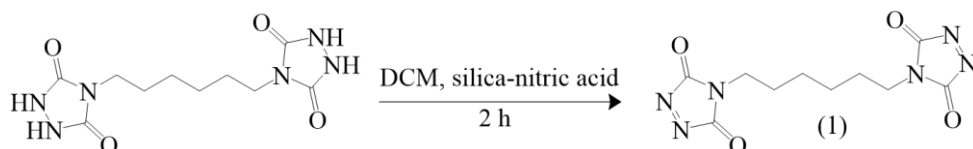
Figure 55 - Hexamethylene bisurazole synthesis.



The urazole obtained in step 2 was added to a flask and suspended in 250 mL of dichloromethane (DCM) under nitrogen atmosphere. A mixture of nitric acid and silica was prepared and added slowly to the flask. Typically, for 5g of urazole a respective amount of 15 g of oxidizer was used (11.28 g of nitric acid + 8 g of silica). After 2 h, the mixture was filtered,

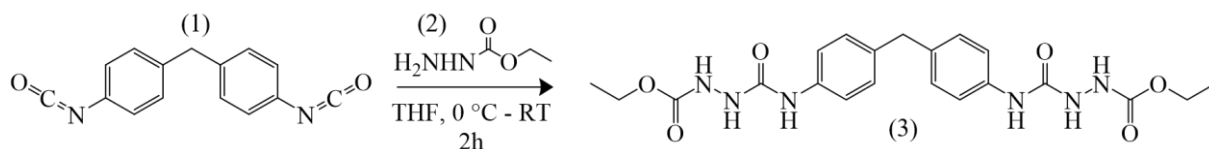
dried over anhydrous magnesium sulfate (MgSO_4) and the DCM was evaporated to obtain the final product (hexamethylene bis-TAD, 1 in Figure 56) with 62% yield.

Figure 56 - Hexamethylene bis-TAD synthesis.



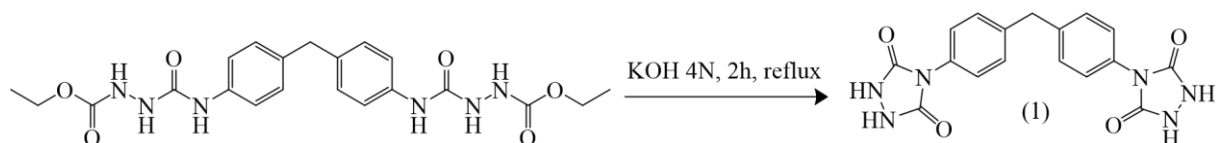
MDP bis-TAD synthesis was also conducted from diisocyanate. Ethyl carbazate (2 in Figure 57) (5 g) was dissolved in 30 mL of anhydrous THF under inert atmosphere in an ice bath. Then, methylenediphenyl diisocyanate (1 in Figure 57) (6 g) was added in 30 mL of anhydrous THF and added dropwise in the previous solution at 0°C . After addition, the reaction proceeded at room temperature during 1 h. The final mixture was filtrated, and the product (3 in Figure 57) (methylene diphenyl bishydrazine carboxylate) was washed with THF and dried overnight under vacuum to give a pure product with 100% yield.

Figure 57 - Methylene diphenyl bishydrazine carboxylate.



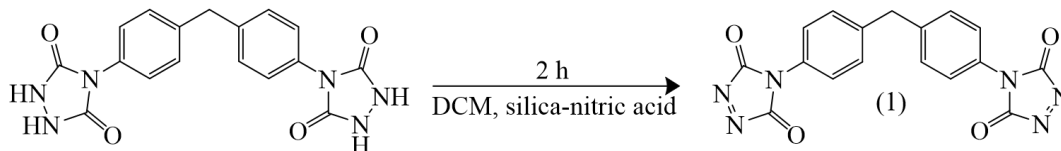
The product obtained in step 1 (5 g) and a 4 N solution of potassium hydroxide (KOH) (25 mL) were added in a flask and refluxed for 2 h. The suspension was cooled down and the pH was adjusted to 1.5 by the dropwise addition of concentrated HCl at 0°C . After filtration, the precipitated fraction was washed with distilled water and dried to give a pure product (methylene diphenyl bisurazole, 1 in Figure 58) with 77% yield.

Figure 58 - Methylene diphenyl bisurazole synthesis.



The oxidation of the urazole (from step 2) was conducted as described before and methylene bis-TAD was obtained after urazole oxidation in silica-nitric acid to give a 80% yield product (methylene diphenyl bis-TAD, in Figure 59).

Figure 59 - Methylene diphenyl bis-TAD synthesis.

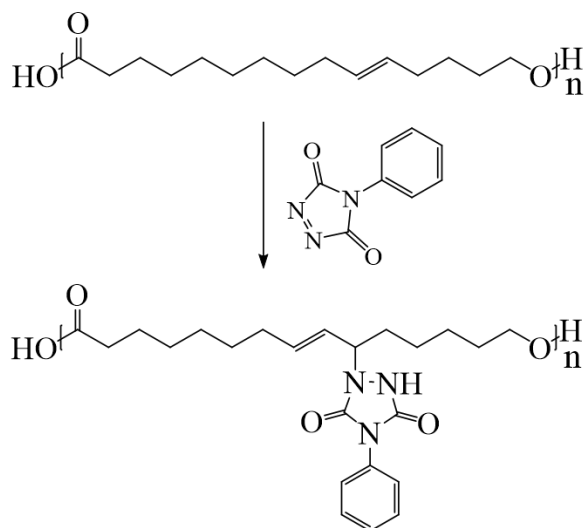


The oxidation procedure for the synthesis of both types of TAD was performed according to a literature procedure (GHORBANI-CHOGHAMARANI; CHENANI; MALLAKPOUR, 2009).

6.2.2.3 Modification of PGI with PTAD

Different organic solvents were tested in the reaction between PGI and PTAD. 100 mg of PGI was dissolved in 0.5 mL of the respective solvent. 72.7 mg of PTAD (TAD:ene molar ratio of 1:1) was dissolved in the proper solvent and then added to PGI solution. The reaction was allowed to proceed at pre-determined times at room temperature. After PTAD addition, the color changed from red to maroon, brown and finally pale yellow. Finally, the solution was precipitated in acetonitrile and the obtained polymer was dried under vacuum for further characterization. Conversion was determined by ¹H-NMR comparing the peaks at 4.1 ppm (corresponding to the methylene group adjacent to the hydroxyl terminal group in PGI) and at 4.6 ppm (corresponding to the new HC-N bond). A schematic representation of PTAD reaction with PGI is shown in Figure 60.

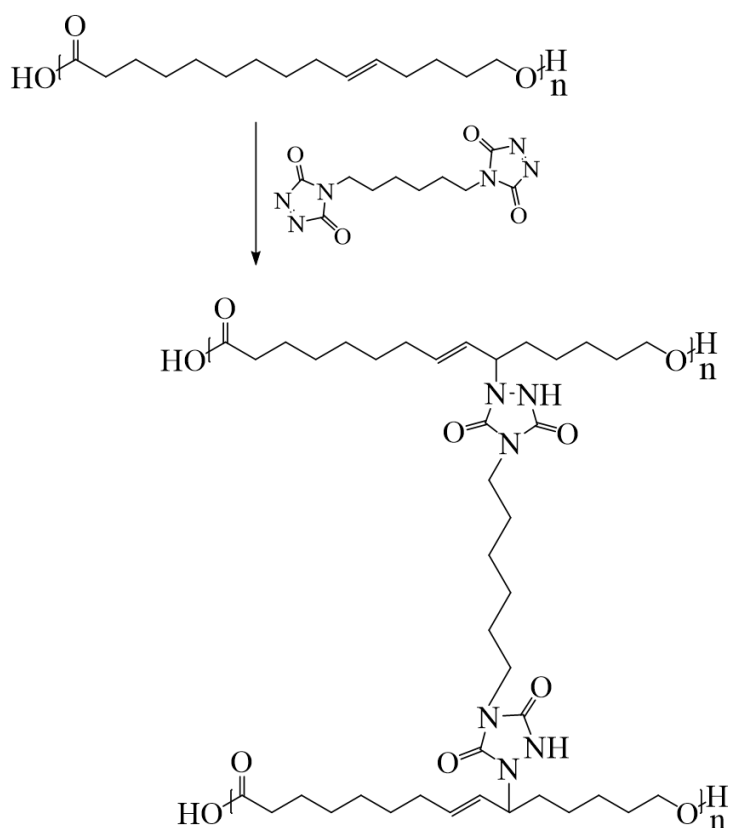
Figure 60 - Modification of PGI with monofunctional PTAD.



6.2.2.4 Crosslinking of PGI with HM-bisTAD

1.5 mg of PGI was dissolved in 0.05 mL of chloroform. 2.18 mg of HM-bisTAD was dissolved in 0.05 mL acetonitrile/chloroform mixture (60/40). Then, the HM-bisTAD solution was added to the PGI solution and the vials were monitored until the disappearance of the pink color to form the crosslinked gel (Figure 61).

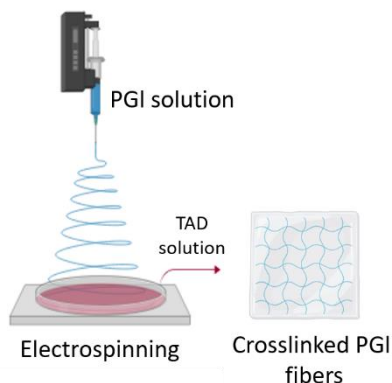
Figure 61 - Crosslinking of PGI with bifunctional HM bis-TAD.



6.2.2.5 *In-situ* crosslinking of PGI fibers

PGI fibers were prepared via electrospinning using a Spraybase electrospinning machine with a stationary collector. The protocol was based as described by Oliveira and co-workers (DE OLIVEIRA et al., 2017a). PGI concentration of 30 wt% in relation to DCM was used. Voltage, flow rate and distance from tip to collector were set at 12 kV, 100 $\mu\text{L}/\text{min}$ and 15 cm, respectively. The PGI fibers were collected in a TAD (HM-bisTAD or MDP-bisTAD) solution in acetonitrile containing 10 wt% of TAD in relation to solvent and the schematic representation is shown in Figure 62. Then, the crosslinked fibers were rinsed in acetonitrile and dried under vacuum prior to characterization. TADs are easily dissolved in acetonitrile while PGI is not soluble in this solvent, preventing non-crosslinked polymer to dissolve in TAD solution.

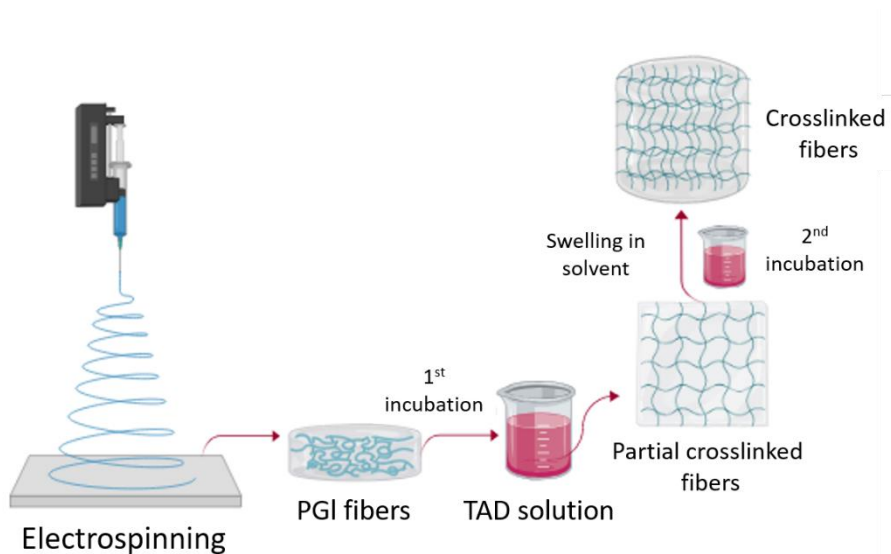
Figure 62 - Schematic illustration of PGI electrospinning followed by fiber deposition in TAD solution.



6.2.2.6 Post-crosslinking of PGI fibers

PGI fibers were obtained using a Spraybase electrospinning machine in the same conditions as described before in exception that this time the fibers were collected on Teflon. The electrospun mats were cut in a dog-bone shape and submerged in a TAD solution (HM-bisTAD or MDP-bisTAD) in acetonitrile using a molar ratio TAD:ene 1:2 and TAD concentration of 0.018 mol/L. After 24 h, the fibers were washed with an excess of acetonitrile to remove any unreacted TAD and dried under vacuum. In order to improve the degree of crosslinking, the partial-crosslinked fibers (prepared previously) were submerged in a second TAD solution using the same parameters as described before but using a mixture of chloroform and acetonitrile as solvents (1:1) - the illustration in Figure 63 shows the procedure. Then, the resultant fibers were rinsed with acetonitrile and dried under vacuum prior to characterization.

Figure 63 - Schematic illustration of post-crosslinking PGI fibers with HM bis-TAD/MDP bis-TAD.



6.2.3 Polymer characterization

6.2.3.1 Chemical Characterization

¹H-NMR was performed using a Bruker spectrometer at 400 MHz at room temperature and samples were solubilized in CDCl₃ ($\delta = 7.26$).

6.2.3.2 Thermal Properties

Thermal analysis of the modified polymers was conducted using a TA Instruments Q200 DSC, using approximately 9.0 mg of dried purified polymer. Temperature profiles from -10 °C to 120 °C with heating and cooling rate of 10 °C/min were applied under nitrogen atmosphere. The melting temperatures were determined by the second heating.

6.2.3.3 Morphology

The fiber morphology was verified by scanning electron microscopy (SEM) with a Zeiss Ultra Plus SEM instrument (Gemini column). Samples were placed on conductive carbon stubs and coated with Pt/Pd. An accelerating voltage of 2 kV was used for all samples. Fiber size

distribution was accessed by selecting randomly at least 100 fibers for each image using the software ImageJ and reported as an average.

6.2.3.4 Mechanical properties

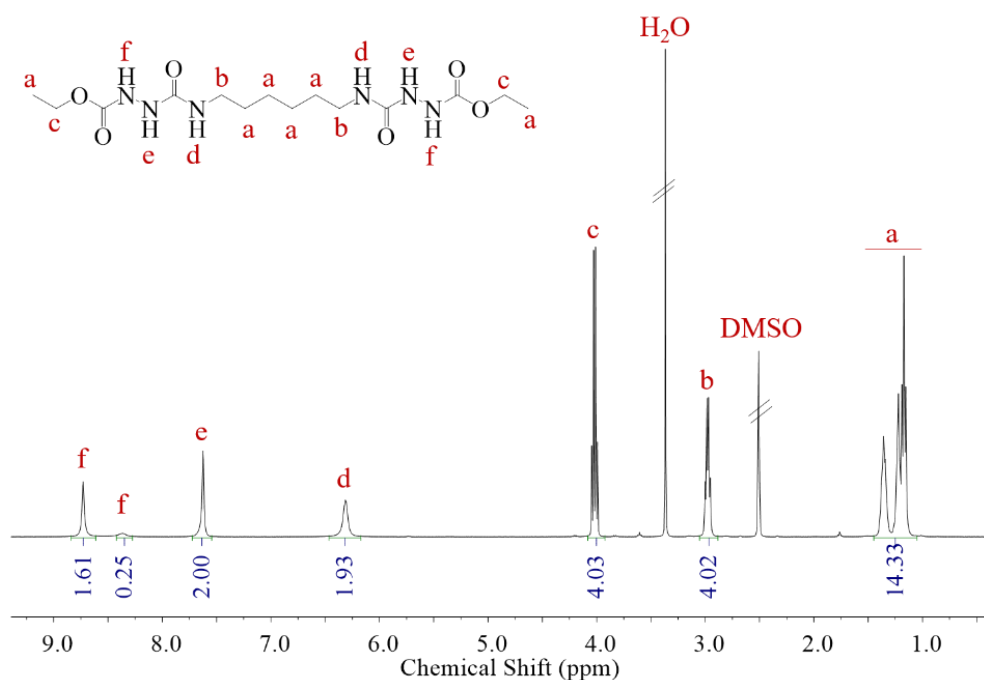
Mechanical properties as tensile strength and elongation at break were measured using a Zwick/Roell model Z2 machine equipped with a 50 N load cell. The electrospun mats were cut in dog-bone shape and 5 measurements of each sample were performed.

6.3 RESULTS AND DISCUSSION

6.3.1 Bifunctional TADs synthesis

HM bis-TAD was synthesized in three steps as described in item 6.2.2.2. First, the semicarbazide was formed upon reaction between ethyl carbazate and hexamethylene diisocyanate. Figure 64 shows the $^1\text{H-NMR}$ of the respective pure product.

Figure 64 - $^1\text{H-NMR}$ of hexamethylene bishydrazine carboxylate in DMSO-d_6 .



In the second step, bisurazole was formed upon hexamethylene bishydrazine cyclization in basic conditions. Figure 65 shows the $^1\text{H-NMR}$ with the corresponding integrals of each hydrogen. Finally, the last step corresponds to HM bis-TAD synthesis via bisurazole oxidation in silica-nitric acid. Figure 66 shows the corresponding peaks of the final structure and the disappearance of the peak at 10 ppm (from bisurazole) confirming HM bis-TAD final structure (62% yield).

Figure 65 - $^1\text{H-NMR}$ of hexamethylene bisurazole in DMSO-d_6 .

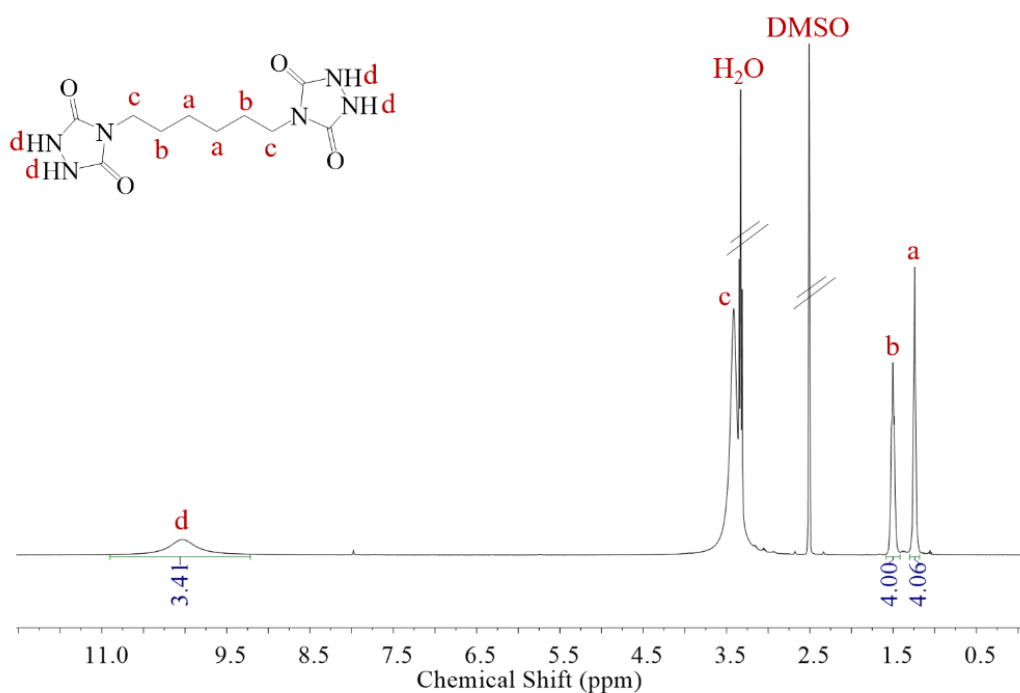
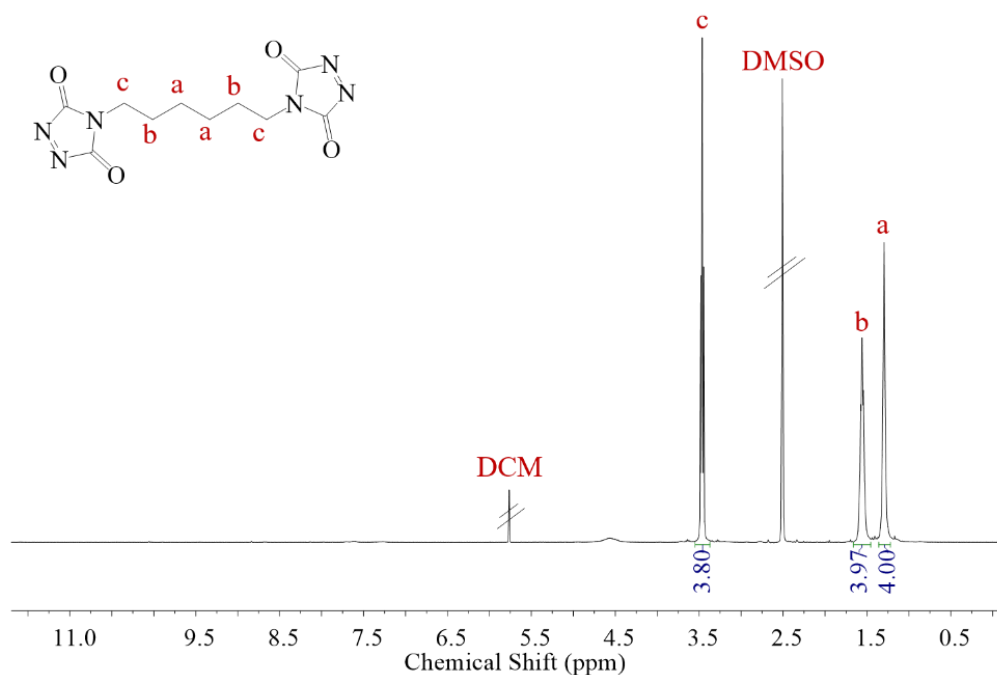


Figure 66 - $^1\text{H-NMR}$ of hexamethylene bisTAD in DMSO-d_6 .

MDP bis-TAD was also synthesized in three steps as described in item 6.2.2.2. First, the semicarbazide was formed upon reaction between ethyl carbazate and methylenediphenyl diisocyanate. Figure 67 shows the $^1\text{H-NMR}$ of the respective pure product.

In the second step, bisurazole was formed upon methylene bishydrazine carboxylate cyclization in basic conditions. Figure 68 shows the $^1\text{H-NMR}$ with the corresponding integrals. The last step corresponds to MDP bis-TAD synthesis via bisurazole oxidation in silica-nitric acid. Figure 69 shows the corresponding peaks of the final structure and the disappearance of the peak at 10.4 ppm (from bisurazole) confirming MDP bis-TAD final structure (80% yield).

Figure 67 - $^1\text{H-NMR}$ of methylene diphenyl bishydrazine carboxylate in DMSO-d_6 .

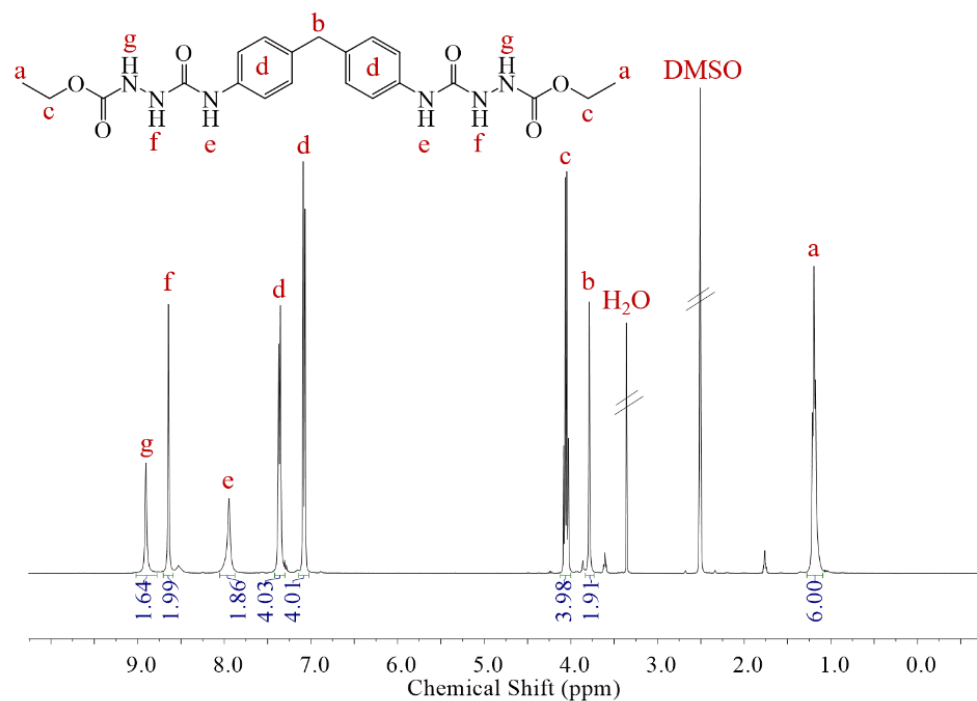


Figure 68 - $^1\text{H-NMR}$ of methylene diphenyl bishydrazine carboxylate in DMSO-d_6 .

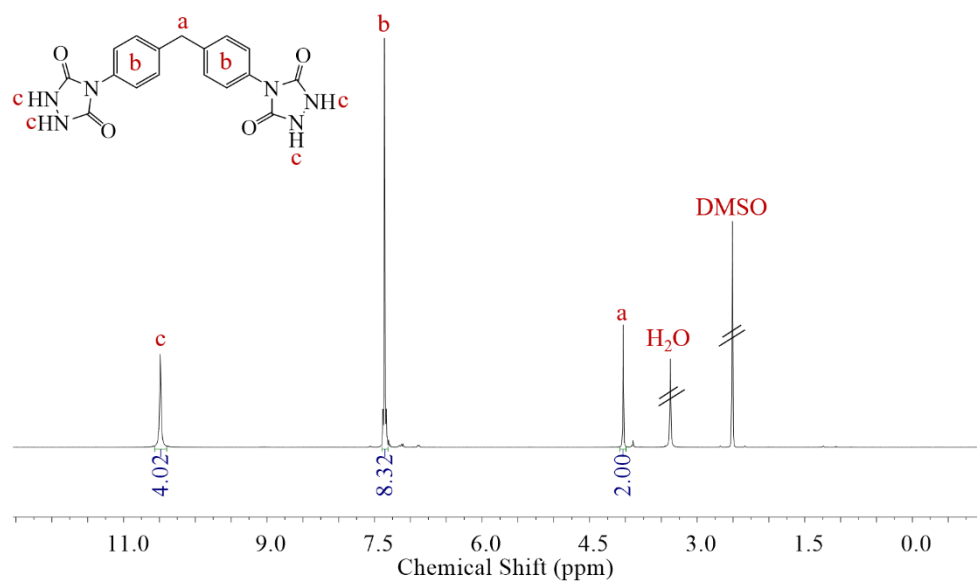
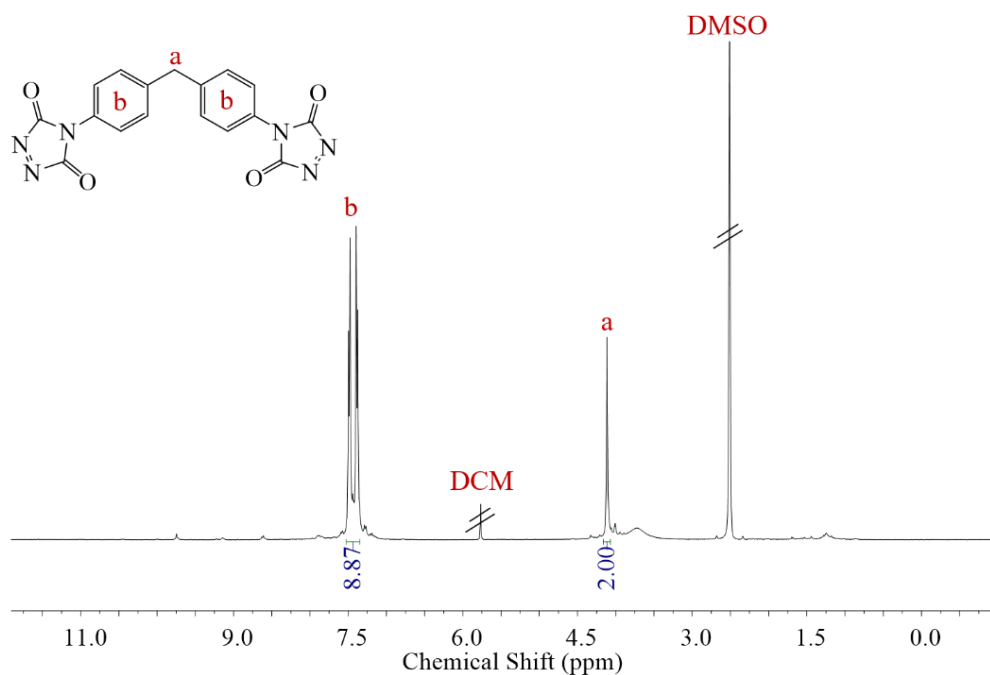


Figure 69 - $^1\text{H-NMR}$ of methylene diphenyl bisTAD in DMSO-d_6 .

6.3.2 PGI modification with PTAD

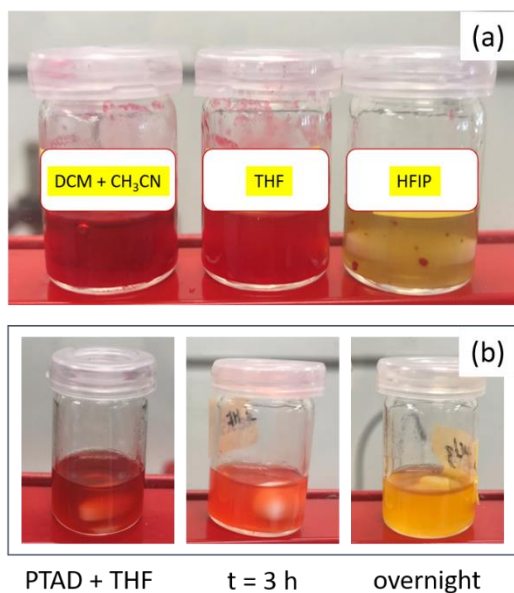
In order to evaluate the feasibility of the modification of PGI via triazolinedione reactions, commercial PTAD was first used. The reaction between PGI and PTAD was investigated using a fixed amount of the reactants (molar ratio PGI:PTAD of 1:1) and using different organic solvents. Table 8 shows the reaction conditions employed for PGI modification and the respective conversions of PTAD. Reactions were allowed to proceed overnight to ensure PTAD consumption. Conversions were obtained by comparison of the signals at 4.1 ppm (corresponding to the methylene group adjacent to the hydroxyl terminal group) and 4.6 ppm (corresponding to HC-N bond). Also, conversions were calculated considering PTAD and PGI purity (97% of purity).

Table 8 - Modification of PGI with PTAD in different solvents using an equivalent molar ratio of the reactants at room temperature.

Entry	Solvent	Conversion (%)
PP1	Chloroform + Acetonitrile	84
PP2	Dichloromethane	64
PP3	Dichloromethane + Acetonitrile	86
PP4	Chloroform	69
PP5	Tetrahydrofuran	97
PP6	Hexafluoro-2-propanol	68

It is possible to observe in Table 8 that conversions from 64 to 97% were found when the same reaction was conducted using different solvents. The highest conversion was observed when tetrahydrofuran was used as solvent albeit it was possible to observe the difference in PTAD consumption when the solvents were changed. When hexafluoro-2-propanol was used, for example, the red color of the reaction medium changed to yellow in the matter of seconds while it took more time when THF was used. Figure 70 shows the system coloration after 3 hours of reaction in different solvents.

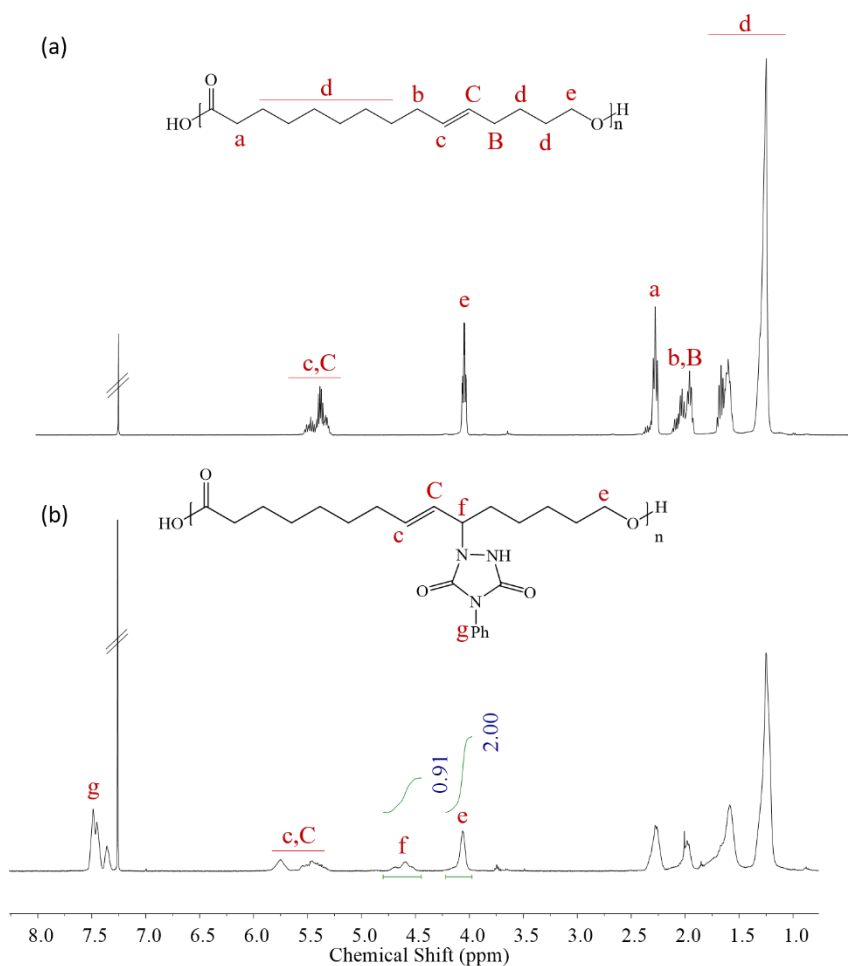
Figure 70 - PTAD reaction (a) after 3 hours in different solvents and (b) in THF.



Despite TAD reactivity can change according to the solvent properties and polarity (ACEVEDO; SQUILLACOTE, 2008; VOUGIOUKALAKIS et al., 2008; SYRGIANNIS et al., 2009), the solubility of PGI and TAD in the respective solvents can affect the final conversion.

$^1\text{H-NMR}$ analysis (Figure 71 a and b) shows $^1\text{H-NMR}$ spectra of PGI and PGI modified with PhTAD, respectively. After PGI modification, it is possible to see the new signals corresponding to the aromatic protons from PTAD (peak g, from 7.3 to 7.54 ppm) and the new bond formed due to the urazole introduction at 4.6 ppm (peak f).

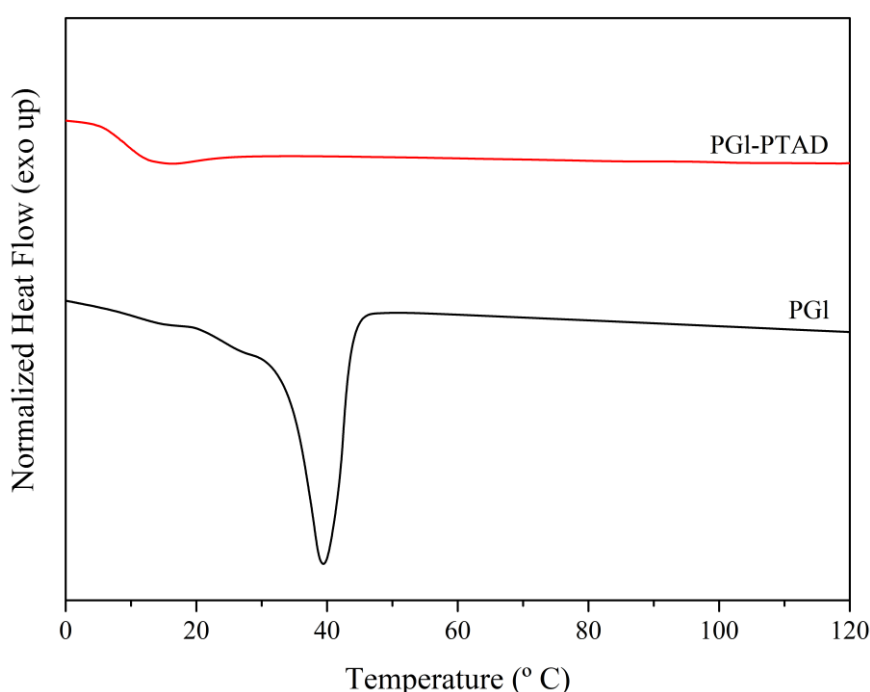
Figure 71 - $^1\text{H-NMR}$ spectra of (a) PGI before and (b) after PTAD conjugation (entry PP5 in table 6) in CDCl_3 (400 MHz).



PGI polymer is a white fluffy solid which is known to have a high degree of crystallinity. After its modification, a transparent yellowish glass-like polymer was obtained. Besides, thermal analysis (Figure 72) confirmed the reduction in polymer crystallinity.

Vlaminck and co-workers used PTAD to modify an unsaturated aliphatic polymer obtained via ADMET polymerization (an ADMET analogue to polydiene). The authors controlled the reaction kinetics and observed that full conversion was reached after 6 h (VLAMINCK et al., 2016b).

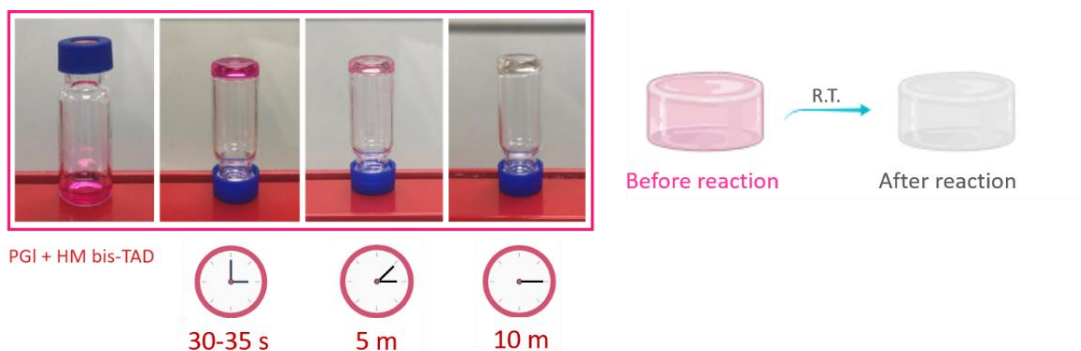
Figure 72 - Differential scanning calorimetry thermograms (second heating curve) before and after modification of PGI with PTAD.



6.3.3 Crosslinking of PGI with HM-bisTAD

Chloroform/acetonitrile solution containing bifunctional HM bis-TAD was added to a solution of PGI in chloroform. The final mixture became viscous within 30 to 35 s and the gelation was observed (Figure 73). Also, after 10 min the pink color was completely changed to transparent indicating the success of the reaction. A swelling test was performed after solvent evaporation and the material absorbed 16 times its own weight when swollen in chloroform.

Figure 73 - Crosslinking reaction between PGI and HM bis-TAD.



6.3.4 *In-situ* crosslinking of PGI fibers

PGI homopolymer was solubilized in DCM and the electrospinning parameters were set according to a literature protocol (DE OLIVEIRA et al., 2017a). The fibers were collected in a mixture of MDP bis-TAD and acetonitrile in order to allow the crosslinking in the collector once PGI is not soluble in the respective solvent. Therefore, the reaction took place in the collector at the same time as the fibers were being formed. As observed in Figure 74, homogeneous PGI fibers with diameters around 10 μm were obtained and the fiber size distribution is presented in Figure 75. Interestingly, there was a change on the surface of the crosslinked fibers and a more wrinkled material could be observed. Also, plain PGI and crosslinked PGI fibers remained in a similar diameter around 10 and 9.8 μm , respectively. The final material was capable to absorb 20 times of its weight when swollen in DCM but most part of the fibers were dissolved in the solvent, indicating that part of the PGI fibers did not react with MDP bis-TAD in the collector. Additionally, it was possible to see some broken fibers (Figure 74 e) by SEM, which is not desirable in the process.

Figure 74 - SEM images of PGI (a, b and c) and PGI modified with MDP bis-TAD during the electrospinning process (d, e and f).

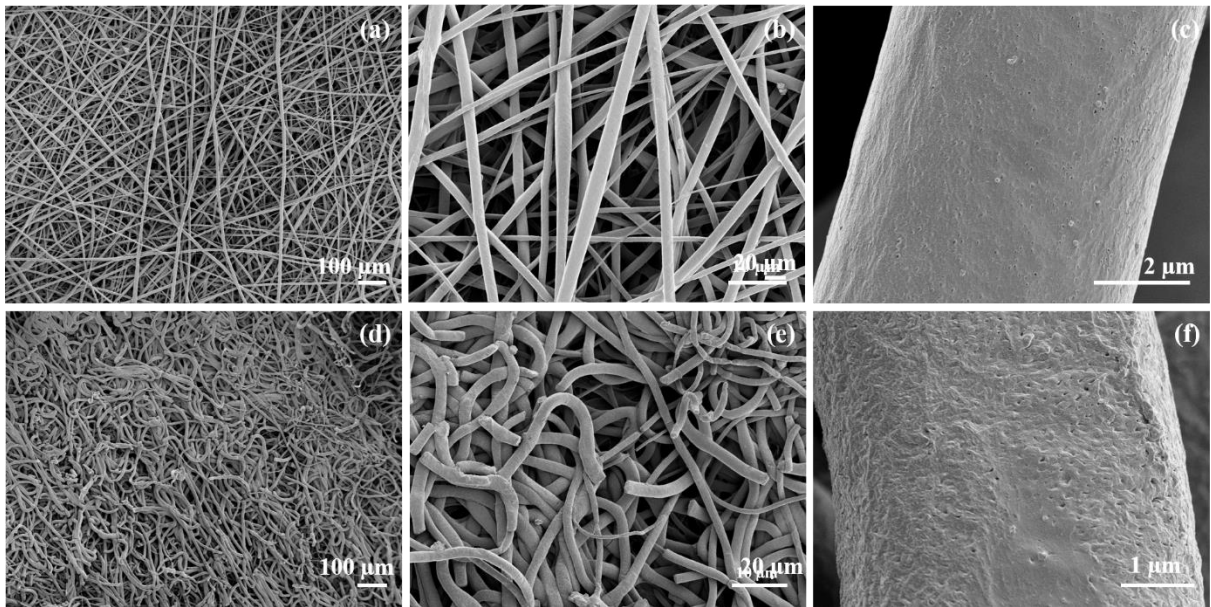
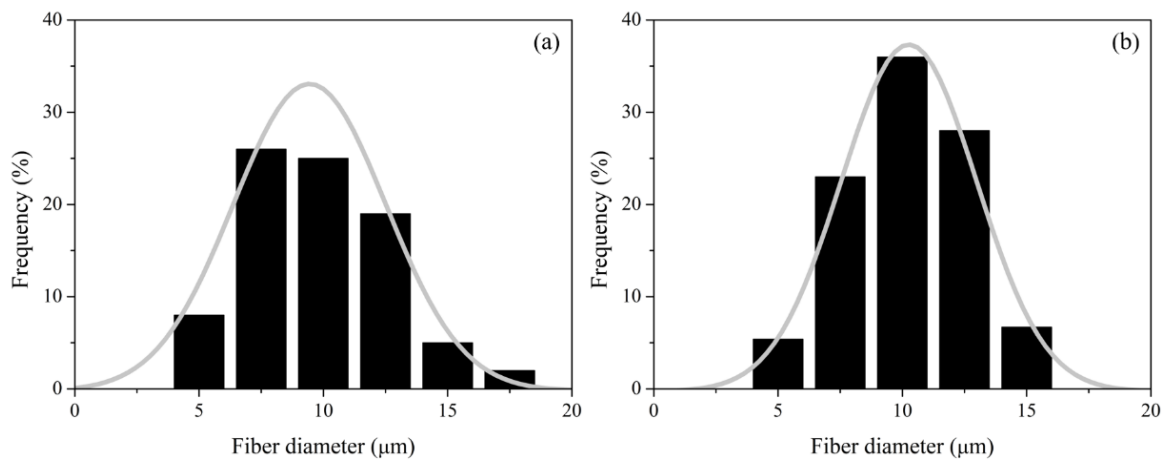


Figure 75 - Fiber size distribution of (a) PGI fibers and (b) crosslinked fibers with MDP bis-TAD after electrospinning of PGI and fiber collection in TAD solution.



6.3.5 Post-crosslinking of PGI fibers

One of the main limitations of using a solution containing TAD and PGI to produce crosslinked fibers by electrospinning is the high reaction rate. After a few seconds it is possible to observe the system gelation and consequently the crosslinked polymer stays entrapped in the tubing. To overcome this problem, PGI fibers were obtained via electrospinning and then

incubated in acetonitrile/TAD solution during 24 h at room temperature. After incubation, the fibers were swollen in DCM and the crosslinked materials could swell more than 20 times their own weights. Also, it was estimated by gravimetry that only a fraction of the total amount of TAD (initial mass) reacted with the available double bonds from polymer fibers (22 and 12% for PGI HM bis-TAD and PGI MDP bis-TAD, respectively). Thermal analysis indicated that polymer crystallinity remained unchanged after crosslinking and melting temperatures (T_m) around 40 °C (Figure 79) were observed. It was hypothesized that TAD reacted only with the surface of the fibers forming a crosslinked ‘shell’ while inner parts of the fibers were not crosslinked, and this can be related to the slow diffusion of TAD into the material.

Due to this, the prepared surface crosslinked fibers were swollen in a TAD solution containing acetonitrile and chloroform once this last one allows the partial-crosslinked PGI fibers to swell keeping the non-crosslinked PGI entrapped in the center of the fibers, due to the formed crosslinked ‘shell’ at the fiber surface. This way, swollen fibers were left to react with TAD in the solution for 24 h and this procedure is referred in the text as ‘second incubation’. SEM images in Figure 76 show that the fiber morphology is maintained after the second crosslinking procedure (Figures 76 b, c, e and f) and diameters stayed around 11.5 and 12 μm for crosslinked PGI with HM bis-TAD and crosslinked PGI with MDP bis-TAD, respectively while plain PGI was around 10 μm . Additionally, after swelling in chloroform - followed by solvent evaporation - the fibers kept the initial morphology (Figure 77) with diameters around 8.4 and 9.8 μm for PGI-HM bis-TAD and PGI MDP bis-TAD. The distributions after the second crosslinking can be seen in Figure 78.

Figure 76 - Fig. 8 SEM images of plain PGI (a,d); crosslinked PGI/HM bis-TAD (b, e) and crosslinked PGI MDP bis-TAD (c,f).

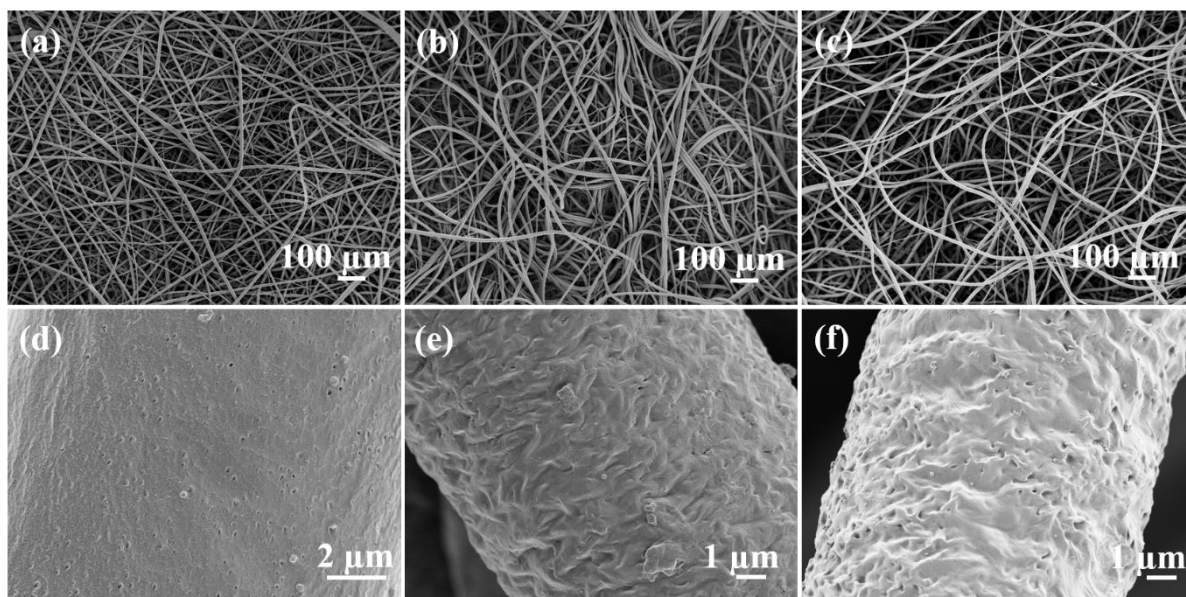


Figure 77 - SEM images of crosslinked (a,c) PGI/HM bis-TAD and (b,d) PGI/MDP bis-TAD after swelling in chloroform.

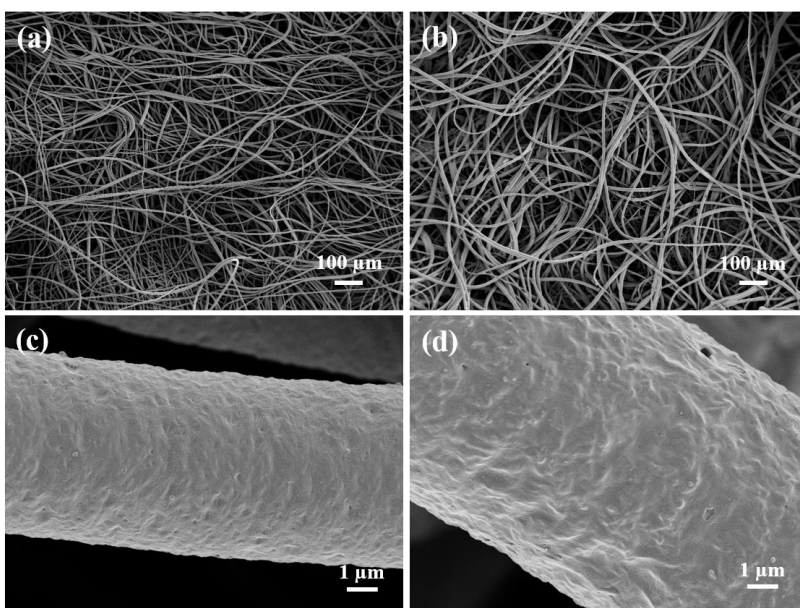
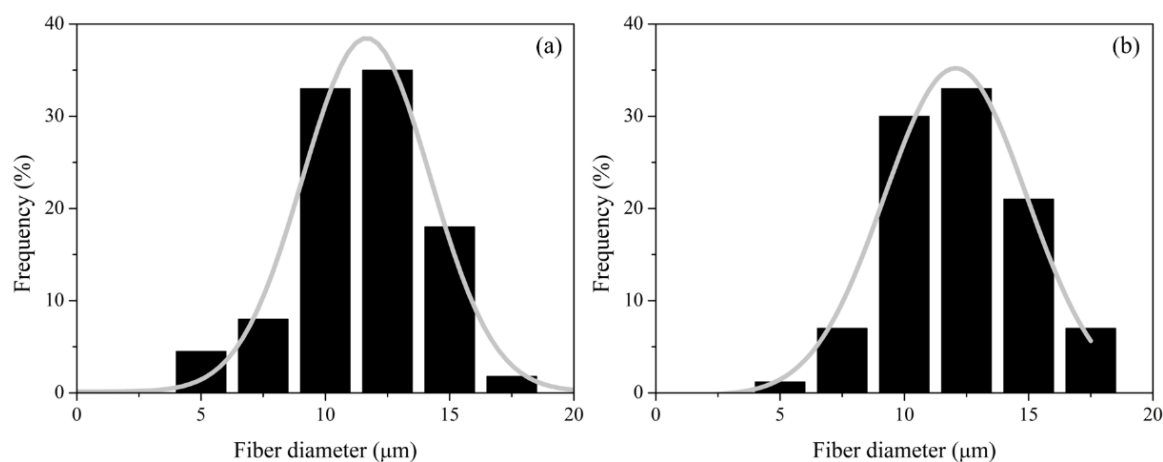
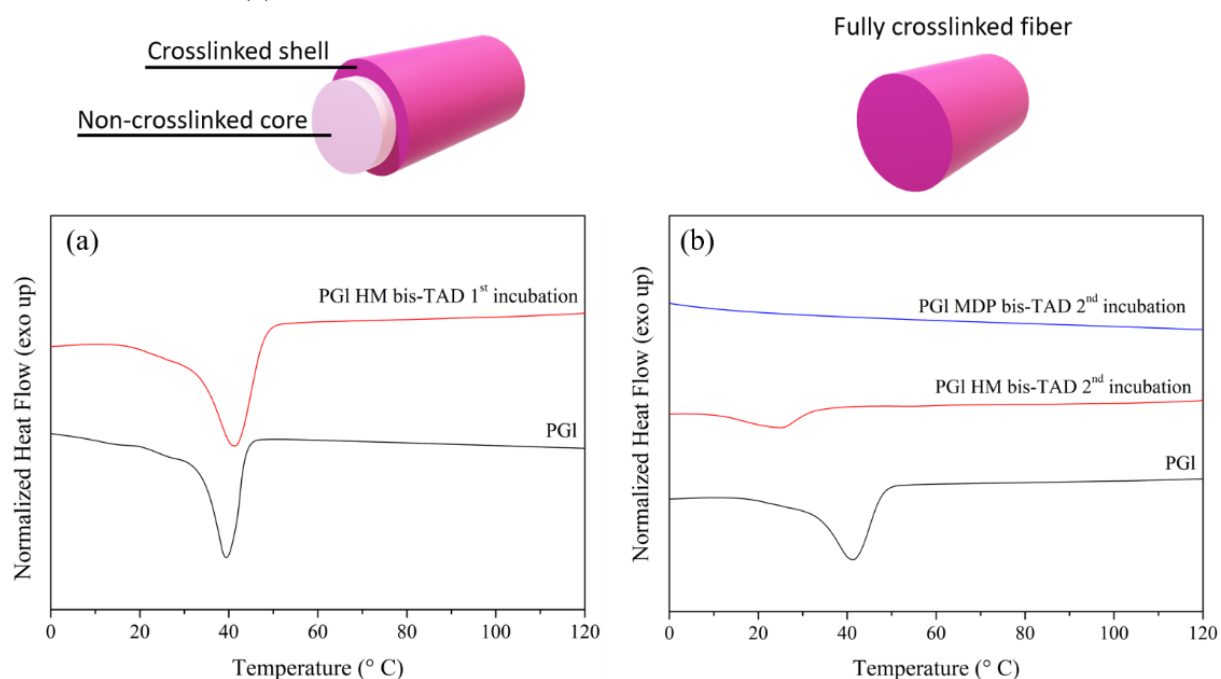


Figure 78 - Fiber size distribution of crosslinked PGI/HM bis-TAD fibers (a) and crosslinked PGI/MDP bis-TAD (b) after second incubation in TAD solutions.



After the second crosslinking, 32 and 37% of initial mass of HM bis-TAD and MDP bis-TAD reacted with the fiber available double bonds. Thermal analysis (Figure 79 b) showed the change in polymer crystallinity and it was observed a decrease in polymer melting temperature due to the introduction of the crosslinker segments into PGI. Also, amorphous polymer was obtained when MDP bis-TAD was used to crosslink PGI which is a result of the decrease in the degree of crystallinity once more amorphous domains are being created. Previous works in literature showed the same behavior when PGI films and fibers were crosslinked via thiol-ene reactions and amorphous polymers were obtained due to the reduction in polymer crystallinity (MEULEN et al., 2008; ATES; HEISE, 2014a; DE OLIVEIRA et al., 2017a).

Figure 79 - Differential scanning calorimetry thermograms (second heating curve) of first incubation of PGI fibers in HM bis-TAD (a) and second incubation of partial crosslinked PGI fibers in HM bis-TAD and MDP bis-TAD (b).



After PGI crosslinking with TADs it was possible to observe the improvement in the fiber's mechanical properties (Figures 80 and 81). While plain PGI fibers presented a tensile strength of 0.3 ± 0.08 MPa, crosslinked ones with HM bis-TAD and MDP bis-TAD presented values around 1.9 ± 0.43 and 2.4 ± 0.44 MPa after first incubation in TAD solution and 2.7 ± 0.8 and 3.9 ± 0.5 MPa after second incubation in TAD solution, which corresponds to 600, 800, 900 and 1,300% times more than plain fibers.

Additionally, after second incubation the fibers showed more elongation at break when comparing with the first crosslinking (from 8.5% to 45% and from 7.5 to 31% when HM bis-TAD and MDP bis-TAD were used as crosslinkers, respectively) once after the second crosslink most part of the PGI reacted with TAD molecules to produce an amorphous material which makes it more resistant to elongation due to the formed network. Oliveira and co-workers studied PGI fibers crosslinking via photoinitiated thiol-ene reactions and the authors observed an increase in mechanical properties after the network formation (DE OLIVEIRA et al., 2017a).

Figure 80 - Stress strain curves of PGI, PGI HM bis-TAD* (first incubation), PGI HM bis-TAD** (second incubation), PGI MDP bis-TAD* (first incubation) and PGI MDP bis-TAD (second incubation) fibers.

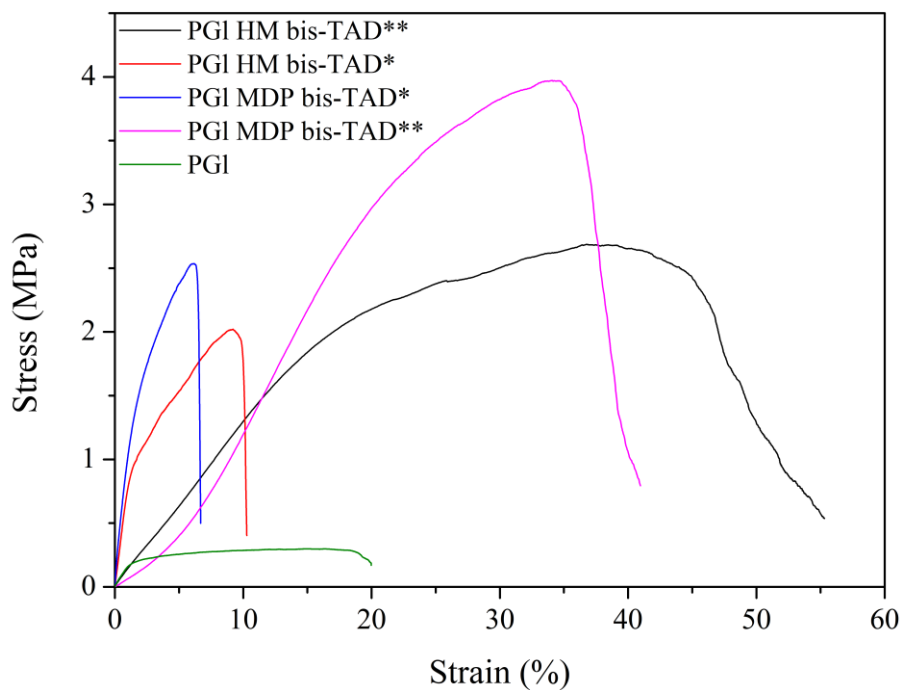
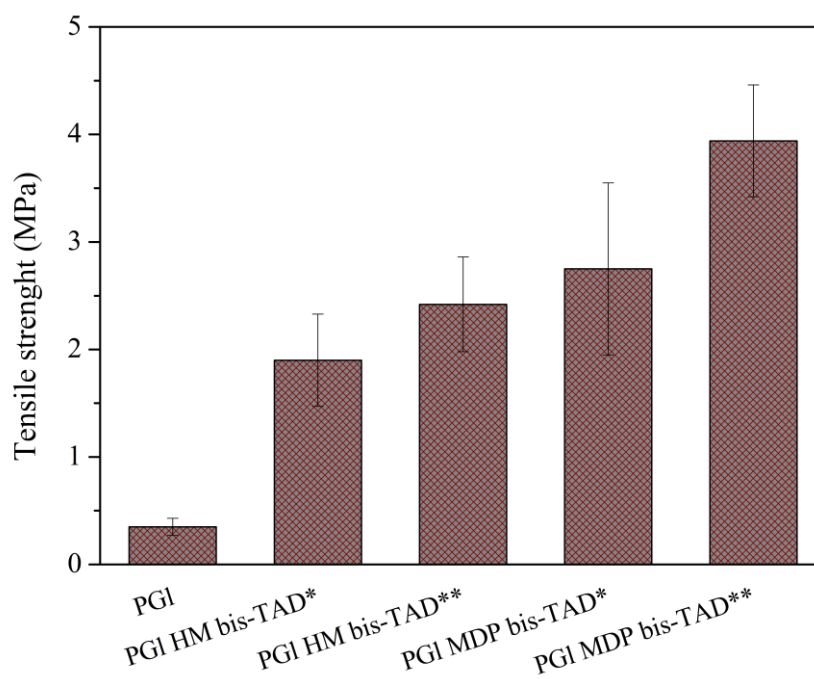


Figure 81 - Tensile strength of PGI, PGI HM bis-TAD* (first incubation), PGI HM bis-TAD** (second incubation), PGI MDP bis-TAD* (first incubation) and PGI MDP bis-TAD (second incubation) fibers.



6.4 CONCLUSIONS

We have investigated the post-polymerization modification and crosslinking of the unsaturated macrolactone PGI using the robust, fast and efficient click chemistry of TADs. High conversion was reached when PGI was reacted with monofunctional PTAD and thermal properties of the modified polymer were changed due to the insertion of urazole groups in PGI structure. Besides, TAD chemistry proved to be efficient to crosslink PGI in order to form polymer networks. PGI fibers were crosslinked by subsequent incubations in bifunctional TAD solutions. In the first incubation in TAD/acetonitrile solution, only the surface of the fibers was crosslinked. In order to increase the crosslinking degree, the fibers with crosslinked surface were swollen in an acetonitrile and chloroform-TAD solution allowing TAD to diffuse and react with all the available double bonds from PGI - to create a fully crosslinked scaffold. Besides, a significant increase in mechanical properties could be observed after crosslinking. Tensile strength increased 1000% after the second incubation in MDP bis-TAD and elongation at break increased from 24.5% (plain PGI) to 45% (in HM bis-TAD) and 32% (in MDP bis-TAD). Both developed systems consisting of surface crosslinked fibers and fully crosslinked fibers are very interesting as platforms for biomedical applications, once their properties can be tuned according to the requirements for specific applications.

CHAPTER VII

7. FINAL CONSIDERATIONS

7.1 CONCLUSION

Polyesters obtained from macrolactones via enzymatic ring-opening polymerization are attractive in the biomedical area due to their biocompatibility and biodegradability. This work is divided in two main topics. The first two chapters correspond to the evaluation of poly(globalide) synthesis via enzymatic ring-opening polymerization in solution (to obtain polymeric films) and in miniemulsion (to obtain nanoparticles).

Polymerizations conducted in solution using toluene as solvent and different enzymes as biocatalysts led to high molecular weight polymers with good dispersity for this kind of polymerization. When Novozym 435 was used as biocatalyst, high yields (88-91%) were obtained in the first minutes of the reaction. Also, high molecular weights were reached in the initial stages and they remained in a similar range within the course of the reaction (M_w from 25,000 to 35,000 g mol^{-1}). Conversely, when NS88011 was used as biocatalyst the reaction kinetics showed to be different and longer reactions times were required to obtain high yields and molecular weights. However, M_w up to 60,500 g mol^{-1} was found when this enzyme was used and the differences in kinetics of each enzyme were related to support characteristics, such as pore size.

Poly(globalide) nanoparticles were prepared by miniemulsion enzymatic ring-opening polymerization using free lipases CALB and NS40116. CALB catalyzed systems lead to nanoparticle diameters between 85 and 283 nm and the diameter was affected by surfactant concentration. $^1\text{H-NMR}$ analysis confirmed polymer formation and yields up to 90% were reached. GPC measurements were performed to check nanoparticles molecular weight - in a range from 6,760 to 23,200 g mol^{-1} . Apart of having reasonable molecular weight, only unstable nanoparticles were produced when NS40116 was employed as biocatalyst.

Unsaturated polyesters can be easily modified via post-polymerization modification by functional groups addition in the polymer main chain to form novel polymers with tunable properties. In this scenario, the second main topic of this thesis was focused in PGI modification

via click-chemistry using two different approaches: thiol-ene addition (Chapter 5) and triazolinedione reactions (Chapter 6).

In chapter 5, three different thiols containing phosphoester groups were synthesized in toluene to obtain yields greater than 60% after silica column purification. After that, these compounds were attached to poly(globalide) backbone via thiol-ene click-like reactions. The effects of the thiol:ene ratio and initiator concentration were evaluated. Low values of double conversion were obtained when diethyl 2-mercaptoethyl phosphate (TF1) was used, with a maximum conversion of 15% in 2:1 thiol:ene molar ratio and 5 mol% of AIBN. The highest double bond conversions were found when diethyl 6-mercapto-1-hexyl phosphate was used, from 14 to 84%. The addition of pendant groups in PGI chain altered polymer crystalline domains and a reduction in polymer melting point and enthalpy of fusion was observed. Also, amorphous materials were obtained in higher concentrations of thiol for modified PGI with TF2 and diphenyl 6-mercapto-1-hexyl phosphate (TF3). Modified PGI-TF2 with a double bond conversion of 14% was used to prepare fibers via electrospinning to form well-defined fibers with diameters around 11 μm . Also, this material demonstrated to be non-toxic in fibroblast cells.

In order to show PGI versatility, in Chapter 6 polymeric chain was modified making use of the robust chemistry of triazolinediones (TADs). First, PGI was modified with a simple monofunctional TAD (PhTAD) to give polymers with high degree of PTAD conjugation - from 64 to 97% - and the conversion was limited by solvent type. Moreover, PGI polymer was processed via electrospinning to obtain submicrometric fibers. In order to improve the properties of the electrospun PGI, the material was crosslinked either *in-situ* (during the electrospinning) and post-electrospinning. Reinforced amorphous fibers were obtained after the immersion of the material in bifunctional TAD solution and the morphology and thermal properties could be tuned with the number of incubations. In summary, an efficient chemistry - that do not make use of catalysts, temperature and initiators - proved to be efficient in introducing functionalities and chemical crosslinks in PGI chain.

7.2 FURTHER WORK

Considering the obtained results in the present work, some ideas are presented in order to complement the work:

1. To investigate ring-opening polymerization of globalide using chemical catalysts to observe the effect on polymer molecular weight and dispersity.
2. To crosslink the obtained PGI nanoparticles and using them to encapsulate bioactive compounds in order to study their release from non-crosslinked and crosslinked nanoparticles.
3. To study the degradation of modified polymers with thiol-phosphoester groups.
4. To study the crosslinking of the modified fibers with TF2 in order to obtain amorphous materials for biomedical use.
5. To study the kinetics of PTAD conjugation in PGI.
6. To obtain fibers from a solution containing PGI and drug and further crosslinking via TAD reactions. Then, the release from the crosslinked and non-crosslinked fibers can be investigated in vitro.
7. To evaluate crosslinked PGI fibers viability and degradation.
8. To analyze the fracture of the crosslinked PGI fibers by SEM.

REFERENCES

- ABDAL-HAY, A. et al. Novel polycaprolactone/hydroxyapatite nanocomposite fibrous scaffolds by direct melt-electrospinning writing. **European Polymer Journal**, v. 105, p. 257–264, 2018.
- ABSIL, R. et al. Click reactive microgels as a strategy towards chemically injectable hydrogels. **Polymer Chemistry**, v. 7, n. 44, p. 6752–6760, 2016.
- ACEVEDO, O.; SQUILLACOTE, M. E. A new solvent-dependent mechanism for a triazolinedione ene reaction. **Journal of Organic Chemistry**, v. 73, n. 3, p. 912–922, 2008.
- AGARWAL, S.; WENDORFF, J. H.; GREINER, A. Use of electrospinning technique for biomedical applications. **Polymer**, v. 49, n. 26, p. 5603–5621, 2008.
- ALBERTSSON, A.-C.; VARMA, I. K.; SRIVASTAVA, K. Polyesters from large lactones. In: DUBOIS, P.; COULEMBIER, O.; RAQUEZ, J.-M. (Ed.). **Handbook of Ring-Opening Polymerization**. Weinheim: Wiley e Sons, 2009. p. 287–306.
- ALBERTSSON, A.-C.; VARMA, I. K. Recent Developments in Ring-opening Polymerization of Lactones for Biomedical Applications. **Biomacromolecules**, v. 4, n. 6, p. 1466–1486, 2003.
- ALBERTSSON, A.; SRIVASTAVA, R. Recent developments in enzyme-catalyzed ring-opening polymerization. **Advanced Drug Delivery Reviews**, v. 60, n. 9, p. 1077–1093, 2008.
- ALDER, K.; PASCHER, F.; SCHMITZ, A. Über die Anlagerung von Maleinsäure-anhydrid und Azodicarbon- säure-ester an einfach ungesättigte Kohlenwasserstoffe. Zur Kenntnis von Substitutionsvorgängen in der Allyl-Stellung. **Ber. Dtsch. Chem. Ges. B**, n. 76, p. 27–53, 1943.
- ALMOUAZEN, E. et al. Development of a nanoparticle-based system for the delivery of retinoic acid into macrophages. **International Journal of Pharmaceutics**, v. 430, p. 207–215, 2012.
- ASUA, J. M. Miniemulsion polymerization. **Progress in Polymer Science**, v. 27, n. 7, p. 1283–1346, 2002.
- ATES, Z. et al. Functional Brush-Decorated Poly(globalide) Films by ARGET-ATRP for Bioconjugation. **Macromolecular Bioscience**, v. 14, n. 11, p. 1600–1608, 2014.
- ATES, Z.; HEISE, A. Functional films from unsaturated poly(macrolactones) by thiol–ene cross-linking and functionalisation. **Polymer Chemistry**, v. 5, n. 8, p. 2936–2941, 2014a.
- ATES, Z.; HEISE, A. Functional films from unsaturated poly(macrolactones) by thiol-ene cross-linking and functionalisation. **Polymer Chemistry**, v. 5, p. 2936–2941, 2014b.
- ATES, Z.; THORNTON, D.; HEISE, A. Side-chain functionalisation of unsaturated polyesters from ring-opening polymerisation of macrolactones by thiol – ene click chemistry. **Polymer**

Chemistry, v. 2, p. 309–312, 2011.

BANSAL, K. K. et al. New biomaterials from renewable resources-amphiphilic block copolymers from δ -decalactone. **Polymer Chemistry**, v. 6, n. 40, p. 7196–7210, 2015.

BARNER-KOWOLLIK, C. et al. “Clicking” polymers or just efficient linking: What is the difference? **Angewandte Chemie - International Edition**, v. 50, n. 1, p. 60–62, 2011.

BASKO, M. et al. Biodegradable polymer networks via triazolinedione-crosslinking of oleyl-functionalized poly(ϵ -caprolactone). **European Polymer Journal**, v. 89, n. November 2016, p. 230–240, 2017.

BAUER, K. N. et al. Main-chain poly(phosphoester)s: History, syntheses, degradation, bio- and flame-retardant applications. **Progress in Polymer Science**, v. 73, p. 61–122, 2017.

BENDER, A. T. Cyclic Nucleotide Phosphodiesterases: Molecular Regulation to Clinical Use. **Pharmacological Reviews**, v. 58, n. 3, p. 488–520, 2006.

BENDER, A. T.; BEAVO, J. A. Cyclic Nucleotide Phosphodiesterases: Molecular Regulation to Clinical Use. **Pharmacological Reviews**, v. 58, n. 3, p. 488–520, 2006.

BERGEMANN, C. et al. Continuous cellularization of calcium phosphate hybrid scaffolds induced by plasma polymer activation. **Materials Science and Engineering C**, v. 59, p. 514–523, 2016.

BHARDWAJ, N.; KUNDU, S. C. Electrospinning: A fascinating fiber fabrication technique. **Biotechnology Advances**, v. 28, n. 3, p. 325–347, 2010.

BISHT, K. S. et al. Enzyme-Catalyzed Ring-Opening Polymerization of. **Macromolecules**, v. 30, p. 2705–2711, 1997.

BOUGARD, F. et al. Synthesis and Supramolecular Organization of Amphiphilic Diblock Copolymers Combining Poly (N,N -dimethylamino-2-ethyl methacrylate) and Poly (ϵ -caprolactone). **Langmuir**, v. 23, p. 2339–2345, 2007.

BRAGHIROLI, D. I.; STEFFENS, D.; PRANKE, P. Electrospinning for regenerative medicine: A review of the main topics. **Drug Discovery Today**, v. 19, n. 6, p. 743–753, 2014.

BRESOLIN, D. et al. Synthesis of a green polyurethane foam from a biopolyol obtained by enzymatic glycerolysis and its use for immobilization of lipase NS-40116. **Bioprocess and Biosystems Engineering**, v. 42, n. 2, p. 213–222, 2019.

BUTLER, G. B. Triazolinedione Modified Polydienes. **Industrial and Engineering Chemistry Product Research and Development**, v. 19, n. 4, p. 512–528, 1980.

CAI, J. et al. Effects of molecular weight on poly(ω -pentadecalactone) mechanical and thermal properties. **Polymer**, v. 51, n. 5, p. 1088–1099, 2010.

CHATTOPADHYAY, S.; DU PREZ, F. Simple design of chemically crosslinked plant oil nanoparticles by triazolinedione-ene chemistry. **European Polymer Journal**, v. 81, p. 77–85, 2016.

CHIARADIA, V. et al. Immobilization of *Candida antarctica* Lipase B on Magnetic Poly(Urea-Urethane) Nanoparticles. **Applied Biochemistry and Biotechnology**, p. 1–18, 2016.

CIPOLATTI, E. P. et al. Enzymatic Immobilization of *Candida antarctica* lipase B on PEGylated poly (urea-urethane) nanoparticles by step miniemulsion polymerization. **Journal of Molecular Catalysis. B, Enzymatic**, v. 109, p. 116–121, 2014.

CLAUDINO, M. et al. Photoinduced thiol-ene crosslinking of globalideε-caprolactone copolymers: Curing performance and resulting thermoset properties. **Journal of Polymer Science, Part A: Polymer Chemistry**, v. 50, n. 1, p. 16–24, 2012.

CLAUDINO, M. **Macromolecular Design : UV-Curable Thiol – Ene Networks Based on Renewable Resources**. 2013. Kungliga Tekniska Högskolan, 2013.

CLOUET, G.; KNIPPER, M. Functionalization of poly(methyl methacrylate) by free radical polymerization, 1. **Makromolekular Chemistry**, v. 188, p. 2597–2604, 1987.

COOKSON, R. C.; GILANI, S. S. H.; STEVENS, D. R. Diels-Alder reactions of 4-phenyl-1,2,4-triazoline-3,5-dione. **Journal of the chemical society**, p. 1905–1909, 1967.

COOKSON, R. C.; GILANI, S. S. H.; STEVENS, I. D. R. 4-phenyl-1,2,4-triazolin-3,5-dione: a powerful dienophile. **Tetrahedron Letters**, v. 1, n. 14, p. 615–618, 1962.

COULEMBIER, O. et al. From controlled ring-opening polymerization to biodegradable aliphatic polyester: Especially poly(β-malic acid) derivatives. **Progress in Polymer Science (Oxford)**, v. 31, n. 8, p. 723–747, 2006.

COULEMBIER, O.; DUBOIS, P. **Polyesters from β-Lactones**. Weinheim: Wiley e Sons, 2009.

DAS, N. G.; DAS, S. K. Controlled-Release of Oral Dosage Forms. **Pharmaceutical Technology**, v. 15, p. 10–17, 2003.

DAS, S.; KAR, M.; GUPTA, S. Sen. Synthesis of end-functionalized phosphate and phosphonate-polypeptides by ring-opening polymerization of their corresponding N-carboxyanhydride. **Polymer Chemistry**, v. 4, n. 15, p. 4087–4091, 2013.

DE BRUYCKER, K. et al. Triazolinediones as Highly Enabling Synthetic Tools. **Chemical Reviews**, v. 116, n. 6, p. 3919–3974, 2016.

DE GEUS, M. et al. Performance polymers from renewable monomers: high molecular weight poly(pentadecalactone) for fiber applications. **Polymer Chemistry**, v. 1, n. 4, p. 525, 2010.

DE MENESES, A. C. et al. Benzyl butyrate esterification mediated by immobilized lipases: Evaluation of batch and fed-batch reactors to overcome lipase-acid deactivation. **Process Biochemistry**, v. 78, n. October 2018, p. 50–57, 2019.

DE OLIVEIRA, F. C. S. et al. Direct UV-Triggered Thiol–ene Cross-Linking of Electrospun Polyester Fibers from Unsaturated Poly(macrolactone)s and Their Drug Loading by Solvent Swelling. **Biomacromolecules**, v. 18, n. 12, p. 4292–4298, 2017a.

DEFIZE, T. et al. Reversible TAD Chemistry as a Convenient Tool for the Design of (Re)processable PCL-Based Shape-Memory Materials. **Macromolecular Rapid Communications**, v. 38, n. 1, p. 1–7, 2017.

DU, J.-Z. et al. Synthesis and micellization of amphiphilic brush-coil block copolymer based on poly(epsilon-caprolactone) and PEGylated polyphosphoester. **Biomacromolecules**, v. 7, n. 6, p. 1898–1903, 2006.

DUBOIS, P.; COULEMBIER, O.; RAQUEZ, J.-M. **Handbook of ring-opening polymerization**. Wiley-VCH ed. Weinheim: Wiley e Sons, 2009.

DUDA, A. et al. Kinetics of the ring-opening polymerization of 6-, 7-, 9-, 12-, 13-, 16-, and 17-membered lactones. Comparison of chemical and enzymatic polymerizations. **Macromolecules**, v. 35, n. 11, p. 4266–4270, 2002.

DUQUE SÁNCHEZ, L. et al. Surface modification of electrospun fibres for biomedical applications: A focus on radical polymerization methods. **Biomaterials**, v. 106, p. 24–45, 2016.

DURHAM, O. Z. et al. Radical Mediated Thiol-Ene Emulsion Polymerizations. **Macromolecules**, v. 50, p. 775–783, 2017.

FERNÁNDEZ, J. et al. A new generation of poly(lactide/ε-caprolactone) polymeric biomaterials for application in the medical field. **Journal of Biomedical Materials Research - Part A**, v. 102, n. 10, p. 3573–3584, 2014.

FERNÁNDEZ, J. et al. Mechanical properties and fatigue analysis on poly(ε-caprolactone)-polydopamine-coated nanofibers and poly(ε-caprolactone)-carbon nanotube composite scaffolds. **European Polymer Journal**, v. 94, n. July, p. 208–221, 2017.

FERNÁNDEZ, J.; ETXEBERRIA, A.; SARASUA, J. R. Synthesis and properties of ω-pentadecalactone-co-δ-hexalactone copolymers: a biodegradable thermoplastic elastomer as an alternative to poly(ε-caprolactone). **RSC Advances**, v. 6, n. 4, p. 3137–3149, 2016.

FOCARETE, M. L. et al. Physical Characterization of Poly (pentadecalactone) Synthesized by Lipase-Catalyzed Ring-Opening Polymerization. **J. Polym. Sci. Part B: Polym. Phys.**, v. 39, p. 1721–1729, 2001.

GAO, H. et al. Synthesis, characterization and micellization of amphiphilic polyethylene-b-

polyphosphoester block copolymers. **RSC Advances**, v. 5, p. 49376–49384, 2015.

GHORBANI-CHOGHAMARANI, A.; CHENANI, Z.; MALLAKPOUR, S. Supported Nitric Acid on Silica Gel and Polyvinyl Pyrrolidone (PVP) as an Efficient Oxidizing Agent for the Oxidation of Urazoles and Bis-urazoles. **Synthetic Communications**, v. 39, n. 2009, p. 4264–4270, 2009.

GRIESBAUM, K. Problems and Possibilities of the Free-Radical Addition of Thiols to Unsaturated Compounds. **Angewandte Chemie - International Edition**, v. 9, n. 4, p. 273–287, 1970.

GROSS, R. a; KUMAR, A.; KALRA, B. Polymer synthesis by in vitro enzyme catalysis. **Chemical Reviews**, v. 101, n. 7, p. 2097–2124, 2001.

GUINDANI, C. et al. Enzymatic ring opening copolymerization of globalide and ϵ -caprolactone under supercritical conditions. **Journal of Supercritical Fluids**, v. 128, n. April, p. 404–411, 2017.

GUINDANI, C. et al. N-acetylcysteine side-chain functionalization of poly(globalide-co-caprolactone) through thiol-ene reaction. **Materials Science & Engineering C**, p. 477–483, 2019.

HAJIPOUR, A. R.; MALLAKPOUR, S. E.; ADIBI, H. Oxidation of Urazoles to Triazolinediones with Benzyltriphenylphosphonium Peroxymonosulfate under Solvent-Free Conditions. p. 13–14, 2001.

HANAY, S. B. et al. Investigation of the triazolinedione (TAD) reaction with tryptophan as a direct route to copolypeptide conjugation and cross-linking. **Polymer Chemistry**, v. 8, n. 43, p. 6594–6597, 2017a.

HANAY, S. B. et al. Exploring Tyrosine-Triazolinedione (TAD) Reactions for the Selective Conjugation and Cross-Linking of N -Carboxyanhydride (NCA) Derived Synthetic Copolypeptides. **Macromolecular BioscienceJournals**, v. 17, p. 1–7, 2017b.

HANAY, S. B. et al. Facile Approach to Covalent Copolypeptide Hydrogels and Hybrid Organohydrogels. **ACS Macro Letters**, v. 7, n. 8, p. 944–949, 2018.

HE, C.; NIE, W.; FENG, W. Engineering of biomimetic nanofibrous matrices for drug delivery and tissue engineering. **Journal of Materials Chemistry B**, v. 2, n. 45, p. 7828–7848, 2014.

HEIJDEN, S. Van Der et al. Use of Triazolinedione Click Chemistry for Tuning the Mechanical Properties of Electrospun SBS-Fibers. **Macromolecules**, v. 48, p. 6474–6481, 2015.

HEIJDEN, S. Van Der et al. Novel composite materials with tunable delamination resistance using functionalizable electrospun SBS fibers. **Composite structures**, v. 159, p. 12–20, 2017.

HEISE, A.; DUXBURY, C. J.; PALMANS, A. R. A. Enzyme-Mediated Ring-Opening Polymerization. In: DUBOIS, P.; COULEMBIER, O.; RAQUEZ, J.-M. (Ed.). **Handbook of Ring-Opening Polymerization**. Weinheim: Wiley e Sons, 2009. p. 379–397.

HOLZ, J. C. P. et al. Enzyme-catalyzed production of emollient cetostearyl stearate using different immobilized commercial lipases under vacuum system. **Biocatalysis and Agricultural Biotechnology**, v. 15, n. May, p. 229–234, 2018.

HOMEM, V. et al. Long lasting perfume e A review of synthetic musks in WWTPs. **Journal of Environmental Management**, v. 149, n. 1, p. 168–192, 2015.

HOYLE, C. E.; BOWMAN, C. N. Thiol-ene click chemistry. **Angewandte Chemie - International Edition**, v. 49, n. 9, p. 1540–1573, 2010.

HOYLE, C. E.; LEE, T. Y.; ROPER, T. Thiol-enes: Chemistry of the past with promise for the future. **Journal of Polymer Science, Part A: Polymer Chemistry**, v. 42, n. 21, p. 5301–5338, 2004.

HU, W. et al. Modification of chitosan grafted with collagen peptide by enzyme crosslinking. **Carbohydrate Polymers**, v. 206, p. 468–475, 2019.

IDASZEK, J. et al. How important are scaffolds and their surface properties in regenerative medicine. **Applied Surface Science**, v. 388, p. 762–774, 2016.

ITO, Y. Surface micropatterning to regulate cell functions. **Biomaterials**, v. 20, n. 23–24, p. 2333–2342, 1999.

JANIK, H.; MARZEC, M. A review: Fabrication of porous polyurethane scaffolds. **Materials Science and Engineering C**, v. 48, p. 586–591, 2015.

JOHNSON, P. M.; KUNDU, S.; BEERS, K. L. Modeling enzymatic kinetic pathways for ring-opening lactone polymerization. **Biomacromolecules**, v. 12, n. 9, p. 3337–43, 2011.

JOSEPH, P.; TRETSIAKOVA-MCNALLY, S. Reactive modifications of some chain- and step-growth polymers with phosphorus-containing compounds: Effects on flame retardance-a review. **Polymers for Advanced Technologies**, v. 22, n. 4, p. 395–406, 2011.

KADE, M. J.; BURKE, D. J.; HAWKER, C. J. The power of thiol-ene chemistry. **Journal of Polymer Science Part a-Polymer Chemistry**, v. 48, p. 743–750, 2010.

KADOKAWA, J.; KOBAYASHI, S. Polymer synthesis by enzymatic catalysis. **Current opinion in chemical biology**, v. 14, n. 2, p. 145–153, 2010.

KALAOGLU-ALTAN, O. I.; SANYAL, R.; SANYAL, A. “Clickable” polymeric nanofibers through hydrophilic-hydrophobic balance: Fabrication of robust biomolecular immobilization platforms. **Biomacromolecules**, v. 16, n. 5, p. 1590–1597, 2015.

KAMAL, Z. et al. Lipase in aqueous-polar organic solvents: Activity, structure, and stability. **Protein Science**, v. 22, n. 7, p. 904–915, 2013.

KHARAGHANI, D. et al. Electrospun antibacterial polyacrylonitrile nanofiber membranes functionalized with silver nanoparticles by a facile wetting method. **European Polymer Journal**, v. 108, p. 69–75, 2018.

KIRK, O.; CHRISTENSEN, M. W. Lipases from *Candida antarctica*: Unique biocatalysts from a unique origin. **Organic Process Research and Development**, v. 6, n. 4, p. 446–451, 2002.

KNANI, D.; GUTMAN, A. L.; KOHN, D. H. Enzymatic polyesterification in organic media. Enzyme-catalyzed synthesis of linear polyesters. I. Condensation polymerization of linear hydroxyesters. II. Ring-opening polymerization of caprolactone. **Journal of Polymer Science, Part A: Polymer Chemistry**, v. 31, n. 5, p. 1221–1232, 1993.

KOBAYASHI, S. Enzymatic polymerization: a new method of polymer synthesis. **Journal of Polymer Science, Part A: Polymer Chemistry**, v. 37, n. 16, p. 3041–3056, 1999.

KOBAYASHI, S. Lipase-catalyzed polyester synthesis--a green polymer chemistry. **Proceedings of the Japan Academy. Series B, Physical and biological sciences**, v. 86, n. 4, p. 338–365, 2010.

KOBAYASHI, S. Enzymatic ring-opening polymerization and polycondensation for the green synthesis of polyesters. **Polymers for Advanced Technologies**, v. 26, n. 7, p. 677–686, 2015.

KOBAYASHI, S.; UYAMA, H.; TAKAMOTO, T. Lipase-catalyzed degradation of polyesters in organic solvents. A new methodology of polymer recycling using enzyme as catalyst. **Biomacromolecules**, v. 1, n. 1, p. 3–5, 2000.

KOHANE, D. S.; LANGER, R. Polymeric biomaterials in tissue engineering. **Pediatric Research**, v. 63, n. 5, p. 487–491, 2008.

KOLB, H. C.; FINN, M. G.; SHARPLESS, K. B. Click Chemistry: Diverse Chemical Function from a Few Good Reactions. **Angewandte Chemie - International Edition**, v. 40, n. 11, p. 2004–2021, 2001.

KRAFT, P.; EICHENBERGER, W. Synthesis and Odor of Aliphatic Musks: Discovery of a New Class of Odorants. **European Journal of Organic Chemistry**, v. 2004, n. 2, p. 354–365, 2004.

KUMAR, A.; SAWANT, K. Encapsulation of exemestane in polycaprolactone nanoparticles: Optimization, characterization, and release kinetics. **Cancer Nanotechnology**, v. 4, n. 4–5, p. 57–71, 2013.

LANDFESTER, K.; RAMIREZ, L. P. Encapsulated magnetite particles for biomedical

- application. **Journal of Physics: Condensed Matter**, v. 15, p. 1345–1361, 2003.
- LANDFESTER, K.; RAMÍREZ, L. P. Encapsulated magnetite particles for biomedical. **Journal of Physics: Condensed Matter**, p. 1345–1361, 2003.
- LARRAÑAGA, A. et al. A study of the mechanical properties and cytocompatibility of lactide and caprolactone based scaffolds filled with inorganic bioactive particles. **Materials Science and Engineering C**, v. 42, p. 451–460, 2014.
- LEE, J. Y. et al. Polypyrrole-coated electrospun PLGA nanofibers for neural tissue applications. **Biomaterials**, v. 30, n. 26, p. 4325–4335, 2009.
- LI, H. et al. Electrospun membranes: Control of the structure and structure related applications in tissue regeneration and drug delivery. **Journal of Materials Chemistry B**, v. 2, n. 34, p. 5492–5510, 2014.
- LITTLE, T. et al. Efficient synthesis of novel 4-substituted urazoles. **Synthetic Communications**, v. 32, n. 11, p. 1741–1749, 2002.
- LOOS, K. **Biocatalysis in Polymer Chemistry**. Groningen: Wiley e Sons, 2010.
- LOWE, A. B. Thiol-ene “click” reactions and recent applications in polymer and materials synthesis. **Polymer Chemistry**, v. 1, n. 1, p. 17, 2010.
- LOWE, A. B. Thiol-ene “click” reactions and recent applications in polymer and materials synthesis: a first update. **Polymer Chemistry**, v. 5, p. 4820–4870, 2014.
- MACHADO, T. O.; SAYER, C.; ARAUJO, P. H. H. Thiol-ene polymerisation : A promising technique to obtain novel biomaterials. **European Polymer Journal**, v. 86, p. 200–215, 2017.
- MADER, M. et al. Ultraporous, Compressible, Wetttable Polylactide/Polycaprolactone Sponges for Tissue Engineering. **Biomacromolecules**, v. 19, n. 5, p. 1663–1673, 2018.
- MÅLBERG, S.; FINNE-WISTRAND, A.; ALBERTSSON, A. C. The environmental influence in enzymatic polymerization of aliphatic polyesters in bulk and aqueous mini-emulsion. **Polymer**, v. 51, n. 23, p. 5318–5322, 2010.
- MALLAKPOUR, S. E.; BUTLER, G. B. Polymerization of N-Methylpyrrole with bis-Triazolinediones via Electrophilic Aromatic Substitution. **Journal of Polymer Science Part a-Polymer Chemistry**, v. 25, p. 2781–2790, 1987.
- MARSICO, F. et al. Unsaturated poly(phosphoester)s via acyclic diene metathesis polymerization. **Macromolecules**, p. 8511–8518, 2012a.
- MATSUMURA, S.; EBATA, H.; TOSHIMA, K. A new strategy for sustainable polymer recycling using an enzyme: poly(ϵ -caprolactone). **Macromolecular Rapid Communications**, v. 21, n. 12, p. 860–863, 2000.

MCGINTY, D.; LETIZIA, C. S.; API, A. M. Fragrance material review on w-pentadecalactone. **Food and Chemical Toxicology**, v. 49, n. 2, p. S193–S201, 2011.

MEI, Y.; KUMAR, A.; GROSS, R. Kinetics and Mechanism of *Candida antarctica* Lipase B Catalyzed polymerization.pdf. **Macromolecules**, p. 5530–5536, 2003.

MEI, Y.; KUMAR, A.; GROSS, R. A. Probing Water-Temperature Relationships for Lipase-Catalyzed Lactone Ring-Opening Polymerizations. **Macromolecules**, n. 35, p. 5444–5448, 2002.

MELCHELS, F. P. W. et al. Photo-cross-linked poly(DL -lactide)-based networks. structural characterization by HR-MAS NMR spectroscopy and hydrolytic degradation behavior. **Macromolecules**, v. 43, n. 20, p. 8570–8579, 2010.

MEULEN, I. V. D. et al. Copolymers from unsaturated macrolactones: Toward the design of cross-linked biodegradable polyesters. **Biomacromolecules**, v. 12, n. 3, p. 837–843, 2011.

MEULEN, I. Van Der et al. Polymers from Functional Macrolactones as Potential Biomaterials: Enzymatic Ring Opening Polymerization, Biodegradation, and Biocompatibility. **Biomacromolecules**, v. 9, p. 3404–3410, 2008.

MILETIĆ, N. .; LOOS, K. .; GROSS, R. . Enzymatic polymerization of polyester. In: LOOS, K. (Ed.). **Biocatalysis in Polymer Chemistry**. Groningen: Wiley e Sons, 2010. p. 83–130.

MILETIĆ, N.; NASTASOVIĆ, A.; LOOS, K. Immobilization of biocatalysts for enzymatic polymerizations: Possibilities, advantages, applications. **Bioresource Technology**, v. 115, p. 126–135, 2012.

MONGE, S. et al. Phosphorus-containing polymers: A great opportunity for the biomedical field. **Biomacromolecules**, v. 12, n. 6, p. 1973–1982, 2011a.

MONGE, S. et al. Polymerization of Phosphorus- Containing (Meth) acrylate Monomers. **Phosphorus-Based Polymers: From Synthesis to Applications**, n. 11, p. 1–18, 2014.

MONTANIER, C. Y. et al. Engineering of *Candida antarctica* lipase B for poly (ϵ -caprolactone) synthesis. **European Polymer Journal**, v. 95, p. 809–819, 2017.

MURA, S. et al. Biodegradable nanoparticles meet the bronchial airway barrier: How surface properties affect their interaction with mucus and epithelial cells. **Biomacromolecules**, v. 12, n. 11, p. 4136–4143, 2011.

MURAKAMI, K. et al. Hydrogel blends of chitin/chitosan, fucoidan and alginate as healing-impaired wound dressings. **Biomaterials**, v. 31, n. 1, p. 83–90, 2010.

NAKANE, K. et al. Blends of Poly(L-lactic acid) with Poly(pentadecalactone) synthesized by enzyme-catalyzed polymerization. **Journal of Applied Polymer Science**, v. 108, p. 2139–2143, 2008.

NARAYANAN, G. et al. Fabrication and Characterization of Poly(ϵ -caprolactone)/ α -Cyclodextrin Pseudorotaxane Nanofibers. **Biomacromolecules**, v. 17, n. 1, p. 271–279, 2016.

O'BRIEN, F. J. Biomaterials & scaffolds for tissue engineering. **Materials Today**, v. 14, n. 3, p. 88–95, 2011.

OLIVEIRA, D. et al. Assessment of two immobilized lipases activity treated in compressed fluids. **Journal of Supercritical Fluids**, v. 38, n. 3, p. 373–382, 2006.

PASCUAL, A.; LEIZA, J. R.; MECERREYES, D. Acid catalyzed polymerization of macrolactones in bulk and aqueous miniemulsion: Ring opening vs. condensation. **European Polymer Journal**, v. 49, n. 6, p. 1601–1609, 2013a.

PAWAR, M. D. et al. Bioactive thermoresponsive polyblend nanofiber formulations for wound healing. **Materials Science and Engineering C**, v. 48, p. 126–137, 2015.

PELAZ, B. et al. Surface Functionalization of Nanoparticles with Polyethylene Glycol: Effects on Protein Adsorption and Cellular Uptake. **ACS NANO**, n. 7, p. 6996–7008, 2015.

PEREIRA, G. N. et al. Solvent-Free Production of Ethylene Glycol Monostearate through Enzymatic Esterification. **Industrial and Engineering Chemistry Research**, v. 57, n. 19, p. 6627–6632, 2018.

POLLONI, A. E. et al. Enzymatic ring opening polymerization of ω -pentadecalactone using supercritical carbon dioxide. **The Journal of Supercritical Fluids**, v. 119, p. 221–228, 2016.

POLLONI, A. E. et al. Polyesters from Macrolactones Using Commercial Lipase NS 88011 and Novozym 435 as Biocatalysts. **Applied Biochemistry and Biotechnology**, v. 184, p. 659–672, 2017.

POSNER, T. Beitrage zur Kenntniss der ungesattigten Verbindungen. Uber die Addition von Meroaptsnen an ungesattigte Kohlenwasserstoffe. **Berichte der deutschen chemischen Gesellschaft**, v. 1, p. 646–657, 1905.

PUPPI, D. et al. Polymeric materials for bone and cartilage repair. **Progress in Polymer Science**, v. 35, n. 4, p. 403–440, 2010.

RAVICHANDRAN, R. et al. Advances in Polymeric Systems for Tissue Engineering and Biomedical Applications. **Macromolecular Bioscience**, v. 12, n. 3, p. 286–311, 2012.

RODRIGUES, R. C. et al. Modifying enzyme activity and selectivity by immobilization.

Chemical Society Reviews, p. 6290–6307, 2013.

ROMIO, A. P. et al. Nanocapsules by miniemulsion polymerization with biodegradable surfactant and hydrophobe. **Macromolecular Chemistry and Physics**, v. 210, n. 9, p. 747–751, 2009.

RONCO, L. I. et al. Incorporation of Magnetic Nanoparticles in Poly(Methyl Methacrylate) Nanocapsules. **Macromolecular Chemistry and Physics**, v. 219, n. 6, p. 1–7, 2018.

ROPER, T. M. et al. Influence of the alkene structure on the mechanism and kinetics of thiol-alkene photopolymerizations with real-time infrared spectroscopy. **Journal of Polymer Science, Part A: Polymer Chemistry**, v. 42, n. 24, p. 6283–6298, 2004.

SÁ, A. G. A. et al. Biocatalysis of aromatic benzyl-propionate ester by different immobilized lipases. **Bioprocess and Biosystems Engineering**, v. 41, n. 5, p. 585–591, 2018.

SAGITHA, P. et al. Recent Advances in Post-modification Strategies of Polymeric Electrospun Membranes. **European Polymer Journal**, v. 105, n. January, p. 227–249, 2018.

SAMANTA, A. et al. Facile Fabrication of Composite Electrospun Nanofibrous Matrices of Poly(ϵ -caprolactone)–Silica Based Pickering Emulsion. **Langmuir**, v. 33, p. 8062–8069, 2017.

SAMPATH, M.; LAKRA, R.; KORRAPATI, P. Biointerfaces Curcumin loaded poly (lactic-co-glycolic) acid nanofiber for the treatment of carcinoma. **Colloids and Surfaces B: Biointerfaces**, v. 117, p. 128–134, 2014.

SAVIN, C. L. et al. Polyglobalide-Based Porous Networks Containing Poly(ethylene glycol) Structures Prepared by Photoinitiated Thiol–Ene Coupling. **Biomacromolecules**, v. 19, p. 3331–3342, 2018.

SCHÖTTLER, S. et al. Protein adsorption is required for stealth effect of poly(ethylene glycol)- and poly(phosphoester)-coated nanocarriers. **Nature Nanotechnology**, v. 11, n. 4, p. 372–377, 2016.

SEITZ, H. et al. Three-dimensional printing of porous ceramic scaffolds for bone tissue engineering. **Journal of Biomedical Materials Research - Part B Applied Biomaterials**, v. 74, n. 2, p. 782–788, 2005.

SETTANNI, G. et al. Protein corona composition of poly(ethylene glycol)- and poly (phosphoester)-coated nanoparticles correlates strongly with the amino acid composition of the protein surface. **Nanoscale**, v. 9, n. 6, p. 2138–2144, 2017a.

SEYEDNEJAD, H. et al. Functional aliphatic polyesters for biomedical and pharmaceutical applications. **Journal of Controlled Release**, v. 152, n. 1, p. 168–176, 2011.

SEZER, A. D. et al. Chitosan film containing fucoidan as a wound dressing for dermal burn

healing: Preparation and in vitro/in vivo evaluation. **AAPS PharmSciTech**, v. 8, n. 2, p. E94–E101, 2007.

SHADI, L.; KARIMI, M.; ENTEZAMI, A. A. Preparation of electroactive nanofibers of star-shaped polycaprolactone/polyaniline blends. **Colloid and Polymer Science**, v. 293, n. 2, p. 481–491, 2015.

SHAO, H. et al. Synthesis and characterization of amphiphilic poly(ϵ -caprolactone)-b-polyphosphoester diblock copolymers bearing multifunctional pendant groups. **Polymer (United Kingdom)**, v. 53, n. 14, p. 2854–2863, 2012.

SHODA, S. et al. Enzymes as Green Catalysts for Precision Macromolecular Synthesis. **Chemical Reviews**, v. 116, n. 4, p. 2307–2413, 2016.

SOEDA, Y.; TOSHIMA, K.; MATSUMURA, S. Synthesis and chemical recycling of novel poly(ester-urethane)s using an enzyme. **Macromolecular Bioscience**, v. 5, n. 4, p. 277–288, 2005.

SONG, R. et al. Current development of biodegradable polymeric materials for biomedical applications. **Drug design, development and therapy**, v. 12, p. 3117–3145, 2018.

SONG, W.-J. et al. Functionalized Diblock Copolymer of Poly (ϵ -caprolactone) and Polyphosphoester Bearing Hydroxyl Pendant Groups : Synthesis ., **Macromolecules**, v. 41, p. 6935–6941, 2008.

STEINBACH, T.; ALEXANDRINO, E. M.; WURM, F. R. Unsaturated poly(phosphoester)s via ring-opening metathesis polymerization. **Polymer Chemistry**, v. 4, n. 13, p. 3800, 2013.

STEINMACHER, F. et al. Design of Cross-Linked Starch Nanocapsules for Enzyme-Triggered Release of Hydrophilic Compounds. **Processes**, v. 5, n. 4, p. 25, 2017.

STEMPFLE, F. et al. Long-chain aliphatic polyesters from plant oils for injection molding, film extrusion and electrospinning. **Green Chemistry**, v. 16, p. 2008–2014, 2014.

SYRGIANNIS, Z. et al. Reaction of a triazolinedione with simple alkenes. Isolation and characterization of hydration products. **Tetrahedron Letters**, v. 50, n. 3, p. 277–280, 2009.

TADEN, A.; ANTONIETTI, M.; LANDFESTER, K. Enzymatic polymerization towards biodegradable polyester nanoparticles. **Macromolecular Rapid Communications**, v. 24, n. 8, p. 512–516, 2003.

TEBALDI, M. L. .; BELARDI, R. M. .; MONTORO, S. R. Polymers with nano-encapsulated functional polymers - Encapsulated nanoparticles for treatment of cancer cells. In: THOMAS, S.; SHANKS, R.; CHANDRAN, S. (Ed.). **Design and Applications of Nanostructured Polymer Blends and Nanocomposite Systems**. [s.l: s.n.]p. 171–186.

THAUVIN, C. et al. Functionalized PLA polymers to control loading and/or release properties

of drug-loaded nanoparticles. **International Journal of Pharmaceutics**, v. 548, n. 2, p. 771–777, 2018.

TORABINEJAD, B. et al. Synthesis and characterization of nanocomposite scaffolds based on triblock copolymer of l-lactide, caprolactone and nano-hydroxyapatite for bone tissue engineering. **Materials Science and Engineering C**, v. 42, p. 199–210, 2014.

TÜRÜNÇ, O. et al. From plant oils to plant foils: Straightforward functionalization and crosslinking of natural plant oils with triazolinediones. **European Polymer Journal**, v. 65, p. 286–297, 2015.

TURUNC, O.; MEIER, M. A. R. The thiol-ene (click) reaction for the synthesis of plant oil derived polymers. **European Journal of Lipid Science and Technology**, v. 115, p. 41–54, 2013.

ULERY, B. D.; NAIR, L. S.; LAURENCIN, C. T. Biomedical applications of biodegradable polymers. **Journal of Polymer Science, Part B: Polymer Physics**, v. 49, n. 12, p. 832–864, 2011.

UYAMA, H. et al. Lipase-Catalyzed Ring-Opening Polymerization of 12-Dodecanolide. **Macromolecules**, v. 28, p. 7046–7050, 1995.

UYAMA, H. et al. Lipase-catalyzed ring-opening polymerization and copolymerization of 15-pentadecanolide. **Acta Polymerica**, v. 47, p. 357–360, 1996.

UYAMA, H.; TAKEYA, K.; KOBAYASHI, S. Synthesis of Polyesters by Enzymatic Ring-Opening Copolymerization Using Lipase Catalyst. **Proceedings of the Japan Academy Series B-Physical and Biological Sciences**, v. 69, n. 8, p. 203–207, 1993.

UYAMA, H.; TAKEYA, K.; KOBAYASHI, S. **Enzymatic Ring-Opening Polymerization of Lactones to Polyesters by Lipase Catalyst: Unusually High Reactivity of Macrolides.** **Bulletin of the Chemical Society of Japan**, 1995. .

VAIDA, C.; KEUL, H.; MOELLER, M. Tailor-made polyesters based on pentadecalactone via enzymatic catalysis. **Green Chem.**, v. 13, n. 4, p. 889–899, 2011.

VAKILI, M. et al. Enhancing reactive blue 4 adsorption through chemical modification of chitosan with hexadecylamine and 3-aminopropyl triethoxysilane. **Journal of Water Process Engineering**, v. 15, p. 49–54, 2017.

VALÉRIO, A. et al. Synthesis of PEG-PCL-based polyurethane nanoparticles by miniemulsion polymerization. **Colloids and Surfaces B: Biointerfaces**, v. 135, p. 35–41, 2015.

VAN DER MEULEN, I. et al. Catalytic ring-opening polymerization of renewable macrolactones to high molecular weight polyethylene-like polymers. **Macromolecules**, v. 44, n. 11, p. 4301–4305, 2011a.

VAN DER MEULEN, I. et al. Copolymers from unsaturated macrolactones: Toward the design of cross-linked biodegradable polyesters. **Biomacromolecules**, v. 12, n. 3, p. 837–843, 2011b.

VAN DER VEEN, I.; DE BOER, J. Phosphorus flame retardants: Properties, production, environmental occurrence, toxicity and analysis. **Chemosphere**, v. 88, n. 10, p. 1119–1153, 2012.

VANDEWALLE, S. et al. Macromolecular Coupling in Seconds of Triazolinedione End-Functionalized Polymers Prepared by RAFT Polymerization. **ACS Macro Letters**, n. 5, p. 766–771, 2016.

VANDEWALLE, S. et al. Polycaprolactone-b-poly(N-isopropylacrylamide) nanoparticles: Synthesis and temperature induced coacervation behavior. **European Polymer Journal**, v. 98, p. 468–474, 2018.

VLAMINCK, L. et al. ADMET and TAD chemistry: A sustainable alliance. **Polymer Chemistry**, v. 7, n. 36, p. 5655–5663, 2016a.

VOUGIOUKALAKIS, G. C. et al. Solvent-dependent changes in the triazolinedione-alkene ene reaction mechanism. **Chemistry - A European Journal**, v. 14, n. 31, p. 9697–9705, 2008.

WANG, D. A. et al. Bioresponsive phosphoester hydrogels for bone tissue engineering. **Tissue Engineering**, v. 11, n. 1–2, p. 201–213, 2005.

WANG, S. et al. A new nerve guide conduit material composed of a biodegradable poly(phosphoester). **Biomaterials**, v. 22, n. 10, p. 1157–1169, 2001.

WANG, Y. C. et al. Self-assembled micelles of biodegradable triblock copolymers based on poly(ethyl ethylene phosphate) and poly(caprolactone) as drug carriers. **Biomacromolecules**, v. 9, n. 1, p. 388–395, 2008.

WANG, Y. C. et al. Recent progress in polyphosphoesters: From controlled synthesis to biomedical applications. **Macromolecular Bioscience**, v. 9, n. 12, p. 1154–1164, 2009.

WANG, Z. et al. Sustainable thermoplastic elastomers derived from plant oil and their “click-coupling” via TAD chemistry. **Green Chemistry**, v. 17, n. 7, p. 3806–3818, 2015.

WANG, Z. et al. Biomass Approach toward Robust, Sustainable, Multiple-Shape-Memory Materials. **ACS Macro Letters**, v. 5, n. 5, p. 602–606, 2016.

WEBB, K.; HLADY, V.; TRESKO, P. A. Relative importance of surface wettability and charged functional groups on NIH 3T3 fibroblast attachment, spreading, and cytoskeletal organization. **Journal of Biomedical Materials Research part B - Applied Biomaterials**, v. 41, n. 3, p. 422–430, 1998.

WEN, J.; KIM, G. J. A.; LEONG, K. W. Poly(D,Llactide-co-ethyl ethylene phosphate)s as new drug carriers. **Journal of Controlled Release**, v. 92, n. 1–2, p. 39–48, 2003.

WILSON, J. A. et al. Synthesis of ω -Pentadecalactone Copolymers with Independently Tunable Thermal and Degradation Behavior. **Macromolecules**, v. 48, n. 4, p. 950–958, 2015a.

WILSON, J. A. et al. Synthesis and Postpolymerization Modification of One-Pot Pentadecalactone Block-like Copolymers. **Biomacromolecules**, v. 16, n. 10, p. 3191–3200, 2015b.

YANG, X.-Z. et al. Block Copolymer of Polyphosphoester and Poly(L-Lactic Acid) Modified Surface for Enhancing Osteoblast Adhesion, Proliferation, and Function. **Biomacromolecules**, v. 10, n. 8, p. 2213–2220, 2009..

YANG, Y. et al. Lipase/esterase-catalyzed ring-opening polymerization: A green polyester synthesis technique. **Process Biochemistry**, v. 46, n. 10, p. 1900–1908, 2011.

YANG, Y. et al. Chemoenzymatic synthesis of polymeric materials using lipases as catalysts: A review. **Biotechnology Advances**, v. 32, n. 3, p. 642–651, 2014.

ZANETTI, M. et al. Synthesis of geranyl cinnamate by lipase-catalyzed reaction and its evaluation as an antimicrobial agent. **Journal of Chemical Technology and Biotechnology**, n. April, 2016.

ZHANG, J. et al. Recent developments in lipase-catalyzed synthesis of polymeric materials. **Process Biochemistry**, v. 49, p. 797–806, 2014.

ZHAO, W. et al. Fabrication of functional PLGA-based electrospun scaffolds and their applications in biomedical engineering. **Materials Science and Engineering C**, v. 59, p. 1181–1194, 2016.

ZHONG, Z.; DIJKSTRA, P. J.; FEIJEN, J. Controlled ring-opening polymerization of ϵ -pentadecalactone with yttrium isopropoxide as an initiator. **Macromolecular Chemistry and Physics**, v. 201, n. 12, p. 1329–1333, 2000.

ZHOU, X.; HONG, L. Controlled ring-opening polymerization of cyclic esters with phosphoric acid as catalysts. **Colloid and Polymer Science**, v. 291, n. 9, p. 2155–2162, 2013.

ZHU, W. et al. Synthesis, characterization, and properties of poly(ester-phosphoester)s by lanthanum triphenolate-catalyzed ring-opening copolymerization. **Journal of Polymer Science, Part A: Polymer Chemistry**, v. 49, n. 23, p. 4987–4992, 2011.

ZIEMBA, A. M. et al. Poly-L-lactic acid-co-poly(pentadecalactone) Electrospun Fibers Result in Greater Neurite Outgrowth of Chick Dorsal Root Ganglia in Vitro Compared to Poly-L-lactic Acid Fibers. **ACS Biomaterials Science & Engineering**, v. 4, p. 1491–1497, 2018.

ZOLFIGOL, M. A. et al. An Efficient Method for the Oxidation of Urazoles Under Mild and Heterogeneous Conditions. **Synthetic Communications**, v. 30, n. 14, p. 2573–2585, 2000.

ZOLFIGOL, M. A. et al. Oxidation of urazoles to their corresponding triazolinediones under

mild and heterogeneous conditions via in situ generation of NO^+ IO_x^- . **Synthetic Communications**, v. 31, n. 13, p. 1965–1970, 2001.

ZOLFIGOL, M. A.; GHAEMI, E.; NIKNAM, K. PEG- N_2O_4 System as an Efficient Reagent both for the Rapid Oxidation of Urazoles and 1, 4-Dihydropyridines under Nonaqueous Conditions. **Journal of the Chinese Chemical Society**, v. 55, p. 704–711, 2008.